DYNAMIC ANALYSIS OF RECTANGULAR LIQUID CONTAINERS WITH ELASTIC BAFFLE

A Thesis

Submitted by

SUPRIYA DEB
Class Roll No-002210402031
Reg. No-163474 of 2022-23
Exam Roll No-M4CIV24028

In partial fulfilment of the requirements
for the award of the degree of

Master of Engineering

In

Civil Engineering
(Structural Engineering)

Under the Guidance of
Dr. Kalyan Kumar Mandal

Department Of Civil Engineering
Jadavpur University
Kolkata-700 032
May-2024

DEPARTMENT OF CIVIL ENGINEERING
FACULTY OF ENGINEERING AND TECHNOLOGY
JADAVPUR UNIVERSITY
KOLKATA – 700 032

CERTIFICATE OF RECOMMENDATION

This is to certify that the thesis entitled, "**DYNAMIC ANALYSIS OF RECTANGULAR LIQUID CONTAINERS WITH ELASTIC BAFFLE**" submitted by **Supriya Deb**, Class Roll No. **002210402031**, Exam. Roll No. **M4CIV24028**, Registration No. **163474 of 2022-2023** in partial fulfilment of the requirements for the award of Master of Engineering degree in Civil Engineering with specialization in "**Structural Engineering**" at Jadavpur University, Kolkata is an authentic work carried out by him under my supervision and guidance. I hereby recommend that the thesis be accepted in partial fulfilment of the requirements for awarding the degree of **"Master of Engineering in Civil Engineering (Structural Engineering)"**.

Dr. Kalyan Kumar Mandal
Associate Professor
Department of Civil Engineering
Jadavpur University
Kolkata- 700032

Dr. Partha Bhattacharya
Head of the Department
Department of Civil Engineering
Jadavpur University
Kolkata-700032

Prof. Dipak Laha
DEAN, FET
Jadavpur University
Kolkata- 700032

DEPARTMENT OF CIVIL ENGINEERING
FACULTY OF ENGINEERING AND
TECHNOLOGY JADAVPUR UNIVERSITY
KOLKATA – 700032

CERTIFICATE OF APPROVAL

This thesis paper is hereby approved as a credible study of an engineering subject carried out and presented in a manner satisfactorily to warrant its acceptance as a pre-requisite for the degree for which it has been submitted. It is understood that, by this approval the undersigned do not necessarily endorse or approve any statement made, opinion expressed or conclusion drawn therein but approved the thesis paper only for the purpose for which it is submitted.

Committee of Thesis Paper Examiners

Signature of Examiner

Signature of Examiner

DECLARATION

I, Supriya Deb, Master of Engineering in Civil Engineering (Structural Engineering), Jadavpur University, Faculty of Engineering & Technology, hereby declare that the work being presented in the thesis work entitled, "**Dynamic Analysis of Rectangular Liquid Containers with Elastic Baffle"** is authentic record of work that has been carried out at the Department of Civil Engineering, Jadavpur University, Kolkata under the guidance of Dr. Kalyan Kumar Mandal, Associate Professor, Department of Civil Engineering, Jadavpur University. The work contained in the thesis has not yet been submitted in part or full to any other university or institution or professional body for award of any degree or diploma or any fellowship.

Place: Kolkata
Date: 29.05.2024

Supriya Deb
Class Roll No: 002210402031
Exam Roll No:M4CIV24028
Reg. No.: 163474 of 2022-23

ACKNOWLEDGEMENT

I would like to take this opportunity to convey my sincere gratitude and appreciation for my supervisor **Dr. Kalyan Kumar Mandal.** I am indebted to him for his methodical guidance, motivation and constant support given to me throughout the thesis work. He has identified my potentials and kept faith in me. It is because of his confidence that I was able to successfully accomplish the targets. I am extremely thankful to him as without him my thesis could not have reached this stage.

I also thankfully acknowledge my gratefulness to all Professors and staffs of Civil Engineering Department, Jadavpur University, Kolkata, for extending all facilities to carry out the present study.

I also thankfully acknowledge the assistance and encouragement received from my family members, friends and others during the preparation of this Thesis.

Place: Kolkata
Date: 29.05.2024

Supriya Deb
Class Roll No.: 002210402031
Reg No.: 163474 of 2022-23
Exam Roll No-M4CIV24028

ABSTRACT

In the present study, fundamental time period and the hydrodynamic pressure exerted by the fluid on walls of rectangular tanks due to sinusoidal excitations are investigated by pressure based finite element method. The fluid within the tank is considered to be water and tank walls are assumed as rigid. However, the baffle within the tanks is considered to be flexible. The fluid within the tank is considered as inviscid and fluid motion is irrotational. Galerkin approach is used for finite element formulation of wave equation. Newmark's average integration method which is unconditionally stable is used to obtain the response of baffle-liquid coupled system. The present algorithm also includes the compressibility of water within tank.

The efficacy of the present algorithm has been demonstrated through numerous examples both for free and forced vibration analysis. The time period increases with presence of elastic baffle within the tanks. The time period of baffle-liquid coupled system also increases with the increase of tank length. An increasing trend of fundamental time period of baffle-liquid coupled system is also observed with the increase of liquid height within the tanks. However, the influence of height of fluid in fundamental time period of this coupled system is greater than those for the length of tanks. The free vibration responses of this coupled system also increase with the increase of flexibility of baffle wall. Position of the baffle within the tanks also influences the free vibration response of the tank with baffle. Similar to the height of baffle, the thickness of baffle also changes the flexibility of baffle within tanks hence the increase in baffle thickness reduces the time period of the baffle-fluid coupled system.

Similar to the fundamental time period of baffle-fluid coupled system, the hydrodynamic pressure within the tanks due to different excitations depends on the different parameters of tank and baffle. The hydrodynamic pressure at the bottom of tank wall increases with the increase of baffle thickness. However, this hydrodynamic pressure at free surface decreases with the increase of baffle thickness. Hydrodynamic pressure at bottom surface of tank increases with decrease in fluid height. Hydrodynamic pressure at bottom surface of tank increases with increase in tank length. However, there is no notable variation in hydrodynamic pressure at free surface due to change in tank length.

The dynamic response is amplified when the system is experienced external loadings having frequency close to natural frequency of the system.

KEYWORDS: *Compressibility of water, Finite element method, Fluid-Baffle interaction, Forced Vibration analysis, Pressure coefficient*

LIST OF SYMBOLS

Symbols	Description
a	Acceleration of excitation
Amp	Amplitude of excitation
C	Acoustic wave speed
C_P	Hydrodynamic pressure coefficient
g	Gravitational acceleration
H	Height of fluid, Height of tank
L	Length of the tank
ρ	Mass density of fluid
N_t	No of time steps
N_h	Nos. of horizontal division of mesh
N_v	Nos. of vertical division of mesh
P	Hydrodynamic Pressure
T	Time period of excitation
V_t	Velocity of fluid at time t
U_t	Displacement of fluid at time t
W	Exciting frequency
w	Fundamental frequency of water within tank

CONTENTS

List of Figures

List of Tables

CHAPTER-1
INTRODUCTION

1.1 General

Fluid containers are integral components in various engineering fields, including civil, mechanical, marine, and aerospace engineering. These containers are used to store and transport liquids and gases, ranging from water and oil to chemicals and other hazardous materials. The need for water tank systems is as old as civilized man. A ground water tank provides for the storage of drinking water, irrigation, fire suppression, agricultural farming and livestock, chemical manufacturing, food processing, rainwater harvesting as well as many other possible solutions. Storage reservoirs and overhead tanks are used to store water, liquid petroleum, petroleum products and similar liquids. Damage in tanks may cause a loss of liquid content, which could result in economic damage, as well as in long-term contamination of soil for tanks resting on soil. Tanks in the seismic area should be functional after earthquakes. This is due to the need of water after earthquakes. However, the tanks of the nuclear power plant and oil could cause the irreparable environmental pollution. Many tanks have been severely damaged and some have collapsed with disastrous results due to past seismic events. Therefore, understanding the dynamic behavior of these containers under various loading conditions is critical to ensure their structural integrity, safety, and functional performance.

Dynamic analysis refers to the study of the response of fluid containers to time-varying loads such as seismic forces, wind loads and other dynamic excitations. Unlike static analysis, which considers only constant loads, dynamic analysis accounts for the time-dependent nature of loads and their impact on the container's structure and the fluid within. Sloshing effect and the hydrodynamic pressure act on walls are the major guiding parameters in the design of such tanks. The clear understanding of sloshing characteristics is essential for the determination of required freeboard to prevent overflow of the fluid and also for the estimation of hydrodynamic pressure on the fluid retaining container such as tank.

Different types of numerical schemes, such as the finite difference method, the finite volume method, the boundary element method and finite element method may be used to obtain the responses of the fluid within the tank.

The analysis of water tank is a perfect example of fluid-structure interaction problem or in other word, the proper and precise responses of the tank is obtained if the fluid-structure interaction

effect is considered in the analysis. Further, the responses will be so realistic if this problem is dealt in 3D. However, in existing literatures it is reported that the effect of the flexibility of the tank does not change the pressure distribution if the tank wall is sufficiently thick. Therefore, the assumption of rigid tank is a good approximation to evaluate the hydrodynamic pressures due to the sloshing component of the liquid in tanks. Similarly, 2D approximation of rectangular water tank may be considered for a certain value of width to length ratio of rectangular tanks.

The Hydrodynamic pressure exerted by the fluid on the tank wall and amplitude of slosh depends on the amplitude and frequency of the tank motion, liquid depth, liquid properties, tank geometry, and also the size, shape and location of the internal baffle. Abundant research has been carried out on the seismic response of cylindrical liquid storage tanks mainly to know the sloshing behaviour and mode shape but very few contributions have been published for determining total hydrodynamic pressure of rectangular tank and analysis is carried out considering fluid as incompressible, irrotational and inviscid. However, the compressibility effect of fluid may play an important role for precise estimation of total hydrodynamic pressure and the sloshed deformation for calculation of free board in tanks.

1.2 Objective of the present study

The objective of the present thesis is to study the dynamic behavior of rectangular fluid container with elastic baffle subjected to different dynamic excitations.

CHAPTER-2
LITERATURE REVIEW

2.1 General

Detailed review of the literature carried out related to the dynamic analysis of liquid storage containers would be difficult to address completely in this chapter. A summarized review of the previous studies related to dynamic analysis of liquid storage tank is presented in this section which is associated to the present study. This literature review focuses on recent contributions related to this work and past efforts most closely related to the needs of the present work.

2.2 Literature Review

Adhikary and Mandal (2017) dealt with the finite element analysis of water tanks of different sizes and locations with rigid baffle wall at tank bottom. Fluid was considered to be compressible as well as incompressible and was discretized by two dimensional eight-noded isoparametric elements and the governing equation was simulated by pressure-based formulation to reduce the degrees of freedom in the domain. The fundamental frequency of the tank water decreases with the increase of the block height and variations are different for different fundamental frequencies. The hydrodynamic pressure on tank wall depends on the exciting frequencies and it has comparatively higher value when the exciting frequency is equal and lower than the first fundamental frequency of the water in the tank. Further, the hydrodynamic pressure increases with the increases of width of the block for all exciting frequencies when the block was at the center of the tank. The similar trend of hydrodynamic pressure was observed for different height of block at exciting frequency equal and less than the fundamental frequency of the reservoir and this was due to the reduction of fundamental frequency with the height of the block. However, the trend became reverse for frequency greater than the fundamental frequency of reservoir. The left and right walls of tank experienced different hydrodynamic pressure when the block was placed at off-centre and its magnitude also depends on the exciting frequency and the position of the block. The pressure on the wall became higher magnitude when the block was closer to that wall. However, the increase in the pressure became insignificant after a certain value of the distance between the wall and the rigid block.

Study on behavior of elevated water storage tanks under seismic occurrence was carried out by **Waghmare et al. (2015)**. The objective of the study was to investigate the uncontrolled response of steel and RCC elevated water reservoirs of different aspect ratio S = H/R (height of the container to its radius) and subjected to different strong ground motion earthquakes. The simulation of water tank using three-mass model concept was carried out through MATLAB. The response of the tanks to different real earthquake ground excitations was investigated using simplified three mass model of the tank. The response quantities such as sloshing displacement, impulsive displacement, tower displacement and base shear are measured by varying the characteristics of earthquake time history. The sloshing displacement is greatly influenced by the characteristics of the time history compared to other response quantities. Base shear depends upon the amplitude, magnitude and on number of times the maximum amplitude frequencies hits the surface.

Hadj-Djelloul et al. (2020) dealt with dynamic behavior of elevated water tanks under seismic excitation using the finite element-based technique taking into account fluid- structure interaction and sloshing effect. Modal and transient analysis were carried out on two types of the elevated tanks support system keeping the same quantity of concrete and the same fluid volume. The period of the convective mode and the sloshing displacements are the same for the shaft and frame supports which mean that the convective component is independent of the supporting system. The period of impulsive mode and the displacement at the top of the tank vary depending upon the rigidity of the structure and the shaft support is more rigid than the frame support. Displacements at the top of the tank and fundamental period of the impulsive mode of the elevated water tank with shaft support is less compared to the elevated water tank with frame support.

Finite element analysis of infinite reservoir adjacent to gravity dam was carried out by **Mandal and Aziz (2019)**. The equation of motion for fluid was simulated by pressure-based Eulerian formulation. 2-dimensional eight noded isoparametric elements were used to discretize the domain. Variation of hydrodynamic pressures on concrete gravity dam were studied for different exciting frequencies. Different truncation boundary conditions for infinite reservoir were compared and the Gogoi and Maity boundary condition was implemented at the truncation surface and the infinite reservoir was truncated at a distance of 0.5H from the upstream face of the dam. Analysis of infinite reservoir was carried out with different inclinations of upstream face ($q=30^0$, 45^0 and 60^0) both for compressible and incompressible fluid. The hydrodynamic pressure on dam remains independent of exciting frequencies when water is modelled as incompressible one. The

hydrodynamic pressure coefficient very much depends on the exciting frequency for compressible water. Similarly, the effect of reservoir bottom absorption is small for lower values of excitation frequencies. However, this effect may not be neglected if the excitation frequency becomes equal to or more than the fundamental frequency of the reservoir. The hydrodynamic pressure increases with increase in the slope of the upstream face of the rigid dam. The distribution of hydrodynamic pressure also varies with the inclination slope.

Mandal (2023) dealt with finite element based total response analysis of rectangular liquid containers for different excitations. The total hydrodynamic pressure exerted by the fluid on walls of rectangular tanks due to horizontal excitations of different frequencies were studied by pressure based finite element method. Fluid within the tanks was considered as inviscid, linearly compressible and its motion was considered to be irrotational and it was simulated by two dimensional eight noded isoparametric element. The tank walls were considered as rigid. The total hydrodynamic pressure within tank depends on exciting frequencies and also height of rectangular water tank. Total hydrodynamic pressure increases with the increases of exciting frequency when the exciting frequency is less than the fundamental frequency of the liquid and it reaches maximum value when exciting frequency is equal to fundamental frequency. The total hydrodynamic pressure decreases for exciting frequency greater than the fundamental frequency of liquid. For a particular exciting frequency, the total hydrodynamic pressure at the free surface of liquid is independent of tank length. The sloshed displacement increases with the increase of exciting frequency and has maximum value when the exciting frequency is equal to the fundamental frequency of liquid within the tank. However, the sloshing is much less when the exciting frequency is greater than the fundamental frequency. Freeboard within the tank is required to provide to overcome sloshing displacement due to dynamic excitation.

Das et al. (2022) dealt with finite element based direct coupling approach for dynamic analysis of dam–reservoir system for different excitation. Dam and reservoir both were discretized by eight noded isoparametric elements. Both the domains were coupled and analyzed as a single system to get the responses of dam–reservoir coupled system subjected to dynamic excitation taking into account the fluid– structure interaction effect. Absorption effect of reservoir bottom was considered. Length of the reservoir was truncated at a suitable distance (L/H_f=0.5), and the non-reflecting boundary condition proposed by Gogoi and Maity was applied along the truncated face. Koyna dam was considered for numerical study. Slope of reservoir bed, inclined length of

reservoir and bottom absorption coefficient are the important factors governing the hydrodynamic pressure as well as responses of gravity dam. Hydrodynamic pressure and stresses of gravity dam increase with increase in slope angles for positive slope of reservoir bottom. Pressure coefficient and stresses of dam decrease with increase in negative slope of reservoir bottom. Inclined length of reservoir is also a dominant factor which influences pressure coefficient and stresses of dam. If the inclined length of reservoir is increased, hydrodynamic pressure coefficient and stresses of gravity dam increase for positive slope angle of reservoir base. Pressure coefficient and stresses of dam decrease with increase in inclined length of reservoir for negative bottom slope. Hydrodynamic pressure increases with increase in reservoir bottom coefficient.

Nayana et al. (2015) dealt with dynamic response of ground supported rectangular water tank. Finite element method was used to predict the response of the seismically excited rectangular tanks. The finite element program, ANSYS was used for the dynamic modal and time history analysis. Effect of change in dimension of water tank (length-to-width ratio) and water fill height with particular tank size on dynamic response were studied. The deformation values increase from fully filled to quarterly filled condition of the tank. The deformation value increases with decrease in length-to-width ratio of the tank.

Effect of the vertical baffle height on the liquid sloshing in a laterally moving three-dimensional rectangular tank was carried out by **J. H. Jung et al. (2012)**. The volume of fluid method was used to simulate two-phase flow in laterally moving rectangular unbaffled and baffled tanks. For unbaffled tank, strong liquid sloshing is enough to cause the liquid to reach the top wall of the tank after impacting the side walls, leading to the violence of the liquid in the tank. Also, the free surface reveals the irregular deformation accompanying nonlinear wave depending on the three-dimensions. For small baffle height of $h_B/h=0.2$, the pattern of liquid sloshing is almost similar to the case of the unbaffled tank, and it results in wave breaking after the liquid collides with the ceiling of the tank. But the free surface deformation for $h_B/h=0.2$ is smoother than that for $h_B/h=0$ especially in the region around the tank center. If the baffle height increases, the liquid sloshing becomes more suppressed due to the augmentation of the blockage effect of the baffle, which results in additional viscosity and energy dissipation, also known as hydrodynamic damping.

Lotfi and Samii (2012) dealt with dynamic analysis of concrete gravity dam-reservoir systems by Wavenumber approach in the frequency domain taking into account fluid-structure interaction. The dam was discretized by isoparametric eight noded plane-solid finite elements and

the reservoir was divided into two parts, a near-field region in the vicinity of the dam and a far-field part which extends to infinity in the upstream direction. For the FE-FE method of analysis only the near-field region was considered and discretized by isoparametric eight noded plane-fluid finite elements and the absorbing boundary condition was employed on the upstream truncation boundary. The FE-FE analysis technique was chosen as the basis of a proposed method for dynamic analysis of concrete dam-reservoir system in the frequency domain, which was referred to as the Wavenumber approach. The length of this near-field region was denoted by 'L' and water depth was referred to as 'H' and three cases were considered for the L/H values of 0.2, 1 and 3 which represent low, moderate and high reservoir lengths. The response of an idealized triangular dam was studied due to horizontal ground motion for different absorbing boundary condition alternatives. The Wavenumber approach gives satisfactory results in comparison with the exact response.

Drosos et al. (2008) dealt with finite element method-based formulation for an effective computation of the eigenmode frequencies, the decomposition of total liquid mass into impulsive and convective parts, and the distribution of wall pressures due to sloshing in liquid storage tanks of arbitrary shape and fill height. The fluid motion was considered to be inviscid and linear. The numerical solution presented in this work was based on a finite element model developed within the environment provided by the ANSYS software. The results of the above methodology for cylindrical and spherical tanks are in excellent agreement with results available in the literatures. Hence, the use of the proposed discrete models results in a significant reduction in the size of the dynamic model and it can become a useful tool for quick and accurate analysis in the design office.

A probabilistic model for evaluation of the dynamic behaviour of a concrete gravity dam considering the fluid-structure interaction was developed by **Khiavi et al. (2023)**. The model was developed with programming in the APDL environment of ANSYS to study the interaction effect in the dynamic behaviour of a concrete dam and reservoir, the process of hydrodynamic wave propagation in the reservoir and its effects on the response of a concrete gravity dam. The model was analyzed by considering the range of changes for excitation frequency and reservoir height and length. The probabilistic model with upstream isolation layer gives good idea of its advantage. The model results provided a clear and proper understanding of the dam-reservoir interaction and the process of propagation of hydrodynamic pressure waves in the reservoir, along with the effect of compressibility and excitation frequency. From the wave propagation process and the responses

obtained, the truncated location of the reservoir can be determined in numerical models for any vibrational frequency.

Seismic analysis of Intze type elevated water tank with different staging configuration was carried out by **Bansode and Datye (2018)**. Response Spectrum Analysis were carried out on three different types of bracing systems of elevated water tank. Intze type water tank was modelled without bracing, with X-bracing and with diagonal bracing. Base shear, base moment, lateral displacement and time period were compared for different staging arrangement. Lateral displacement and time period reduces considerably due to increased stiffness of bracing system. Base shear increases as the level of bracing increases as bracing system put an additional mass to the structure.

Malhotra et el. (2000) dealt with development of simple procedure for seismic analysis of liquid storage tanks taking into account impulsive and convective (sloshing) action of the liquid in flexible steel or concrete tanks fixed to rigid foundations. The tank-liquid system was represented by the first impulsive and first convective modes only after combining the higher impulsive modal mass and higher convective modal mass to the first impulsive mode and first convective mode respectively. The base shear, over-turning moment, and sloshing wave height were calculated by using the site response spectra and performing simple calculations. Three steel tanks were selected for comparing the results obtained from the simplified procedure with those from a detailed modal analysis. The results shows that the values obtained from simplified method is slightly on conservative side in comparison to detailed modal analysis.

Aregawi and Kassahun (2017) dealt with studying dynamic response of idealized ground supported rectangular water tanks to earthquake excitation using a linear three-dimensional finite element analysis and SAP-2000 software over five tank models with a capacity of 216, 288, 360, 432 and 504 m^3. The variable analysis parameters considered were the aspect ratio (tank height to length ratio) and tank water level. The results show that, there is a smooth increase in the moment and displacement of both hydrostatic and hydrodynamic analysis with a decrease in aspect ratio (A). The maximum hydrodynamic moment was observed to be 91.3 % higher than the maximum hydrostatic moment. Similarly, the displacement obtained from hydrodynamic analysis was 63.58% more than the corresponding hydrostatic result.

Das et al. (2022) dealt with finite element-based approach to examine hydrodynamic pressure in reservoir adjacent to the concrete gravity dam subjected to dynamic excitation. The domain of reservoir was discretized by eight noded finite element. Pressure was considered as nodal variable following Eulerian approach. Hydrodynamic pressure of infinite reservoir adjacent to gravity dam were studied for different geometrical properties of the reservoir. The value of hydrodynamic pressure coefficient increases with the increase of inclination of dam reservoir interface. Increase in pressure is not uniform at the face of the dam due to increase of slope angle for Tc/H_f=4. However, increase in pressure is uniform at the face of the dam due to increase of slope angle for other frequencies. Velocity distribution of reservoir for different values of inclination of dam reservoir interface is significantly different. There is also change in velocity profile of reservoir with change of absorption coefficient of reservoir bottom. The value of hydrodynamic pressure at the heel of dam increases with increase of reservoir positive bottom slope angle. Hydrodynamic pressure coefficient at the heel of dam decreases with increase of negative slope angle. Hydrodynamic pressure is also a function of inclined length of bottom of reservoir. Pressure coefficient increases at base of dam with increase of inclined length for positive slopes. However, pressure coefficient decreases at base of dam with increase of inclined length for negative slope.

The non-linear vibrations of a structure coupled with water sloshing in a rectangular tank were studied both theoretically and experimentally by **Ikeda and Nakagawa (1996)**. From the theoretical analysis, the modal equations which are needed to analyze the non-linear coupled vibration of the structure with the sloshing could be obtained. The solutions for the harmonic oscillations of the structure and the water surface were determined including their stability analysis. Depending upon the water depth, the shapes of the resonance curves for the structure became soft spring types for a deep depth and hard spring types for a shallow depth. When the magnitude of excitation was small, the amplitude of the structure became infinitesimal near the tuning frequency. If the magnitude of excitation was comparatively large, a super-summed and differential harmonic oscillation may occur near the tuning frequency. The validity of the theoretical analysis was confirmed by the experiments.

Jiaqui Ran et al. (2023) dealt with study on the response characteristics of elevated cylindrical liquid storage tanks under seismic excitation. In seismic analysis, the undesirable mode of oscillation was determined using analytical and numerical approaches. El Centro earthquake

response spectrum plot and El Centro accelerogram were used to compute the response to the seismic event and to compare the results of time-history analysis. The ANSYS software was used for all of the analyses.

The tank's height-to-length ratio, soil type, water level, and tank wall thickness are some of the variables in determining seismic performance of the tank. Full tanks have higher top displacement and axial force components than half-full (31%), and empty tanks (75 percent). According to the underground tank, empty tank top displacement and axial force components are higher than those in half-full (19%) and full tank circumstances (40 percent). Tank cases that are located above ground have higher base shear values than those that are located below ground (19 percent to 37 percent).

Seismic response evaluation of the RC elevated water tank with fluid-structure interaction and earthquake ensemble was carried out by **Omidinasab and Shakib (2011).** Finite element method was employed to model elevated water tank system. A reinforced concrete elevated water tank supported by moment resisting frame, with a capacity of 900 m^3 and height of 32 m had been utilized and subjected to an ensemble of earthquake records considering Eulerian method for modelling of fluid-structure interaction. Seismic responses of the elevated water tank such as base shear force, overturning moment, displacement and hydrodynamic pressure had been assessed for ensemble earthquake records. The seismic responses of the elevated water tank were determined using the nonlinear time history analysis for the empty, half-full and fully filled containers. The study reveals that the maximum response does not always occur in the full tank. The system predominant frequencies are located on the range of high amplitude of frequency content of some of the selected earthquake records and caused amplification of responses. The increase in the percentage of container filling showed that the value of base shear force, overturning moments, displacement and hydrodynamic pressure increased in the range of mean plus and minus standard deviation. Evaluation of the convective pressure revealed that the earthquake records with low predominant frequency caused excitation in the oscillating modes with relatively high period and consequently resulted in high hydrodynamic pressure at fluid free surface.

Nandagopan and Shajee (2017) dealt with dynamic analysis of RCC water tanks with varying height of water level. Ground supported rectangular and circular water tanks, overhead circular and rectangular water tanks were considered. Housner’s two mass model for water tank was selected for dynamic analysis where the whole mass of water was divided into impulsive

liquid mass and convective liquid mass. Analysis was carried out to find the base shear and base moment. The manual dynamic analysis is done with varying height of water level in the tank using IS-1893 (Part 2) guidelines and study the effects due to change in height of water level. The manual dynamic analysis was compared with dynamic analysis performed in FEM software ETABS for varying height of water level. It was observed that base shear and base moment increase with increase in water level. Elevated water tank shows higher base reactions than ground supported tanks. So base reaction increases with increase in staging height. The base shear and base moment of ground supported rectangular tank exceeds ground supported circular tank by 6.89% and 6% respectively at tank full condition. The ground supported circular tank has less base reactions, i.e., it is better than ground supported rectangular tank. In case of elevated tanks the base shear and base moment of circular tank exceeds rectangular tank by 1.37% and 3.69% respectively. The elevated rectangular tank is better than elevated circular tank.

Kotrasova and Kormanikova (2017) dealt with earthquake analysis of liquid storage cylindrical tank. The paper provided the theoretical background for concrete containers fixed to rigid foundations due to earthquake events, describing of fluid hydrodynamic impulsive and convective (sloshing) effects on the tank. Seismic responses such as base shear, the bending moment and overturning moment were calculated by using the elastic response spectra for Slovak republic risk region of seismic risk 2.

Ali and Telang (2017) carried out dynamic analysis of elevated water tanks supported on RC framed structure with different tank storage capacities for different staging configuration. In this study, various capacity circular and rectangular overhead water tank were considered. Analysis was carried out for all four different seismic zones (zone-II to V), and for both tank-full and tank-empty conditions. From the analysis it is observed that seismic base shear of full water tank and empty water tank are increased with seismic zone II-V because of zone factor, response reduction factor etc. Base shear in full condition tank is slightly higher than empty tank due to absence of water or hydro static pressure. Displacement of full water tank and empty water tank are increased with seismic zone II-V. Maximum nodal displacement and minimum nodal displacement found at the wall of water tank when tank is in full condition. Shear force and bending moment of full water tank and empty water tank are increased with seismic zone II-V and these values in full condition tank is slightly higher than empty tank due to absence of water or hydro static pressure.

Mustafa H Arafa (2006) dealt with development of a finite element formulation to examine the sloshing of liquids in partially filled rigid rectangular tanks undergoing base excitation. The liquid domain was discretized into two-dimensional four-node rectangular elements with the liquid velocity potential representing the nodal degrees of freedom. Liquid sloshing effects induced by both steady-state harmonic and arbitrary horizontal base excitation were investigated in terms of the slosh frequencies, liquid velocity field, free surface displacement and hydrodynamic forces acting on the tank walls. The model was employed to study the effects of providing both vertical and horizontal rigid baffles within the liquid domain on the slosh frequencies and free surface motion during forced vibration, in an attempt to investigate their viability in acting as slosh suppression devices. Numerical simulation indicates that significant reduction in the hydrodynamic forces can be achieved for baffled tanks subjected to various external excitation schemes.

Seismic analysis of rectangular concrete tanks by considering fluid and tank interaction was carried out by **Yazdanian et al. (2016)**. For examining seismic behaviour two water storage rectangular concrete tanks were modelled in FEM software and analysed under static, modal, response-spectrum and time-history analysis. In time history analysis, earthquake accelerograms of Tabas, Kobe and Cape Mendocino were applied to tanks. From the analysis it is found that displacement, base shear and wave height obtained from time history analysis are more than those of response spectrum analysis. In time history analysis, the maximum displacement is achieved in highest part of the tanks. The thickness of the wall has a very important effect in the behaviour of the tanks and it is observed the tanks which have the greater dimension, but have bigger wall thickness tolerated less displacement. The tank which has the greater weight has the bigger base shear. Also, the PGA of the earthquake has a strong effect on increasing of base shear.

Seismic response of elevated rectangular water tanks considering soil-structure interaction was carried out by **Visuvasam et al. (2017)**. The base support was considered as flexible instead of rigid by providing spring stiffness in order to consider the effect of soil properties on the seismic behaviour of water tanks using SAP-2000 software and parametric studies had been carried out based on soft, medium and hard types of soils. The result shows that the ratio of fundamental time period of flexible base (T_f) to fixed base (T) behaved linearly for all types of soils and the soil-structure interaction affects the T_f/T ratio by 20% and 10% for soft and medium type soils

respectively. The hard soil behaves similar to fixed base condition where the T_f/T and V_f/V ratios confined to unity. The models analysed and designed considering fixed base condition overestimate the design values.

Dongya Zhao et al. (2017) dealt in developing numerical code based on potential flow theory to investigate nonlinear sloshing in rectangular tanks under forced excitation. The Boundary Element Method (BEM) was used to solve boundary value problems of both velocity potential and acceleration potential. Numerical calculation results were compared with published results to determine the efficiency and accuracy of the numerical code. Using this code, internal free surface elevation and sloshing loads on liquid tanks can be obtained both in time domain and frequency domain. The artificial damping model was adopted to account for energy dissipation during sloshing. Sloshing properties in partially filled rectangular and membrane tank under translational and rotational excitations were investigated. It is found that sloshing under horizontal and rotational excitations share similar properties. The first resonant mode and excitation frequency are the dominant response frequencies. Resonant sloshing will be excited when vertical excitation lies in the instability region. For liquid tank under rotational excitation, sloshing responses including amplitude and phase are sensitive to the location of the center of rotation. Moreover, experimental tests were conducted to analyze viscous effects on sloshing and to validate the feasibility of artificial damping models. The results show that the artificial damping model with modifying wall boundary conditions has better applicability in simulating sloshing under different fill levels and excitations.

Behaviour of elevated water tank under sloshing effect was studied by **Wakchaure and Besekar (2014)** using Finite Element Method (FEM) based computer software ANSYS. Four different RCC elevated service reservoir models such as circular with and without compartment, rectangular with and without compartment were used for study having same capacity, location, staging height, bracing interval and number of columns for all models. Static, modal (dynamic) and Response spectra analysis were carried out and results were compared. From the analyses results it can be stated that critical response of the elevated tank does not always occur in full condition, it may also occur under half condition. The critical response, depends on the earthquake characteristics and particularly frequency content of earthquake records. Elevated water tank with compartment reduces the sloshing effect & stress, deflection, deformations of the tank.

Sloshing response of elevated water tank over alternate column proportionality was carried out by **Chirag N. Patel et al. (2012)** to compare the seismic behaviour of the elevated water tank under alternate column proportionality under different time history records using finite element software SAP-2000. A reinforced elevated water tank with 1000 m^3 capacity and supported by fixed base frame type staging system with different column proportionality had been considered in the study. With considering two-mass water model, seismic responses including sloshing displacement and displacement of tank at various locations from bottom to top were assessed under four earthquake records. It has been observed that sloshing displacement increases with the increase in the panel number and increases against high frequency earthquake. For rectangular deep type of column staging, value of sloshing displacement is high compare to other types and for rectangular wide type of column staging, sloshing displacement is less.

Bhandiwad and Dodamani (2022) dealt with studying performance of porous baffles in a sloshing tank. Analytical investigations were carried out to examine the performance of two vertical porous baffles placed at equal intervals in the rectangular sloshing tank to suppress and control the liquid sloshing variation under a range of excitation frequencies, which cover up to five sloshing mode frequencies. Three different porosities of 4.4%, 6.8%, and 9.2% were considered in the sloshing tank to study the effectiveness of porosities under tank sway motion. The tank with relatively low porous baffles of porosities 4.4%, 6.8%, and 9.2% more effectively reduces the amplification of sloshing motion at first resonant mode.

Chunfeng Zhao et al. (2015) worked on sloshing and vibration mitigation of water storage tank of AP1000. The influence of fluid–structure interaction on the dynamic behaviour of water tank and effects of water sloshing in reducing seismic response of the shield building were investigated considering six cases of water heights in the water tank. The Arbitrary Lagrangian Eulerian algorithm was used to simulate the fluid sloshing and oscillation of water tank under a typical earthquake occurred at nuclear power plant. The numerical results revealed that the fluid–structure interaction effects of various water levels have significant effects on the motion and structural response of water tank, and not all the water levels can reduce the seismic response of shield building.

Dona Rose et al. (2015) dealt in studying overhead water tanks subjected to dynamic loads. Tanks of various capacities with different staging height were modelled using ANSYS software

for tank full and half level condition considering the sloshing effect along with hydrostatic effect. The time history analysis of the water tank was carried out by using earthquake acceleration records of El Centro. From the analysis it is observed that the peak displacement and base shear from the time history analysis increases with staging heights, the displacement for half-filled tanks is lesser than the displacement for tanks with full capacity, base shear for half capacity tanks are lesser than that for full capacity tanks under same staging condition.

Helou (2014) dealt in studying seismic induced forces on rigid water storage tanks where two models of the same tank were constructed. One model focused on a static treatment which considered the hydrostatic loads only while the second model was constructed in accordance with the ACI recommendations for seismic analysis. The tank with no added mass shows a fundamental frequency of 78 Hertz while the same tank with the added masses shows a slightly lower fundamental frequency of 73 Hertz. This was due to the moderate increase in mass but with no obvious increase in stiffness. It was observed that the maximum circumferential moment shifted its position; instead of being at the base of the tank it happened at the height of the impulsive masses and inclusion of the convective water mass resulted moderate increase in any typical moment value. In case tanks were modelled with elastic foundation, soil flexibility increased both the circumferential and the longitudinal stresses and accordingly the plastic strains and radial deformations.

Investigation of sloshing response in rectangular container with flexible baffle were carried out by **Bang-Fuh Chen et al. (2018)**. ANSYS was used to simulate the sloshing response in a rectangular container with bottom mounted flexible baffles and the simulated results of the free surface displacement and the resonant sloshing frequency of a tank with flexible baffles were compared with those of a tank with rigid baffles. From the study it is seen that the sloshing response is significantly affected by the geometry and location of the flexible baffles and wave displacements are significantly influenced by the height and thickness of the baffle. Power spectral analyses were also made to see the sloshing resonance frequency affected by the flexible baffle interaction with sloshing fluids.

Seismic behaviour of elevated storage reservoir was studied by **Nerkar and Nayak (2016)** by finite element method. Circular and rectangular elevated water tank with different water levels were considered for study and static as well as dynamic analyses of time history were performed

on the tanks. Base shear variation, time period for different mode shapes, time history for different earthquakes were calculated by using SAP2000. From the study it is seen that as water level increases base shear for tank also increases and the base shear for circular reservoir is more than rectangular reservoir for every water level. Time period variation for 100% filled water level is greater than 0% water level and as water level increases time period for respective reservoir increases. Displacement of reservoir with empty condition is minimum while for full reservoir displacement is maximum and displacement for circular reservoir is minimum than that of rectangular reservoir.

Chaithra et al. (2017) dealt in analysis of soil-structure interaction on response of tanks filled with fluid and the tank, fluid and soil were modelled using finite element method. Tank was subjected to one far field and one near fault ground accelerations and the displacement, base shear and the pressure in the fluid were obtained. Three types of soil with different flexibility were considered to study the soil-structure interaction effect. The structure was subjected to two earthquake ground motions, one far field i.e., El Centro earthquake and one near fault Imperial Valley ground motions. From the study it is concluded that soil-structure interaction has negligible effect on response of tank resting on hard soil but it has significant effect on the response of the tank and fluid when resting on soft soil.

Capillary effect on the sloshing of a fluid in a rectangular tank submitted to sinusoidal vertical dynamical excitation was carried out by **Bachir and Ouerdia (2014)** in order to derive practical solutions to problems faced in several engineering considering tank containing a fluid with a free surface was submitted to gravity and capillary forces and subjected to external dynamic excitation. It was observed that with increase of the sloshing Eigen frequencies wave lengths decreased. The analysis of sloshing in stable regions showed nonlinear effects depending on the frequency and the amplitude of the dynamic excitation.

Djelloul and Djermane (2019) dealt in studying the effect of geometric imperfection on the dynamic of elevated water tanks. It was aimed to demonstrate the local geometric imperfection effect on dynamic buckling of elevated water tank using the 3D finite element technique to study the seismic response of perfect and imperfect elevated water tank taking into account the effect of fluid structure interaction, wall flexibility, local geometric imperfection, nonlinear time history analysis, material and geometric nonlinearity. It is observed that the convective frequency remains

the same for the perfect and imperfect elevated tank. The maximum deformations are located along the support-tank interface region.

Virella et al. (2008) had carried out linear and nonlinear 2D finite element analysis of sloshing modes and pressures in rectangular tanks subject to horizontal harmonic motions. The influence of nonlinear wave theory on the sloshing natural periods and their modal pressure distributions were investigated for rectangular tanks under the assumption of two-dimensional behaviour. Natural periods and mode shapes were computed and compared for both linear wave theory and nonlinear wave theory models, using the finite element package ABAQUS. Pressure distributions acting on the tank walls were obtained for the first three sloshing modes using both linear and nonlinear wave theory. It is found that the non-linearity does not have significant effects on the natural sloshing periods. For the sloshing pressures on the tank walls, different distributions were found using linear and nonlinear wave theory models. The linear wave theory conservatively estimated the magnitude of the pressure distribution, whereas larger pressures resultant heights were obtained when using the nonlinear theory. It can be concluded that the non-linearity of the surface wave amplitude does not have major effects on the pressure distribution on the walls of rectangular tanks.

Rubesh and Ponnusamy (2022) dealt with numerical modelling of nonlinear baffles on sloshing suppression of rectangular tanks under horizontal excitation. The baffles were placed horizontally in the middle of the liquid container. The two-dimensional numerical analyses were carried out utilizing the VoF method assuming that the flow was laminar. The nonlinear baffles were tested for different excitation amplitudes, fill levels, excitation frequencies and submergence depths. From the analyses, it is found that the presence of nonlinear baffles reduced the sloshing pressure greater than the conventional horizontal baffle. The baffle designed using a negative amplitude cosine curve (NACB) possessed a superior sloshing suppression than other nonlinear baffles. With increased excitation amplitudes at resonance, the NACB baffles provided better sloshing suppression than conventional horizontal baffles. NACB baffles offered better sloshing suppression even at higher submergence depths. The nonlinear baffles of various shapes possessed a superior performance in suppressing sloshing than the conventional horizontal baffles.

Sanapala et al. (2017) had carried out numerical simulations to investigate the sloshing dynamics of a partially filled rectangular container subjected to vertical harmonic as well as seismic excitations. Parametric sloshing in a partially filled 2D rectangular tank was numerically investigated under the influence of vertical excitation. The free surface displacement, magnitude

of velocity, vorticity, pressure distribution and forces on the side walls were analyzed. The results of numerical simulations can be outlined as; (i) under parametric resonance, the slosh response of the liquid depicted a nonlinear behaviour, when the imposed excitation frequency was in the neighbourhood of twice that of natural sloshing frequency, for certain amplitudes of excitation, (ii) under coupled seismic excitation, the optimal baffle position and width was found to be effective in controlling the total response from the resultant slosh wave amplitude.

Quantitative risk analysis of oil storage facilities in seismic areas was carried out by **Fabbrocino et al. (2005)** by a representative case study regarding an oil storage plant with a number of atmospheric steel tanks containing flammable substances. It was observed that quantitative probabilistic seismic risk analysis (QpsRA) can be successfully carried out if seismic fragility analyses of critical components are developed in terms of limit states that may trigger industrial accidents (i.e. hazardous materials release).

Yanmin Guan et al. (2020) dealt in numerical investigation on the effect of baffles on liquid sloshing in 3D rectangular tanks based on nonlinear boundary element method. The numerical simulation of liquid sloshing in the three-dimensional tanks under horizontal excitation and roll excitation was carried out, and the inhibition effect of different baffles on the sloshing phenomenon was investigated. The numerical calculations were carried out by the nonlinear Boundary Element Method (BEM) with Green's theorem based on the potential flow, which was conducted with the governing equation corresponding to the boundaries of each region. The vertical baffle is a more effective way to reduce the sloshing amplitude when the tank is under a horizontal harmonic excitation while the horizontal baffle is a more effective way when the tank is under a roll excitation. The amplitude of free surface elevation at right tank wall decreases with the increasing of the horizontal baffle length and the vertical baffle height.

2.3 Critical Observations

Based on the review of literatures, some critical observations are described below-

- Finite element analysis is recognized to be one of the best numerical tools for dynamic analysis of fluid containers.
- The water within the tank is expressed by several variables such as displacement, velocity potential and pressure. Out of these variables, it is advantageous to model the fluid within the tank by pressure, as the number of degrees of freedom per mode in this case reduced to one.

- The pressure-based formulation has certain advantages in the computational aspect compared to the velocity potential and the displacement-based formulations, as the number of unknown per node is only one and hence it requires less storage and time.
- In pressure-based formulation, fluid satisfies irrotational condition automatically. Otherwise, a complicated condition needs to be incorporated to satisfy the irrotationality condition.
- For dynamic analysis of fluid container, the fluid within the tank may be modelled either as compressible or incompressible fluid.
- 3-D modelling and analyses give more realistic response than 2-D analysis but it requires more space and time. However, up to a certain limit of width to length ratio (B/L) the performance of tank in 2-D and 3-D analyses is almost similar.
- Sloshing Characteristics and hydrodynamic pressure exerted by the fluid on the tanks are influenced by tank parameters such as fluid depth, tank shape, baffle parameters such as size, shape and locations, external excitation and so on.
- The analysis of water tank is a perfect example of fluid-structure interaction and if considered in the analysis provides proper response of the tanks.
- Linear and nonlinear wave theory may be used to model the tanks. However, for water with comparatively smaller depth, linear wave theory is sufficient.

OBJECTIVE- The objective of present thesis is to study the dynamic behavior of rectangular fluid container with elastic baffle.

2.4 Scope of Present Work

- Finite element formulation of fluid within the container
- Finite element formulation of elastic baffle
- Numerical simulation of interaction between fluid and elastic baffle
- Evaluation of responses of fluid-baffle couple systems using average Newmark's Integration method.

CHAPTER-3
THEORITICAL FORMULATION

3.1 Theoretical Formulation for Fluid

The state of stress for a fluid which follows Newton's law is defined by an isotropic tensor as

$$T_{ij} = -p\delta_{ij} + T'_{ij} \tag{3.1}$$

Where, T_{ij} is total stress, T'_{ij} is viscous stress tensor which depends only on the rate of change of deformation in such a manner that the value becomes zero when the fluid is under rigid body motion or rest. The variable p is defined as hydrodynamic pressure whose value is independent explicitly on the rate of deformation and δ_{ij} is Kronecker delta. For an isotropic linear elastic material, T'_{ij} can be written as

$$T'_{ij} = \lambda \Delta \delta_{ij} + 2\mu D_{ij} \tag{3.2}$$

Where, μ and λ are two material properties (constants). μ is the first coefficient of viscosity or simply viscosity and (λ+2μ/3) is the second coefficient of viscosity or bulk viscosity. D_{ij} is the rate of change of deformation tensor and can be written as

$$D_{ij} = \frac{1}{2}\left(\frac{\partial v_i}{\partial y_j} + \frac{\partial v_j}{\partial x_i}\right) and\ \Delta = D_{11} + D_{22} + D_{33} \tag{3.3}$$

Thus, the total stress tensor becomes

$$T_{ij} = -p\delta_{ij} + \lambda \Delta \delta_{ij} + 2\mu D_{ij} \tag{3.4}$$

For fluid which is compressible, bulk viscosity ($\lambda+2\mu/3$) becomes zero. Thus, equation (3.4) reduced to

$$T_{ij} = -p\delta_{ij} - \frac{2\mu}{3}\Delta\delta_{ij} + 2\mu D_{ij} \tag{3.5}$$

If the viscosity of fluid is neglected, equation (3.5) becomes

$$T_{ij} = -p\delta_{ij} \tag{3.6}$$

Generalized Navier-Stokes's equations of motion are given by

$$\rho\left(\frac{\partial v_i}{\partial t} + v_j \frac{\partial v_i}{\partial x_j}\right) = \frac{\partial T_{ij}}{\partial x_j} + \rho B_i \tag{3.7}$$

Where, B_i is the body force and ρ is the mass density of fluid. Substituting equation (3.6) in equation (3.7) the following relations are obtained

$$\rho\left(\frac{\partial v_i}{\partial t} + v_j \frac{\partial v_i}{\partial x_j}\right) = \rho B_i - \frac{\partial p}{\partial x_i} \tag{3.8}$$

Where u and v are the velocity components along x and y axes respectively and f_x and f_y are body forces along x and y direction respectively and if the convective terms are neglected, the equation of motion becomes

$$\frac{1}{\rho}\frac{\partial p}{\partial x} + \frac{\partial u}{\partial t} = f_x \tag{3.9}$$

$$\frac{1}{\rho}\frac{\partial p}{\partial y} + \frac{\partial v}{\partial t} = f_y \tag{3.10}$$

Neglecting the body forces, equations (3.9) and (3.10) become

$$\frac{1}{\rho}\frac{\partial p}{\partial x} + \frac{\partial u}{\partial t} = 0 \tag{3.11}$$

$$\frac{1}{\rho}\frac{\partial p}{\partial y} + \frac{\partial v}{\partial t} = 0 \tag{3.12}$$

The continuity equation of fluid in two dimensions is expressed as:

$$\frac{\partial p}{\partial t} + \rho c^2\left(\frac{\partial u}{\partial x} + \frac{\partial v}{\partial y}\right) = 0 \tag{3.13}$$

Where, c is the acoustic wave speed in fluid. Now, differentiating equation (3.11) and (3.12) with respect to x and y respectively, the following relations are obtained

$$\frac{1}{\rho}\frac{\partial^2 p}{\partial x^2} + \frac{\partial}{\partial x}\left(\frac{\partial u}{\partial t}\right) = 0 \tag{3.14}$$

$$\frac{1}{\rho}\frac{\partial^2 p}{\partial y^2} + \frac{\partial}{\partial y}\left(\frac{\partial v}{\partial t}\right) = 0 \tag{3.15}$$

Adding equation (3.14) and equation (3.15) the following expression is finally arrived.

$$\frac{1}{\rho}\frac{\partial^2 p}{\partial x^2} + \frac{1}{\rho}\frac{\partial^2 p}{\partial y^2} + \frac{\partial}{\partial x}\left(\frac{\partial u}{\partial t}\right) + \frac{\partial}{\partial y}\left(\frac{\partial v}{\partial t}\right) = 0 \tag{3.16}$$

Differentiating equation (3.13) with respect to time, the following expression can be obtained.

$$\frac{\partial^2 p}{\partial t^2} + \rho c^2\left\{\left(\frac{\partial}{\partial x}\left(\frac{\partial u}{\partial t}\right) + \frac{\partial}{\partial y}\left(\frac{\partial v}{\partial t}\right)\right\} = 0 \tag{3.17}$$

Thus, from equation (3.16) and equation (3.17), one can find the following expression**:**

$$\frac{1}{\rho}\frac{\partial^2 p}{\partial x^2} + \frac{1}{\rho}\frac{\partial^2 p}{\partial y^2} - \frac{1}{\rho c^2}\left(\frac{\partial^2 p}{\partial t^2}\right) = 0 \tag{3.18}$$

Simplifying the equation (3.18), the equation for compressible fluid may be obtained as

$$\nabla^2 p(x,y,t) = \frac{1}{c^2}\ddot{p}(x,y,t) \tag{3.19}$$

If, the compressibility of fluid is neglected the equation (3.19) will be modified as

$$\nabla^2 p(x,y,t) = 0 \tag{3.20}$$

The pressure distribution in the fluid domain may be obtained by solving equation (3.19) with the following boundary conditions. A typical geometry of tank-water system is shown in Fig-3.1.

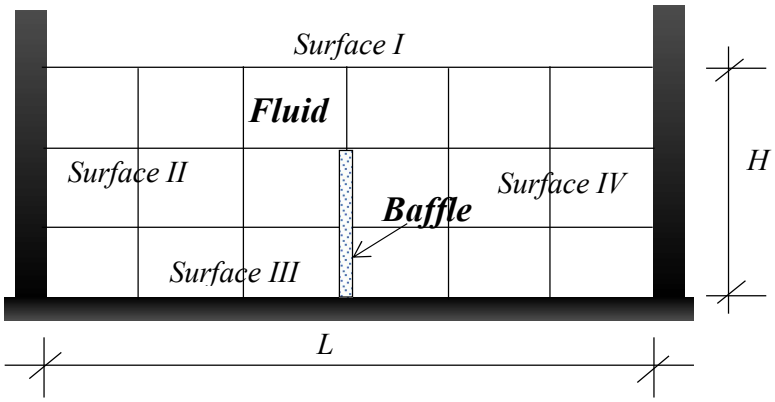

Fig-3.1 Geometry of fluid-tank -baffle system

i) *At surface I*

Considering the effect of surface wave of the fluid, the boundary condition of the free surface is taken as

$$\frac{1}{g}\ddot{p} + \frac{\partial p}{\partial y} = 0 \tag{3.21}$$

ii) *At surface II* and *surface IV*

At water-tank wall interface, the pressure should satisfy

$$\frac{\partial p}{\partial n}(0,y,t) = \rho_f a e^{i\omega t} \tag{3.22}$$

Where $ae^{i\omega t}$ is the horizontal component of the ground acceleration in which, ω is the circular frequency of vibration and $i = \sqrt{-1}$, n is the outwardly directed normal to the element surface along the interface. ρ_f is the mass density of the fluid.

iii) *At surface III*

This surface is considered as rigid surface and thus pressure should satisfy the following condition

$$\frac{\partial p}{\partial n}(x,0,t)=0.0 \tag{3.23}$$

3.2 Finite Element Formulation for Fluid domain

By using Galerkin approach and assuming pressure to be the nodal unknown variable, the discretized form of equation (3.19) may be written as

$$\int_{\Omega} N_{rj}\left[\nabla^2 \sum N_{ri} p_i - \frac{1}{c^2}\sum N_{ri}\ddot{p}_i\right] d\Omega = 0 \tag{3.24}$$

Where, N_{rj} is the interpolation function for the reservoir and Ω is the region under consideration. Using Green's theorem equation (3.24) may be transformed to

$$-\int_{\Omega}\left[\frac{\partial N_{rj}}{\partial x}\sum\frac{\partial N_{ri}}{\partial x}p_i+\frac{\partial N_{rj}}{\partial y}\sum\frac{\partial N_{ri}}{\partial y}p_i\right]d\Omega-\frac{1}{c^2}\int_{\Omega}N_{rj}\sum N_{ri}\,d\Omega\;\ddot{p}_i+\int_{\Gamma}N_{rj}\sum\frac{\partial N_{rj}}{\partial n}d\Gamma\;p_i=0 \tag{3.25}$$

in which i varies from 1 to total number of nodes and Γ represents the boundaries of the fluid domain. The last term of the above equation may be written as

$$\{F\} = \int_{\Gamma} N_{rj}\frac{\partial p}{\partial n}d\Gamma \tag{3.26}$$

The whole system of equation (3.25) may be written in a matrix form as

$$\left[\bar{E}\right]\left\{\ddot{P}\right\}+\left[\bar{G}\right]\{P\}=\{F\ \} \tag{3.27}$$

where,

$$\left[\bar{E}\right]=\frac{1}{C^2}\sum\int_{\Omega}\left[N_r\right]^T\left[N_r\right]d\Omega \tag{3.28}$$

$$\left[\bar{G}\right]=\sum\int_{\Omega}\left[\frac{\partial}{\partial x}\left[N_r\right]^T\frac{\partial}{\partial x}\left[N_r\right]+\frac{\partial}{\partial y}\left[N_r\right]^T\frac{\partial}{\partial y}\left[N_r\right]\right]d\Omega \tag{3.29}$$

$$\left[F\right]=\sum\int_{\Gamma}\left[N_r\right]^T\frac{\partial p}{\partial n}d\Gamma=\left\{F_I\right\}+\left\{F_{II}\right\}+\left\{F_{III}\right\}+\left\{F_{IV}\right\} \tag{3.30}$$

Here the subscript *I, II, III and IV* stand for different surface conditions. For surface wave, the equation (3.21) may be written in finite element form as

$$\left\{F_I\right\}=-\frac{1}{g}\left[R_f\right]\{\ddot{p}\} \tag{3.31}$$

In which,

$$\left[R_f\right]=\sum_{\Gamma_f}\int\left[N_r\right]^T\left[N_r\right]d\Gamma \tag{3.32}$$

At the *Surface II and Surface IV* if $\{a\}$ is the vector of nodal accelerations of generalized coordinates, $\{F_{II}\}$ and $\{F_{IV}\}$ may be expressed as

$$\left\{F_{II}\right\}\ and\ \left\{F_{IV}\right\}=-\rho\left[R_{II}\right]\{a\}\ \ and\ \ -\rho\left[R_{IV}\right]\{a\}\ \ respectively \tag{3.33}$$

in which,

$$\left[R_{II}\right]\ and\ \left[R_{IV}\right]=\sum_{\Gamma_{II\ and\ IV}}\int\left[N_r\right]^T\left[N_r\right]d\Gamma \tag{3.34}$$

At *Surface III*

$$\left\{F_{III}\right\}=0 \tag{3.35}$$

After substitution all terms the equation (3.27) becomes

$$[E]\{\ddot{P}\}+[G]\{P\}=\{F_r\} \tag{3.36}$$

where,

$$\left[E\right]=\left[\bar{E}\right]+\frac{1}{g}\left[R_I\right] \tag{3.37}$$

$$\left\{F_r\right\}=-\rho_f\left[R_{II}\right]\{a\}-\rho_f\left[R_{IV}\right]\{a\} \tag{3.38}$$

For any given acceleration at the fluid-structure interface, the equation (3.36) is solved to obtain the hydrodynamic pressure within the fluid.

3.3 Theoretical Formulation for Elastic Baffle

The baffle is discretized using Bernoulli beam elements with transverse and rotational deformations as shown in fig-3.2.

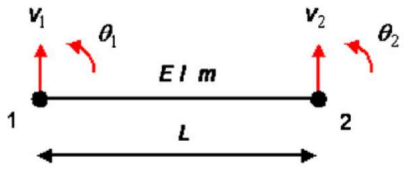

Fig-3.2 A Bernoulli Beam Element

Stiffness and mass matrices of baffle are represented as *[k]* and *[m]* respectively. The mass per unit length of the structure element is $m = \rho A$, where ρ and A are the mass density of baffle material and the cross-sectional area of the beam element. The structural displacements and accelerations within an element are approximated using their nodal values as given by

$$v(x,t) = [N_b]\{d\} \; and \; \ddot{v}(x,t) = [N_b]\{\ddot{d}\} \tag{3.39}$$

Where, *{d}* is the vector of time dependent nodal displacements and $[N_b]$ is interpolation function and expressed as

$$[N_b] = [N_{b1}\; N_{b2}\; N_{b3}\; N_{b4}] \; and \; \{d\} = \begin{bmatrix} V_1(t) \\ \theta_1(t) \\ V_2(t) \\ \theta_2(t) \end{bmatrix} \tag{3.40}$$

and

$$\left.\begin{aligned} N_{b1} &= 1 - 3\left(\frac{x}{l}\right)^2 + 2\left(\frac{x}{l}\right)^3 \\ N_{b2} &= x\left(1 - \frac{x}{l}\right)^2 \\ N_{b3} &= 3\left(\frac{x}{l}\right)^2 - 2\left(\frac{x}{l}\right)^3 \\ N_{b4} &= \frac{x^2}{l}\left(\frac{x}{l} - 1\right) \end{aligned}\right\} \tag{3.41}$$

l is length of the member.

The consistent element mass matrix for the beam element can then be written as

$$m_{ij} = \int_0^l m N_{bi}(x) N_{bj}(x)\, dx \tag{3.42}$$

Assuming a linear elastic material with the stress-strain relation **{σ} = [E]{ε}** and a strain-displacement relation **{ε} = [B]{d}**, the elemental stiffness matrix can be obtained from the following relation:

$$k_{ij} = \int_0^l B^T E\, B\, dx \tag{3.43}$$

On integration using the element shape functions, the elemental stiffness *[k]* and consistent mass matrices *[m]* are found to be as follows:

$$[m] = \frac{ml}{420}\begin{bmatrix} 156 & 22l & 54 & -13l \\ 22l & 4l^2 & 13l & -3l^2 \\ 54 & 13l & 156 & -22l \\ -13l & -3l^2 & -22l & 4l^2 \end{bmatrix} \quad and \quad [k] = \frac{EI}{l^3}\begin{bmatrix} 12 & 6l & -12 & 6l \\ 6l & 4l^2 & -6l & 2l^2 \\ -12 & -6l & 12 & -6l \\ 6l & 2l^2 & -6l & 4l^2 \end{bmatrix} \tag{3.44}$$

The finite element discretized equation for dynamics excitations can now be written in the familiar form given below

$$[m]\{\ddot{d}\} + [k]\{d\} = \{F_{ext}\} \tag{3.45}$$

Where, $\{F_{ext}\}$ is external dynamic force

3.4 Coupling of Fluid-Baffle system

In fluid-baffle interaction problems, the fluid and baffle do not vibrate as separate systems under dynamic excitations, rather they act together in a coupled way. Therefore, the baffle-fluid interaction problem has to be dealt in a coupled way. In the present study, a direct coupling approach is developed to get the responses of baffle-fluid coupled system under external excitations. The discrete baffle equation may be written in the familiar form given below. No damping is considered in the motion of baffle.

$$[m]\{\ddot{d}\}+[k]\{d\}-[Q]\{P\}=\{F_{ext}\} \tag{3.46}$$

Here, [Q] is coupling term arises to satisfy the compatibility condition at the tank baffle-fluid interfaces and is expressed in eq. (3.47). The term [Q]{P} comes to take care of the additional force due to the hydrodynamic pressure within the water, adjacent to the baffle walls. Similarly, in eq. (3.48), the term $[Q^T\{\ddot{d}\}]$, is essential to take care of the effect of additional pressure due to the acceleration of baffle walls, as the flexibility of the baffle walls is considered in present study.

$$\int_{\Gamma_s} N_s^T npd\Gamma = \left(\int_{\Gamma_s} N_s^T nN_f d\Gamma\right) p = [Q]\{p\} \tag{3.47}$$

Where, n is the direction vector of the normal to the fluid-baffle interface. N_s and N_f are the shape functions of baffle wall and fluid at the interface are respectively. Similarly, the finite element equation for the fluid with elastic baffle may be written using eq. (3.36) as

$$[\mathrm{E}]\{\ddot{\mathrm{P}}\}+[\mathrm{G}]\{\mathrm{P}\}+[\mathrm{Q}^{\mathrm{T}}]\{\ddot{\mathrm{d}}\}=\{\mathrm{F_r}\} \tag{3.48}$$

Now, the system of equation (3.46) and (3.48) are coupled in a second-order ordinary differential equations, which defines the coupled fluid-structure system completely. These equations may be written in a combined form as

$$\begin{bmatrix} m & 0 \\ Q^T & E \end{bmatrix}\begin{Bmatrix} \ddot{d} \\ \ddot{P} \end{Bmatrix}+\begin{bmatrix} k & -Q \\ 0 & G \end{bmatrix}\begin{Bmatrix} d \\ P \end{Bmatrix}=\begin{Bmatrix} F_{ext} \\ F_r \end{Bmatrix} \tag{3.49}$$

To solve Equation (3.49), Newmark's average integration method has been adopted and is given by

$$\{u\}_{i+1}=\{u\}_i+\Delta t\{\dot{u}\}_i+\frac{\Delta t^2}{2}[(1-2\beta)\{\ddot{u}\}_i+2\beta\{\ddot{u}\}_{i+1}] \tag{3.50}$$

$$\{\dot{u}\}_{i+1}=\{\dot{u}\}_i+\Delta t[(1-\gamma)\{\ddot{u}\}_i+\gamma\{\ddot{u}\}_{i+1}] \tag{3.51}$$

Here, β and γ are chosen to control stability and accuracy. It is evident from the literature that the integration scheme is unconditionally stable if $2\beta \geq \gamma \geq 0.5$.

CHAPTER 4

RESULTS AND DISCUSSIONS

4.1 Free Vibration Analysis

In this section, changes in time period have been observed by changing various parameters like length and height of tank, baffle height, thickness and baffle position & height of fluid within the tank. Variations in time period are shown in graphical form for three different modes and the graphs are plotted for three time period against the different parameters.

Here, R_T – Reservoir Time Period

Int_T – Coupled system Time Period

4.1.1 Change in Tank length keeping Baffle in middle

The tank with 5m fluid height and 4m baffle height with 100mm baffle wall is considered in this section. The length of the tank has been changed keeping the baffle in the middle of the tank always. The graphs are plotted for changes in time periods (TP) with respect to Length(L) and Fluid height(H)/Tank length(L) ratios (H/L).

a) Graphs for Tank Length vs Time period:

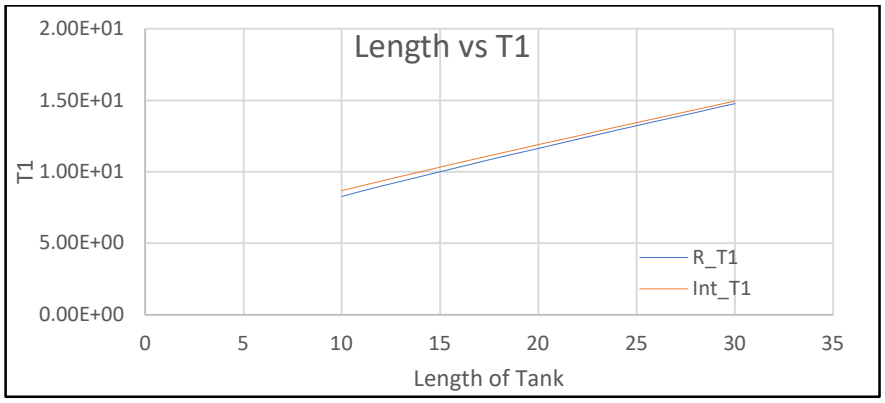

Fig-4.1 First Time Period for different length of tank

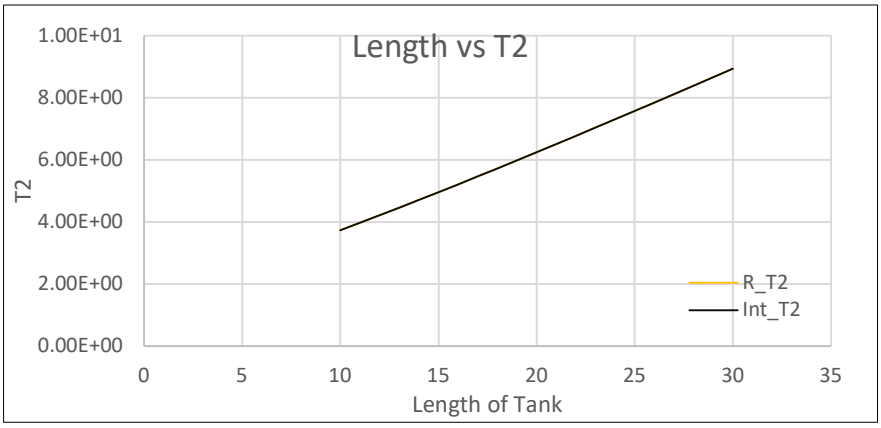

Fig-4.2 Second Time Period for different length of tank

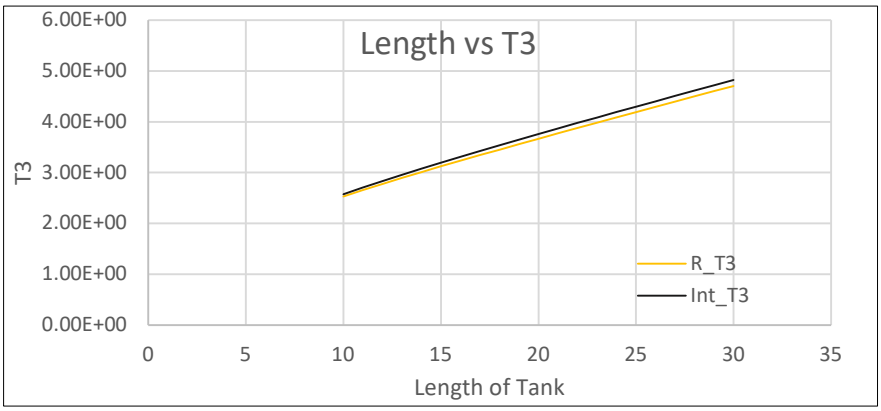

Fig-4.3 Third Time Period for different length of tanks

It is observed that time period of the tank with or without baffle increases with increase in tank length. It is also seen that with increase in the length, for first mode the lines for tank time period and coupled system time period converges towards each other that means the difference between the time period decreases with increase in tank length (fig 4.1), whereas for third mode both lines are diverging from each other that means the difference between the time period increases with the increase of tank length (fig 4.3). But for the second mode no difference is observed for both the time period (fig 4.2).

b) Graphs for H/L vs Time period:

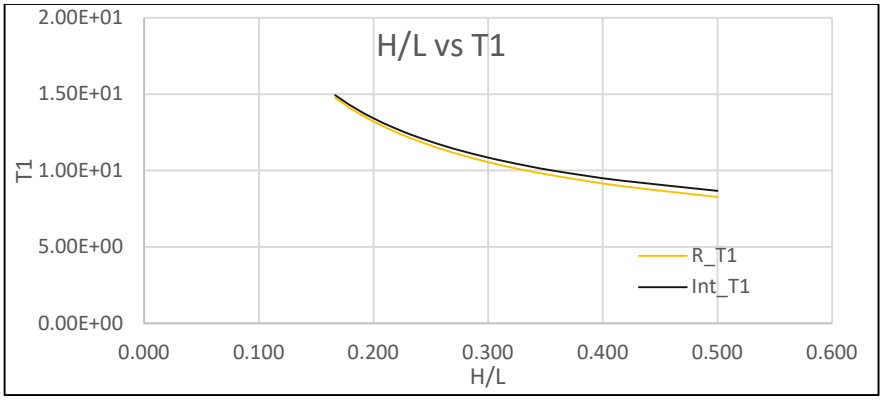

Fig-4.4 First Time Period for different H/L ratios

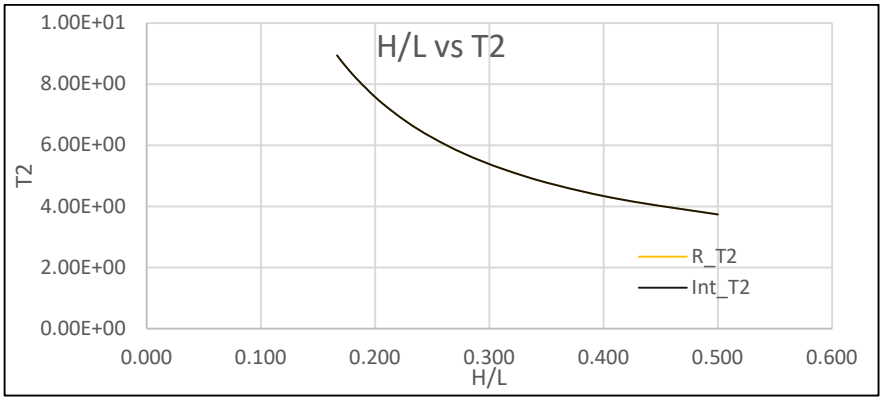

Fig-4.5 Second Time Period for different H/L ratios

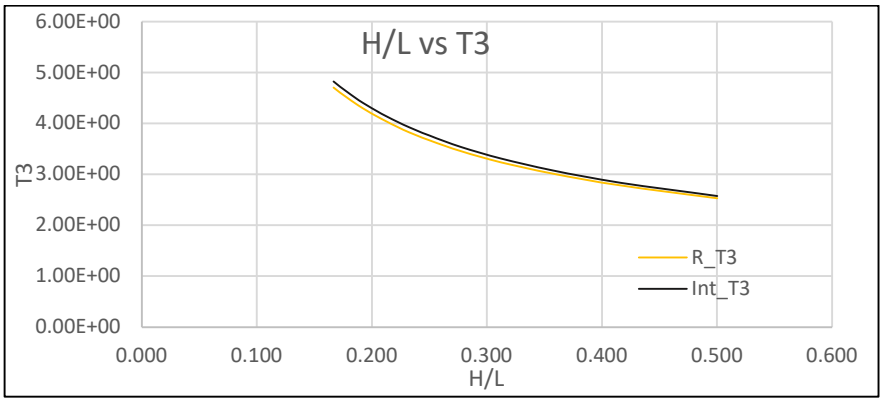

Fig-4.6 Third Time Period for different H/L ratios

For increasing H/L ratio, time period of tank and tank-baffle coupled system decreases. Also, with increase in H/L ratio for first mode the lines are diverging in nature (fig 4.4), whereas for third mode the lines are converging (fig 4.6). Here also there is no difference is observed in second mode for both the time period (fig 4.5).

4.1.2 Change in Fluid height

Here for a 12m tank with baffle wall of 100mm thickness and baffle wall positioned always at middle, fluid height has been changed. But to keep the H/l ratio similar to previous case baffle height (l) has also been changed. The graphs are plotted for changes in time periods with respect to Fluid height(H) and Fluid height(H)/Tank length(L) ratio (H/L ratio).

a) Graphs for Fluid Height vs Time period:

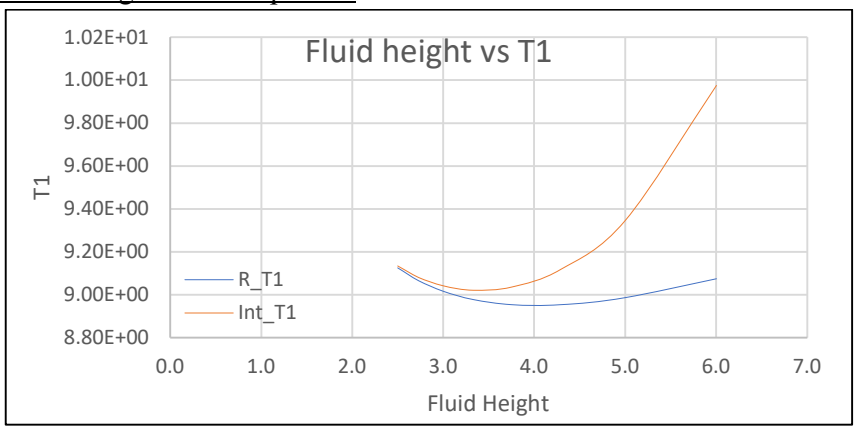

Fig-4.7 First Time Period for different fluid height

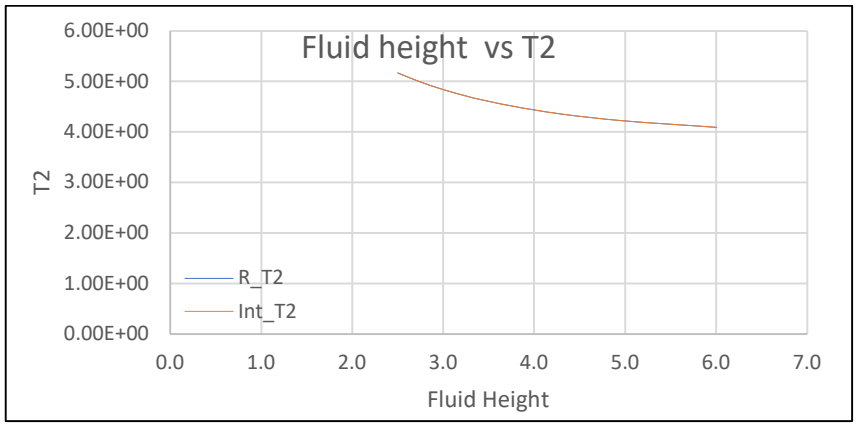

Fig-4.8 Second Time Period for different fluid height

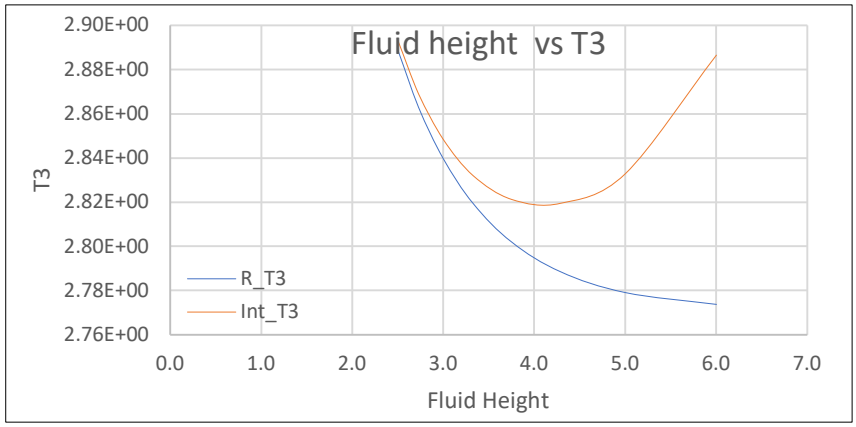

Fig-4.9 Third Time Period for different fluid height

It has been observed that for first and third mode the variation in reservoir time period w.r.t fluid height is less as compared to second mode. It has also been found that for first and third mode time period of tank diverges with coupled time period with increase in fluid height. For second mode, no variation is observed between reservoir time period and coupled system time period (fig 4.8).

b) Graphs for H/L vs Time period:

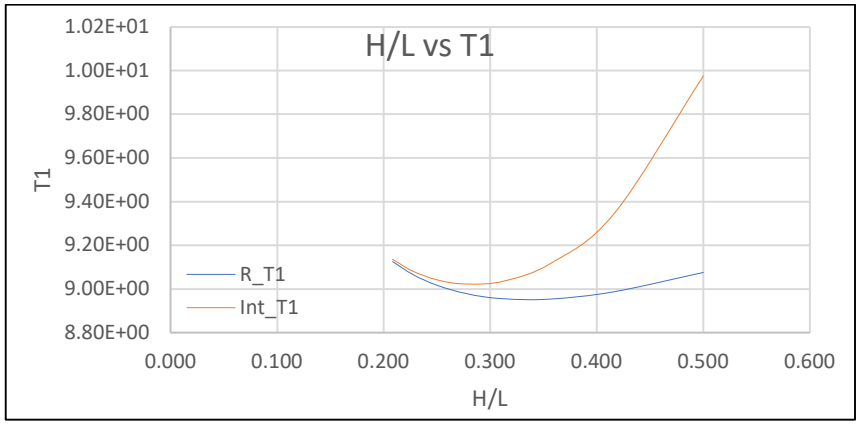

Fig- 4.10 First Time Period for different H/L ratios

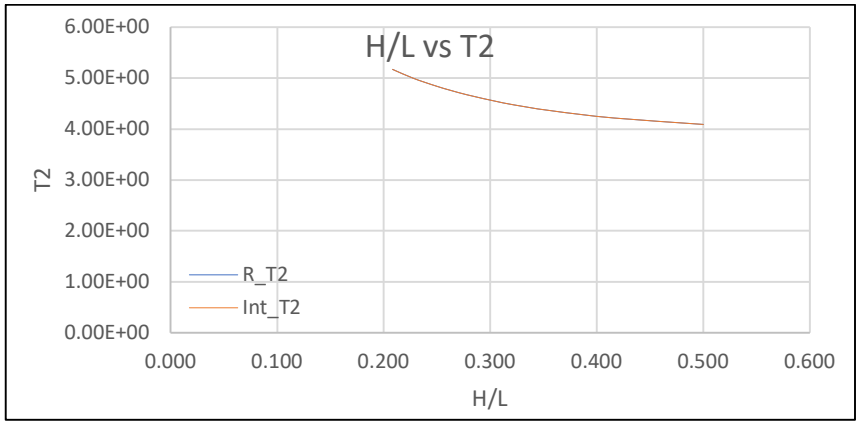

Fig- 4.11 Second Time Period for different H/L ratios

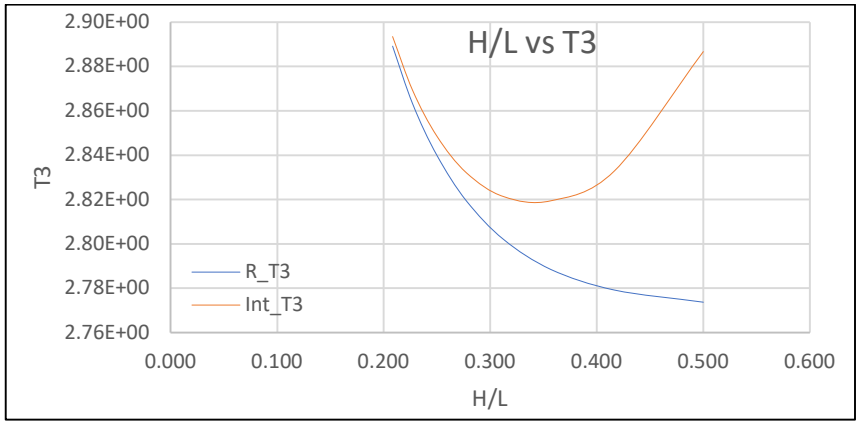

Fig-4.12 Third Time Period for different H/L ratios

It has been observed that first and third fundamental time period T1 and T3 for coupled system increases with increase in H/L ratio, but the value of second fundamental time period T2 decreases with increase in H/L ratio. The impact of baffle is less significant for T1 and T3 when H/L ratio comes closer to 0.2. And there is no difference is observed between reservoir time period and coupling time period for second mode (fig 4.11).

4.1.3 Change in Baffle position

Here the baffle has been positioned in different location of a 20m tank which has 5m of fluid height, 4m of baffle height and 100mm thick baffle wall. The variation in time periods has been observed which has plotted on graph below.

a) Graphs for Baffle position vs Time period:

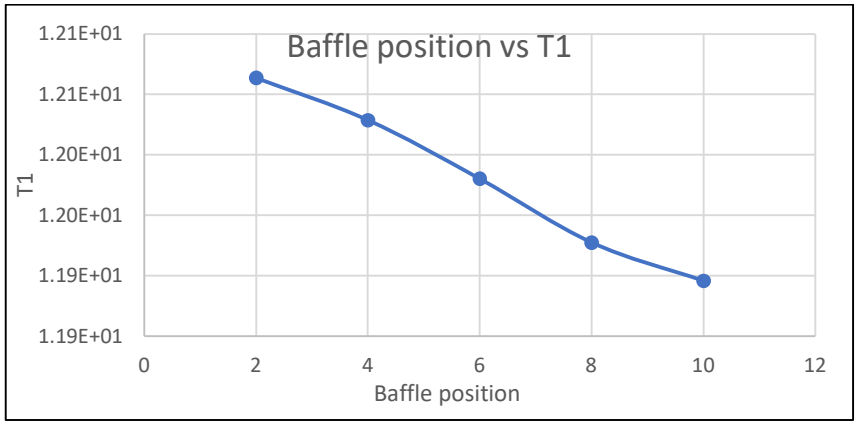

Fig-4.13 First Time Period for different baffle position

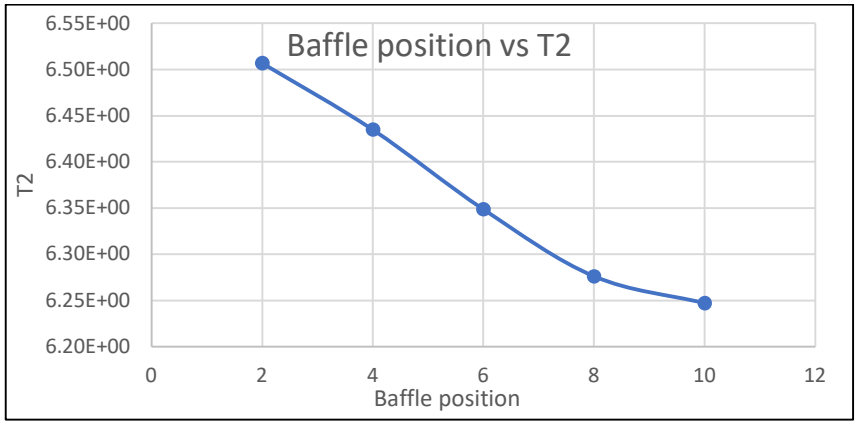

Fig-4.14 Second Time Period for different baffle position

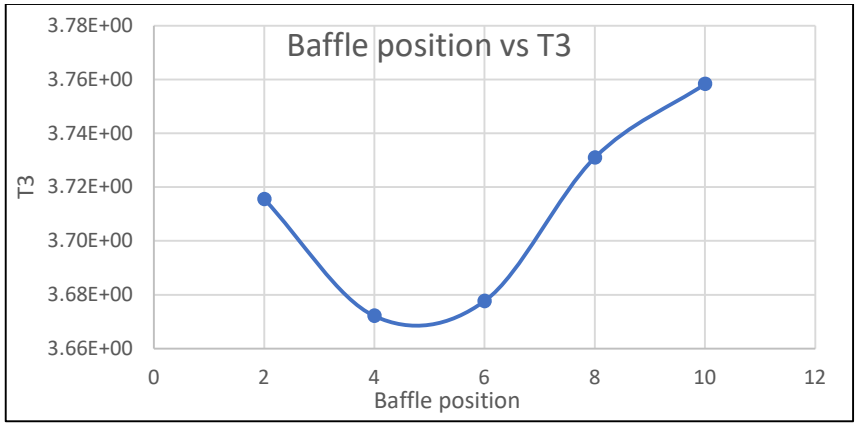

Fig-4.15 Third Time Period for different baffle position

Here for first and second mode time period is decreasing with the baffle wall moving towards middle of the tank. But for the third mode it has been observed that position up to one fourth length of tank time period decreases and after that time period increases and attains maximum value at the middle of the tank (fig 4.15).

4.1.4 Change in Baffle height

Here for a 12m tank with 5m fluid height, 200mm baffle thickness and baffle positioned at middle, the graphs are plotted for time periods against different baffle height.

a) Graphs for Baffle height vs Time period:

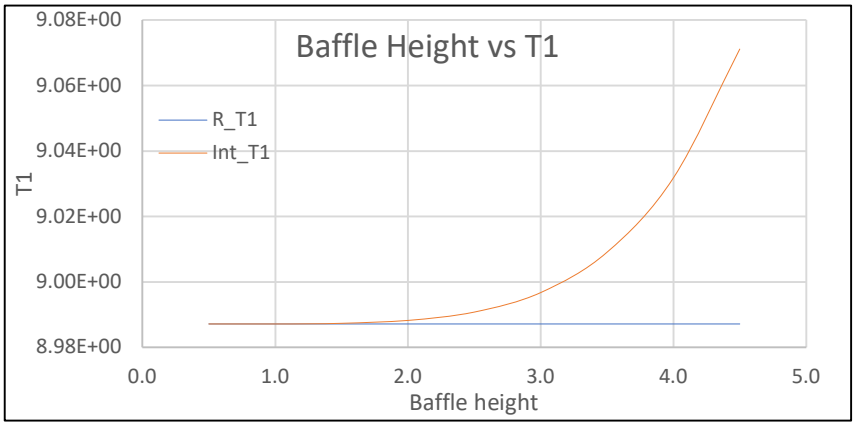

Fig-4.16 First Time Period for different baffle height

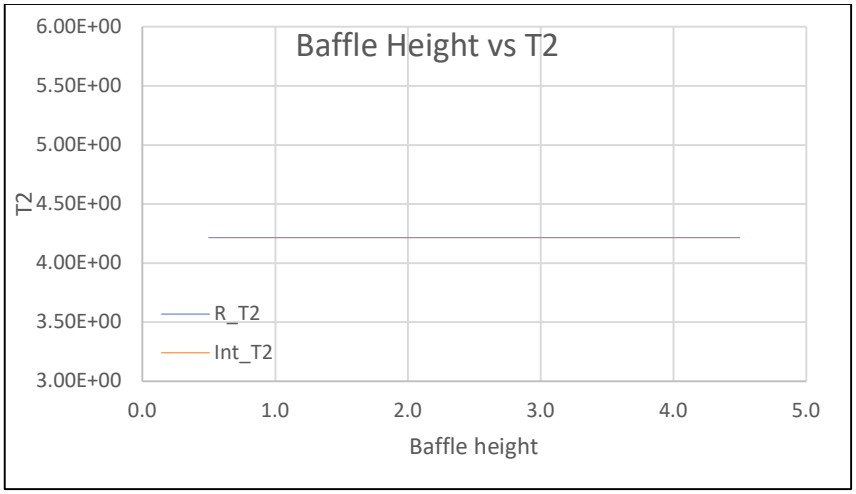

Fig-4.17 Second Time Period for different baffle height

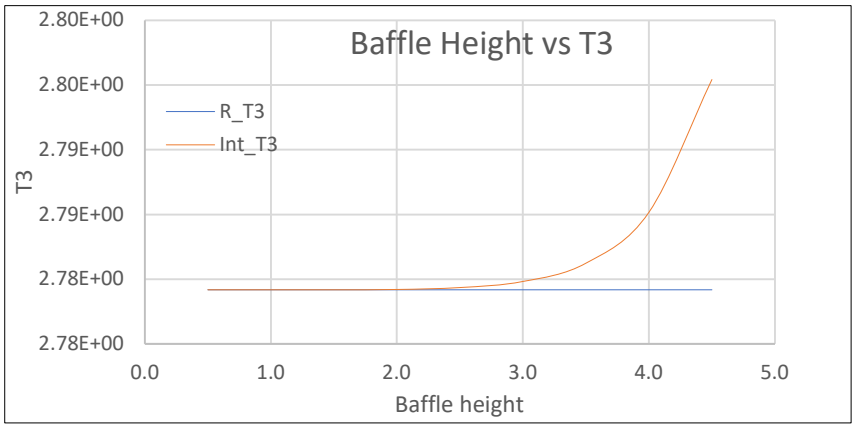

Fig-4.18 Third Time Period for different baffle height

In this case for first and third mode with increase in baffle height the coupling time period increases. But for second mode very little changes at coupling time period is observed which can be ignored.

4.1.5 Change in Baffle thickness

Here for a 12m tank with 5m fluid height, 4m baffle height and baffle positioned at middle, the graphs are plotted for time periods against different baffle thickness.

a) Graphs for Baffle Thickness vs Time period:

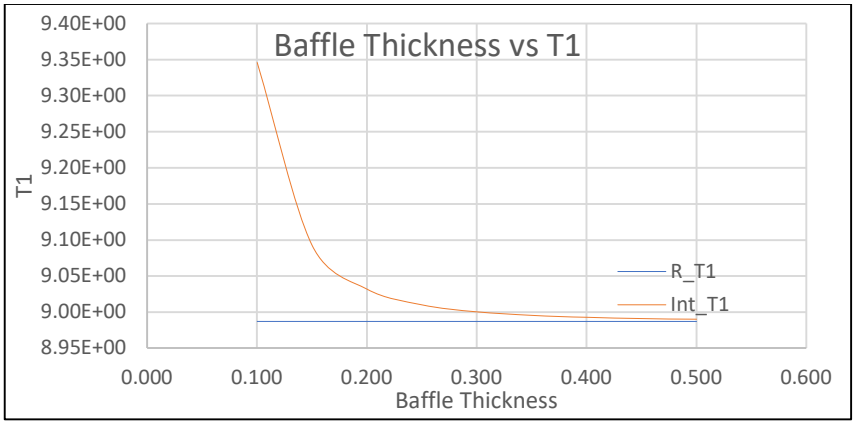

Fig-4.19 First Time Period for different Baffle thickness

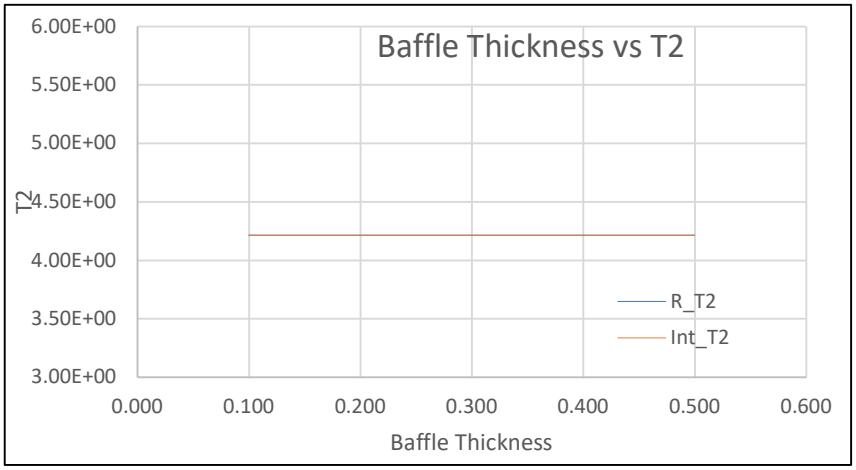

Fig-4.20 Second Time Period for different Baffle thickness

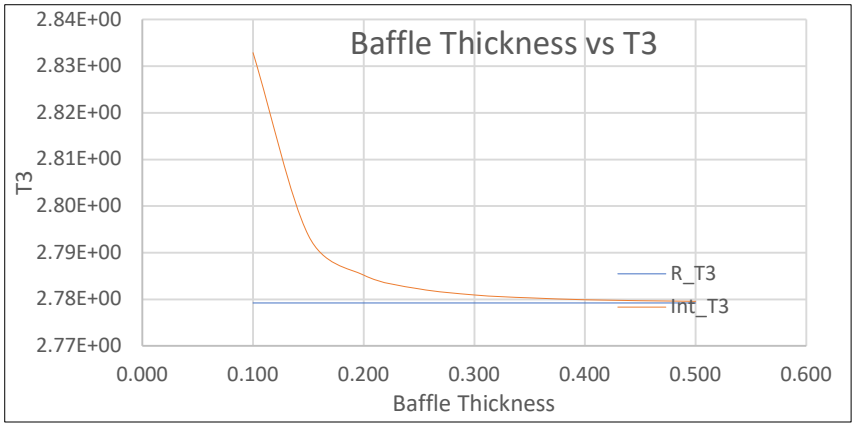

Fig-4.21 Third Time Period for different Baffle thickness

Here for first and third mode with increase in baffle thickness the coupling time period decreases. It has been observed that below baffle thickness of 0.4m or more precisely it can be noted that near

baffle thickness(t)/ baffle height (l) ratio below 0.1 the difference between reservoir time period and coupling time period are almost insignificant. But for second mode very little changes at coupling time period is observed which can be ignored.

4.2 Forced Vibration Analysis

4.2.1 Selection of Time Step

The results from Newmark's integration technique are sensitive to the time step and to determine a suitable time step, tank with following properties is considered. Water depth (H) = 5.0 m, length of tank (L) =12.0 m, acoustic speed (C) = 1440 m/sec, mass density of water (ρ) = 1000 kg/m^3. The study is carried out against sinusoidal excitation of frequency 2.67 rad/sec and 3.60 rad/sec with amplitude of 1.0g. Here, the fluid domain is discretized by 10 × 10 (i.e., N_h = 10 and N_v = 10). Tank walls and the base are assumed to be rigid. The maximum pressure coefficient ($C_p = P/\rho*Amp*H$) for different number of time step (N_t) for different exciting frequencies are summarized in Table 4.1. It is observed from the tabular results that the developed hydrodynamic pressure for different exciting frequencies is converged for values of N_t= 256. Thus, the time step (Δt) for the analysis of water tank is adopted as T/256 (T=time period) for all the case unless it is mentioned.

Table 4.1 Convergence of total hydrodynamic pressure coefficients (C_p) for different time steps

N_t	Excitation frequency	
	2.67 rad/sec	3.60 rad/sec
8	0.0528	0.0303
16	0.0550	0.0322
24	0.0556	0.0326
32	0.0559	0.0327
64	0.0561	0.0329
128	0.0563	0.0329
192	0.0564	0.0329
256	0.0564	0.0329

4.2.2 Forced Vibration Analysis of Tank with Elastic Baffle

The fluid is discretized by mesh of size 10 × 10 (i.e., N_h = 10 and N_v = 10). Similarly, for time history analysis the time step is considered as T/256. Time history analysis for pressure coefficient is carried out at four corner nodes top left(A), bottom left(C), top right(B) and bottom right(D) for different exciting frequencies 0.75ω, ω, 1.5ω, 3ω where 'ω' is the natural frequency of the tank-baffle coupled system corresponding to different tank and baffle parameters and also for arbitrary exciting frequency of 3 rad/sec.

4.2.2.1 Change in Tank length

The tank with 5m fluid height and 4m baffle height with 200mm thick baffle wall is considered in the analysis. The length of the tank has been changed keeping the baffle in the middle of the tank always. Time history for different H/L ratio are presented below.

a) Time history for exciting frequency 'ω'

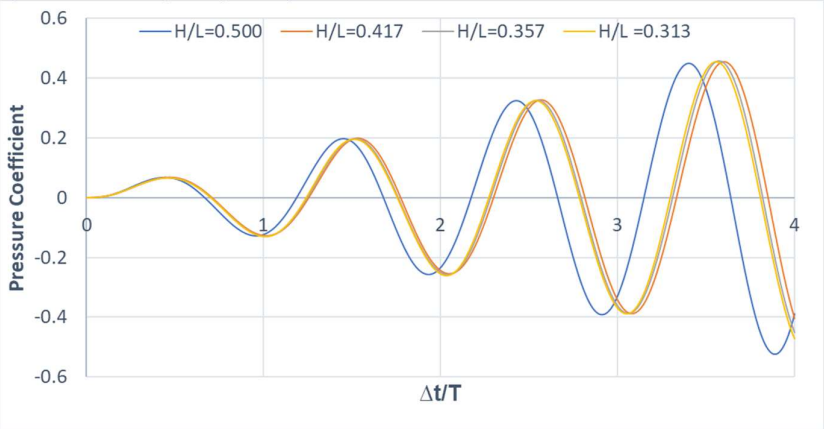

Fig 4.22 Variation of Pressure Co-efficient at 'A' for different H/L ratio

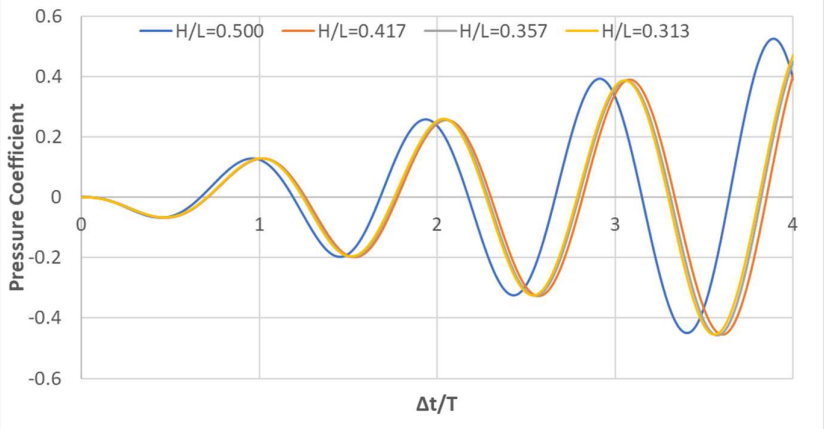

Fig 4.23 Variation of Pressure Co-efficient at 'B' for different H/L ratio

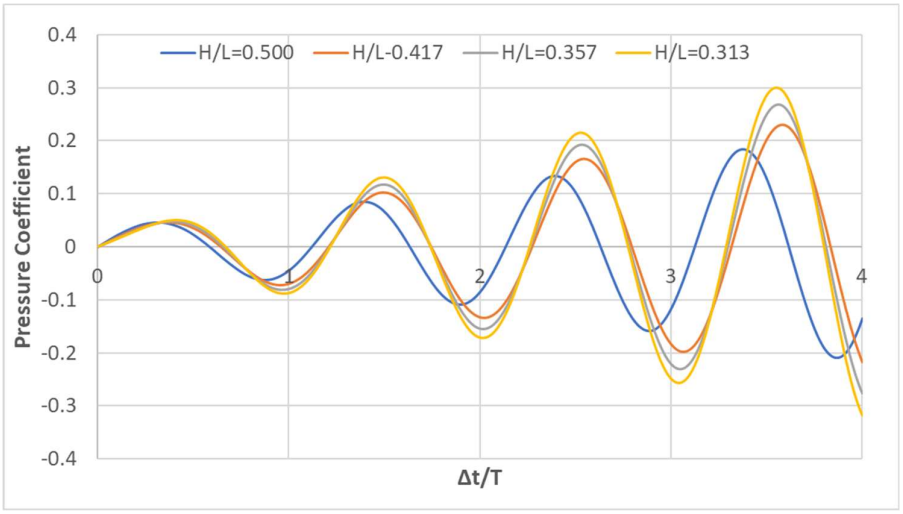

Fig 4.24 Variation of Pressure Co-efficient at 'C' for different H/L ratio

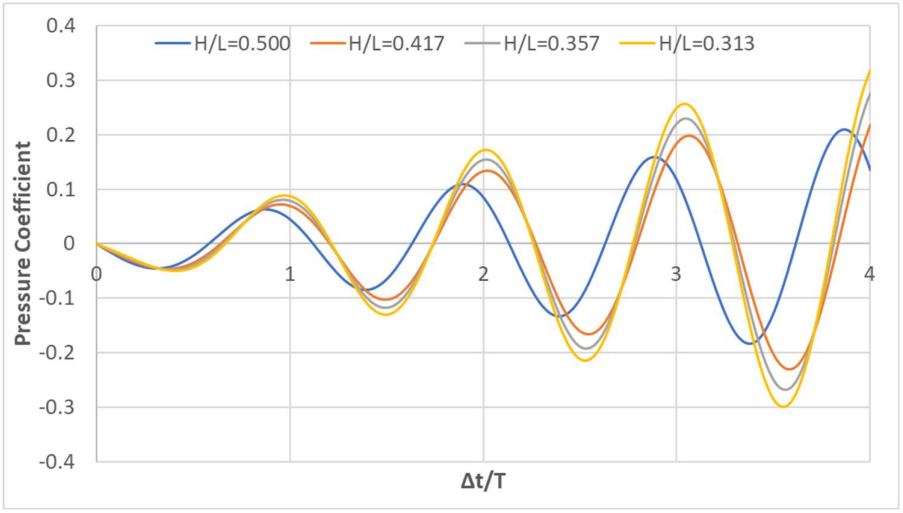

Fig 4.25 Variation of Pressure Co-efficient at 'D' for different H/L ratio

From the figures 4.22-4.25 it is observed that time histories of pressure coefficient for H/L ratio of 0.500 is different from time histories corresponding to other three H/L ratios at node A and B. At node C and D time histories for different H/L ratios are different from each other but significant variation for H/L ratio of 0.500 is observed.

b) Time history for exciting frequency '0.75ω'

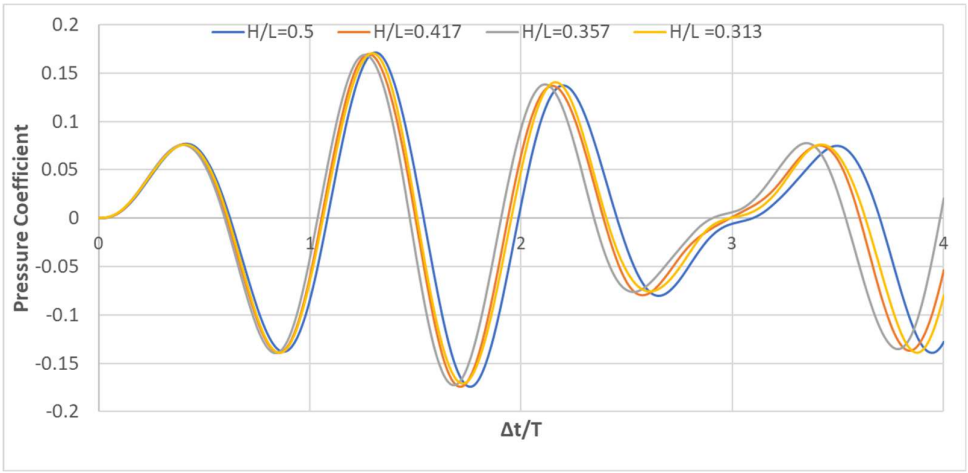

Fig 4.26 Variation of Pressure Co-efficient at 'A' for different H/L ratio

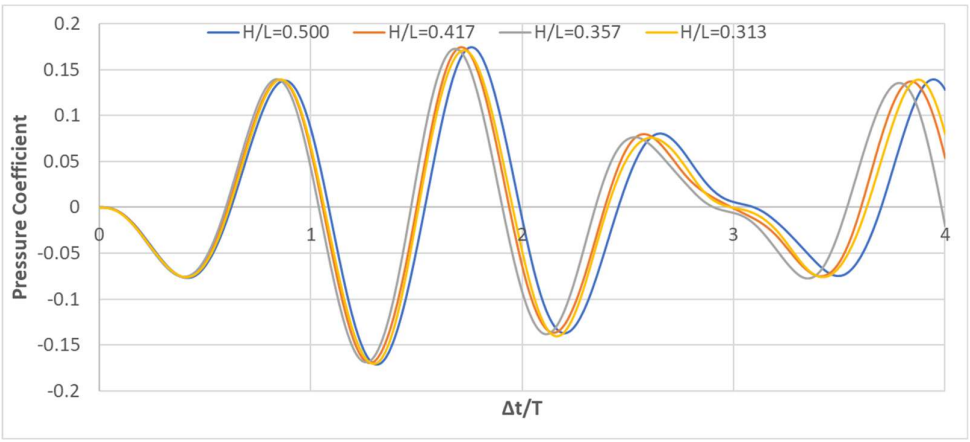

Fig 4.27 Variation of Pressure Co-efficient at 'B' for different H/L ratio

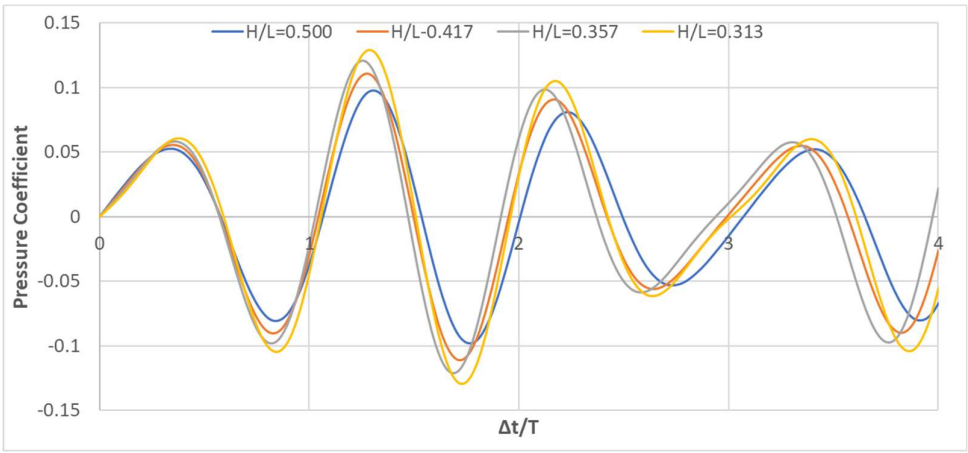

Fig 4.28 Variation of Pressure Co-efficient at 'C' for different H/L ratio

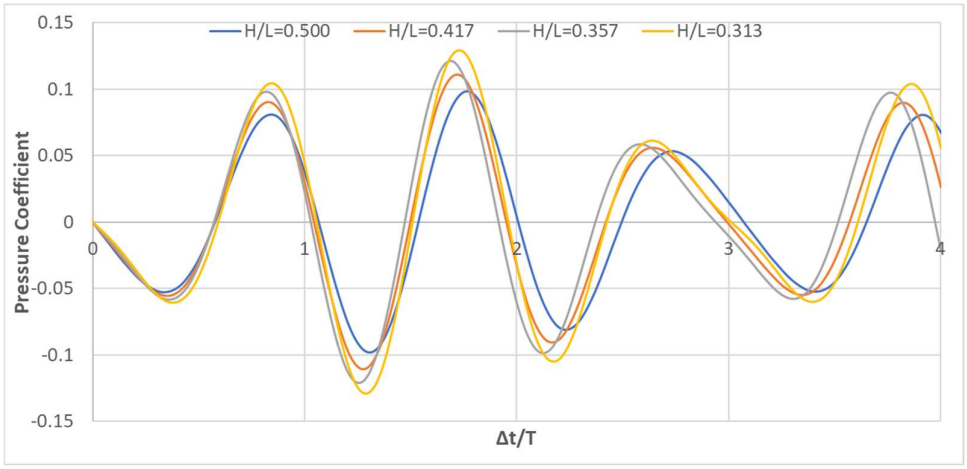

Fig 4.29 Variation of Pressure Co-efficient at 'D' for different H/L ratio

From the figures 4.26-4.29 it is observed that variation of pressure coefficients at four corner nodes corresponding to forcing frequency 0.75ω for different H/L ratios is not significant.

c) Time history for exciting frequency '1.5ω'

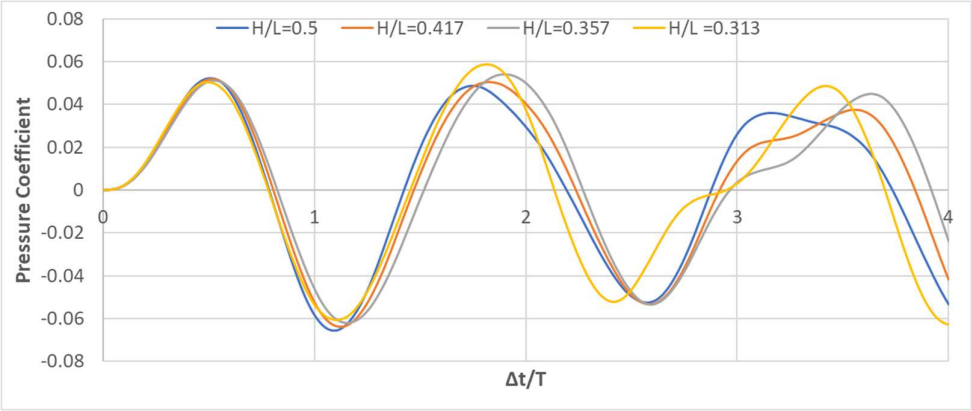

Fig 4.30 Variation of Pressure Co-efficient at 'A' for different H/L ratio

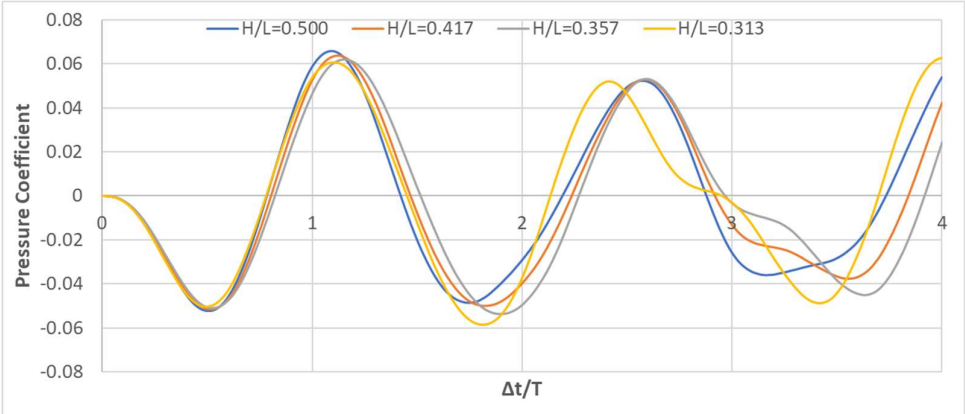

Fig 4.31 Variation of Pressure Co-efficient at 'B' for different H/L ratio

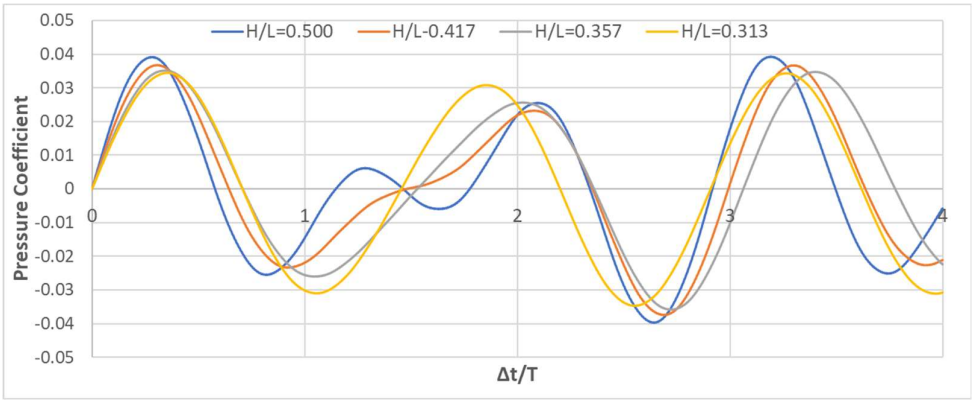

Fig 4.32 Variation of Pressure Co-efficient at 'C' for different H/L ratio

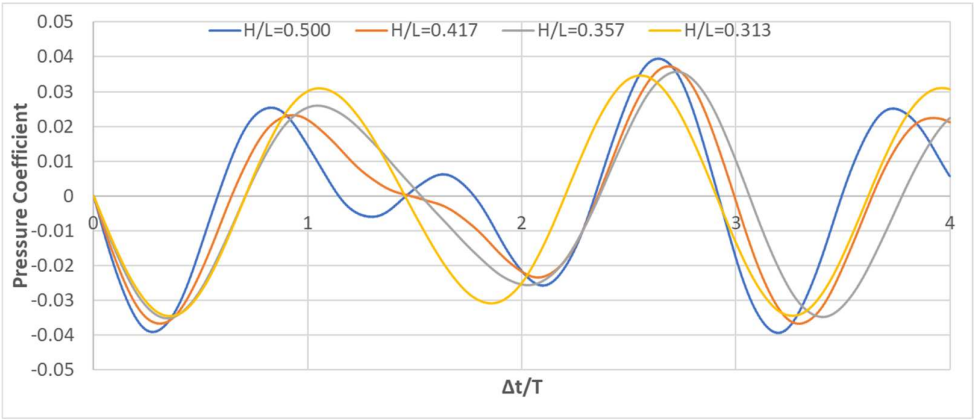

Fig 4.33 Variation of Pressure Co-efficient at 'D' for different H/L ratio

From the figures 4.30-4.33 it is observed that there is a variation of pressure coefficients at four corner nodes corresponding to forcing frequency of 1.5ω for different H/L ratios. However, pressure coefficient time history for H/L ratio of 0.500 is notably different from other three H/L ratios.

d) Time history for exciting frequency '3ω'

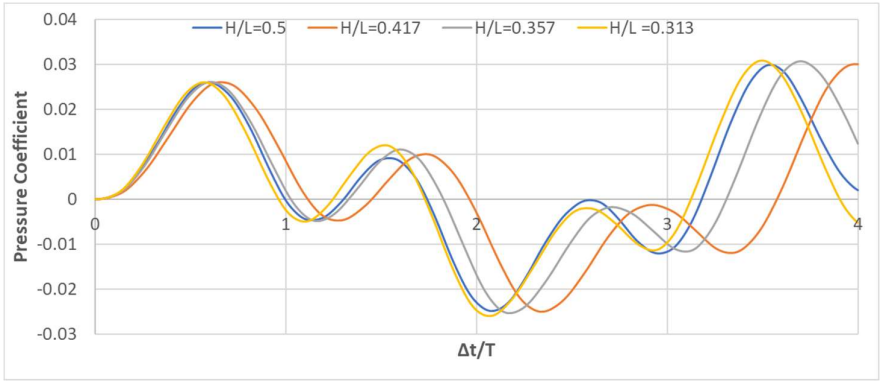

Fig 4.34 Variation of Pressure Co-efficient at 'A' for different H/L ratio

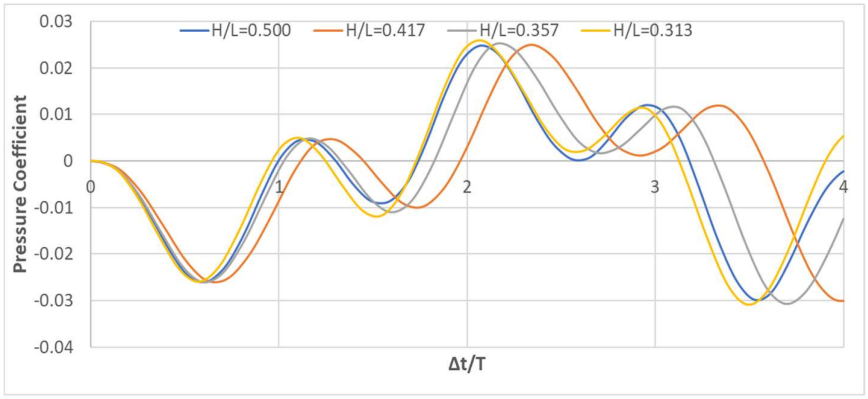

Fig 4.35 Variation of Pressure Co-efficient at 'B' for different H/L ratio

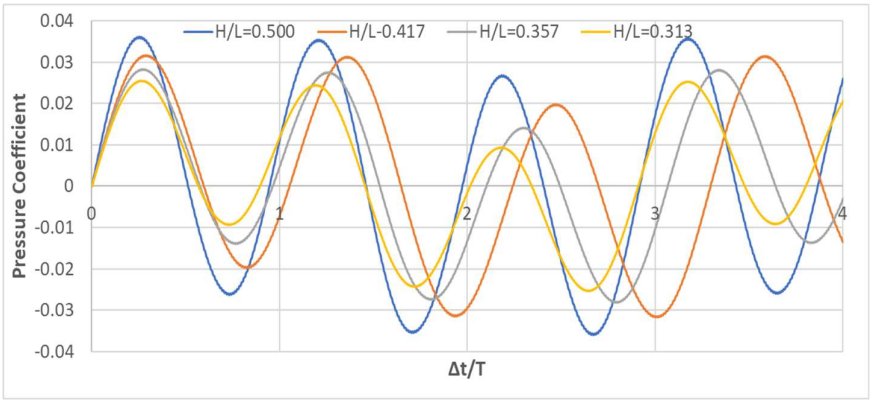

Fig 4.36 Variation of Pressure Co-efficient at 'C' for different H/L ratio

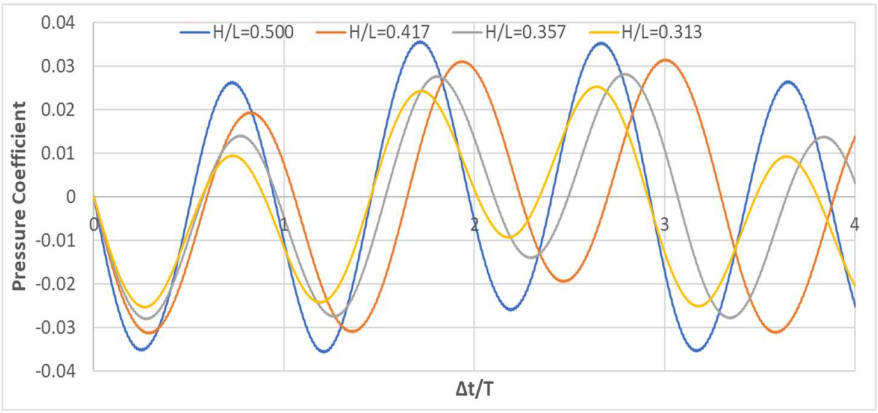

Fig 4.37 Variation of Pressure Co-efficient at 'D' for different H/L ratio

It is observed that there is a wide variation of pressure coefficients at four corner nodes corresponding to forcing frequency of 3ω for different H/L ratios (fig 4.34-4.37). Among these pressure coefficient time history at node C and D for H/L ratio of 0.500 is significantly different from time history corresponding to other three H/L ratios.

e) Time history corresponding to exciting frequency 3 rad/sec

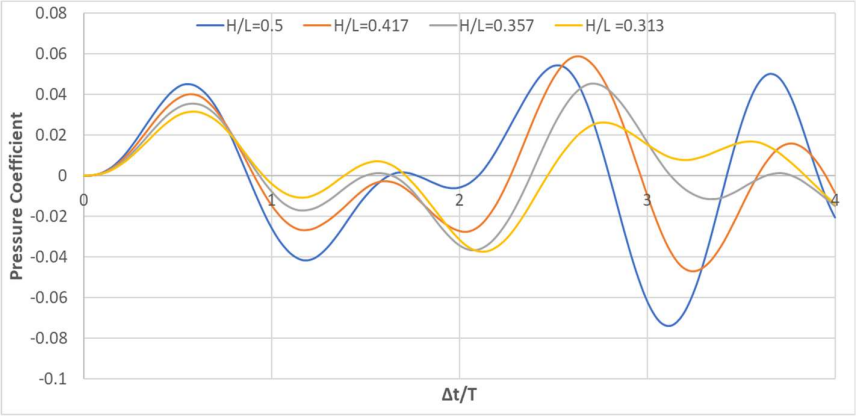

Fig 4.38 Variation of Pressure Co-efficient at 'A' for different H/L ratio

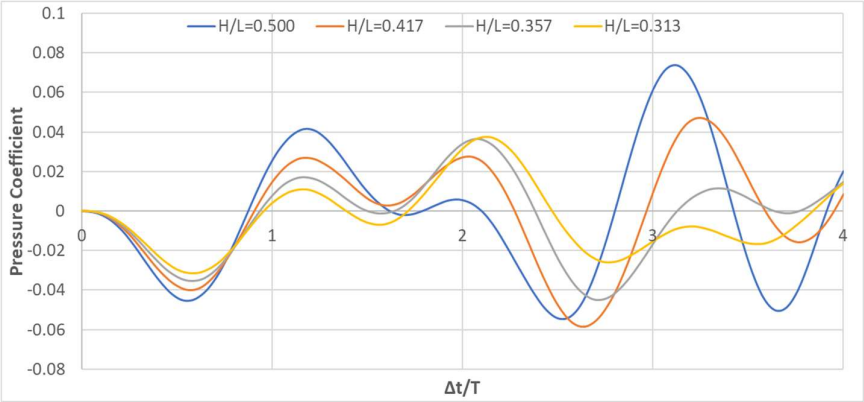

Fig 4.39 Variation of Pressure Co-efficient at 'B' for different H/L ratio

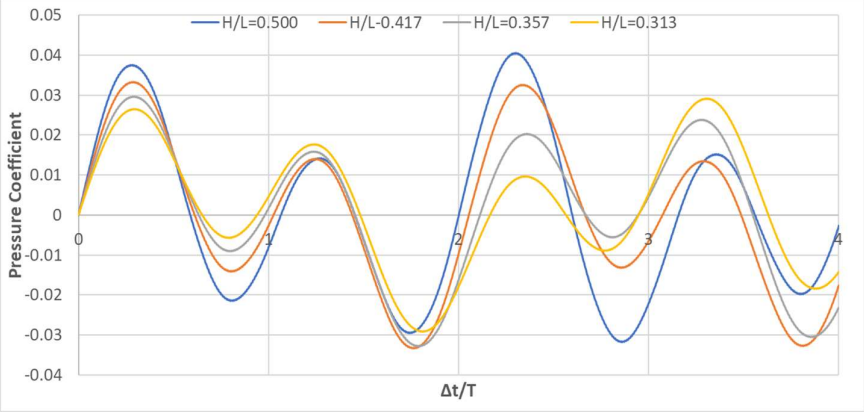

Fig 4.40 Variation of Pressure Co-efficient at 'C' for different H/L ratio

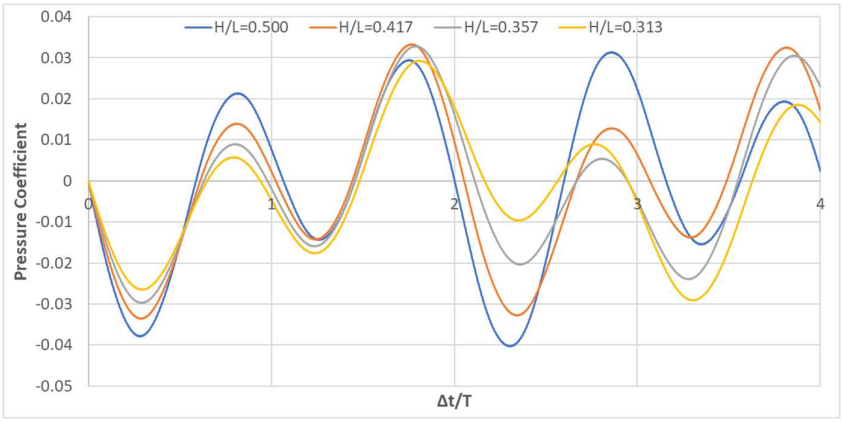

Fig 4.41 Variation of Pressure Co-efficient at 'D' for different H/L ratio

Variation of pressure coefficients at four corner nodes corresponding to forcing frequency 3 rad/sec for different H/L ratios are plotted in the figure 4.38-4.41. Pressure coefficient time history for H/L ratio of 0.500 is notably different from time histories corresponding to other H/L ratios.

4.2.2.2 Change in Baffle thickness

Here for a 12m tank with fluid height of 5m and baffle wall of 4m height and baffle wall positioned at 2.4m, baffle thickness has been changed. Time histories for different baffle thicknesses are presented below.

a) Time history corresponding to exciting frequency 'ω'

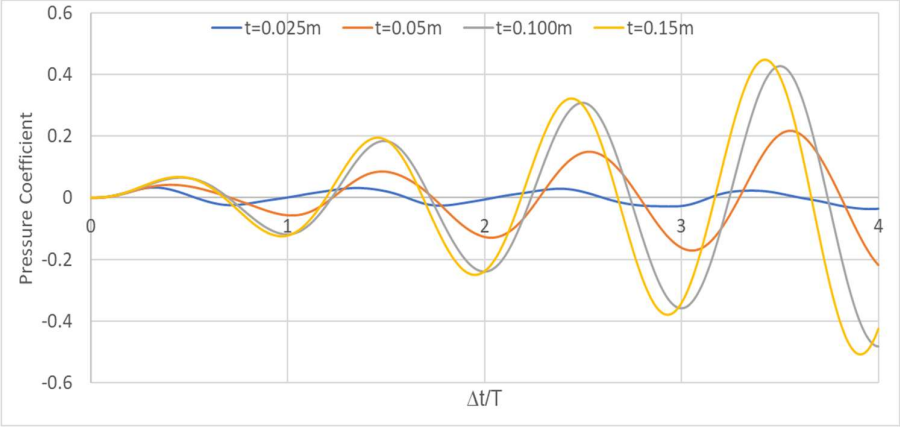

Fig 4.42 Variation of Pressure Co-efficient at 'A' for different baffle thickness

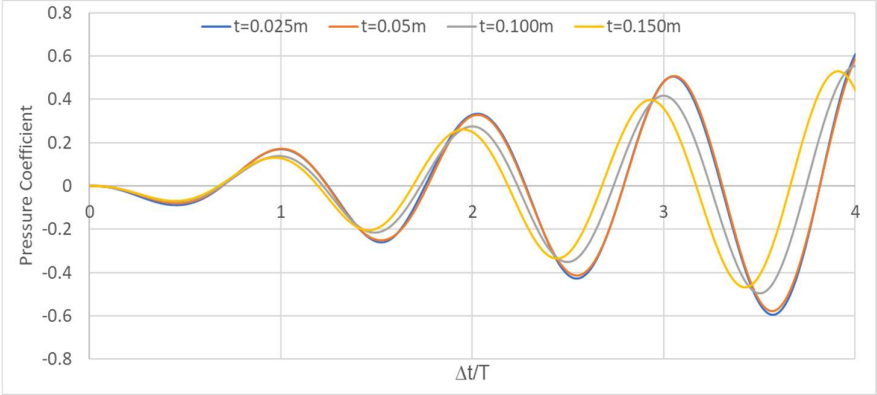

Fig 4.43 Variation of Pressure Co-efficient at 'B' for different baffle thickness

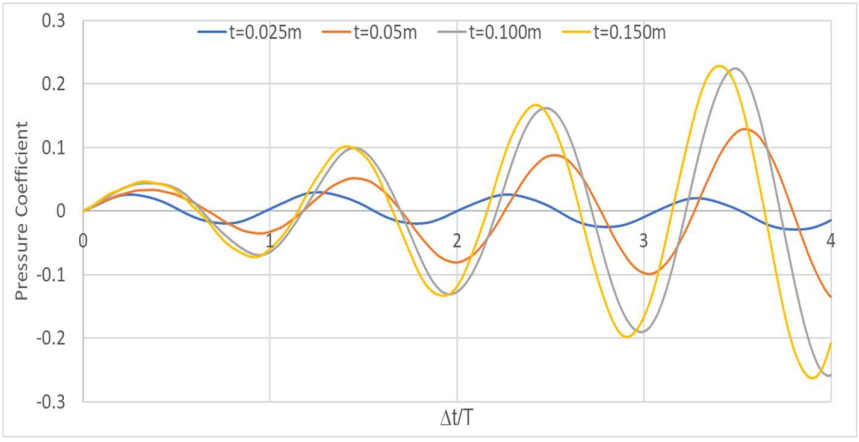

Fig 4.44 Variation of Pressure Co-efficient at 'C' for different baffle thickness

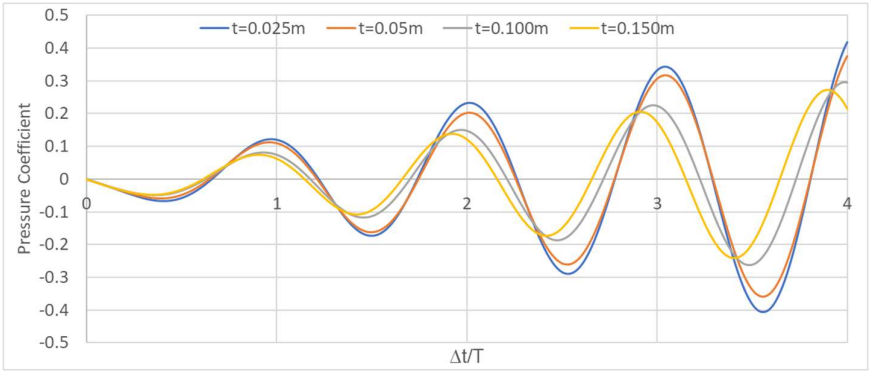

Fig 4.45 Variation of Pressure Co-efficient at 'D' for different baffle thickness

Variation of pressure coefficients at four corner nodes for forcing frequency equal to natural frequency for different baffle wall thickness are plotted (fig 4.42-4.45). Time histories corresponding to baffle thickness 25 mm at node A and C (near end of baffle wall) are flat in nature. For 50 mm thickness it is slightly steeper than 25 mm thickness. No such variation is

observed for 100 mm and 150 mm at node A and C. But at far end nodes B and D, baffle thickness has less effect in the dynamic response.

b) Time history corresponding to exciting frequency '0.75ω'

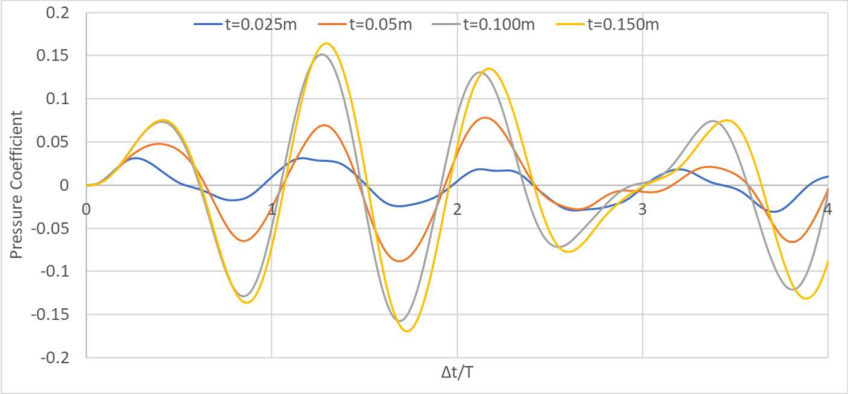

Fig 4.46 Variation of Pressure Co-efficient at 'A' for different baffle thickness

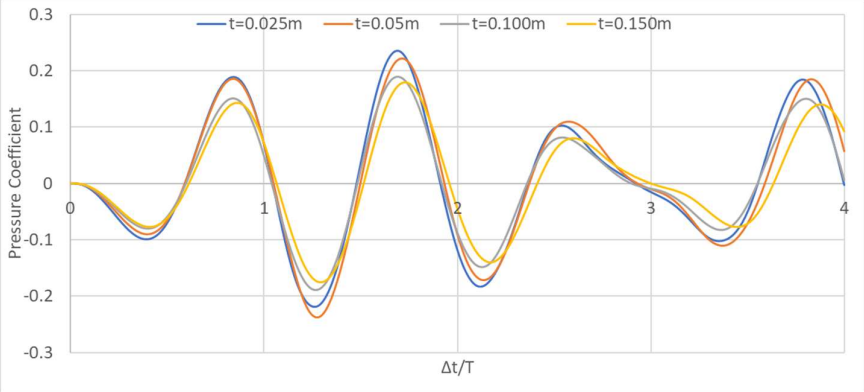

Fig 4.47 Variation of Pressure Co-efficient at 'B' for different baffle thickness

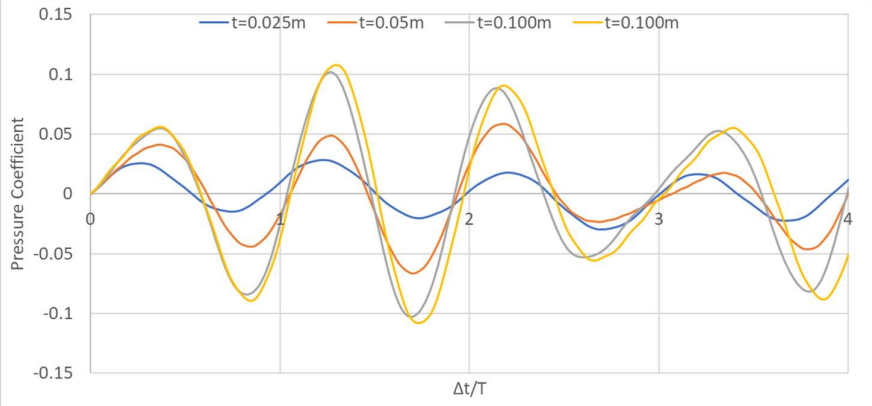

Fig 4.48 Variation of Pressure Co-efficient at 'C' for different baffle thickness

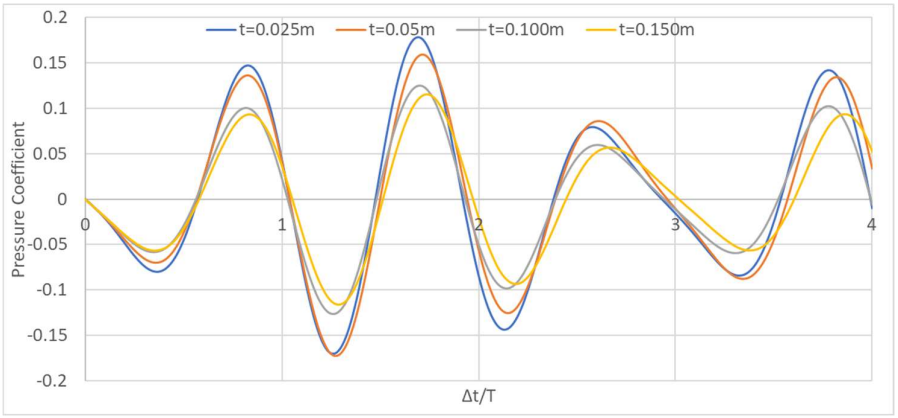

Fig 4.49 Variation of Pressure Co-efficient at 'D' for different baffle thickness

It is observed from the pressure coefficient time histories above (fig 4.46 to 4.49) that baffle thickness has significant impact in the dynamic response. For wall thickness of 25mm and 50 mm, pressure coefficient is less at near end (node A and C) of baffle wall. Thickness above 100 mm has less impact in the dynamic response. But for far end (node B and D) baffle thickness has less effect in the dynamic response.

c) Time history corresponding to exciting frequency '1.5ω'

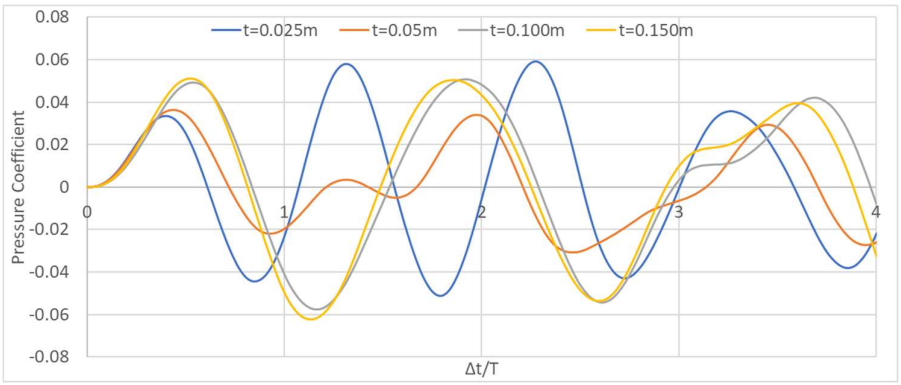

Fig 4.50 Variation of Pressure Co-efficient at 'A' for different baffle thickness

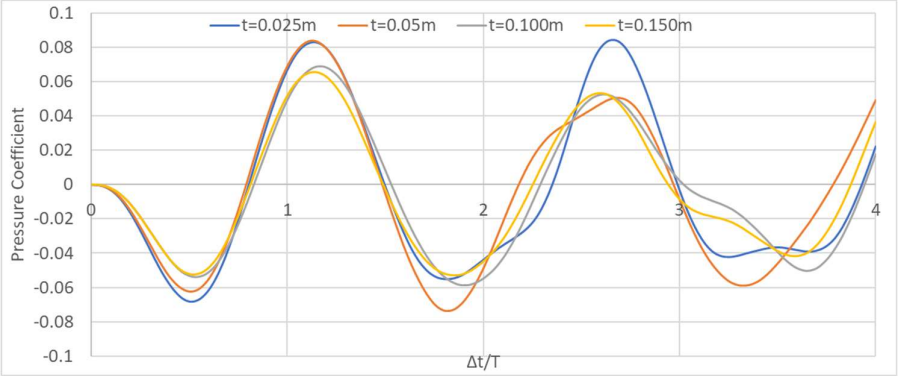

Fig 4.51 Variation of Pressure Co-efficient at 'B' for different baffle thickness

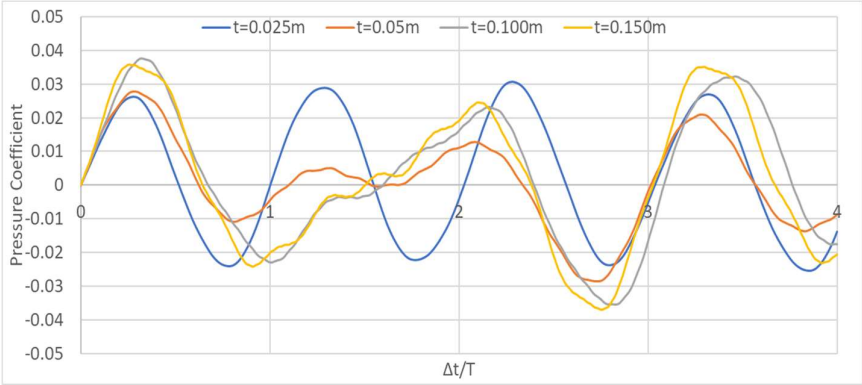

Fig 4.52 Variation of Pressure Co-efficient at 'C' for different baffle thickness

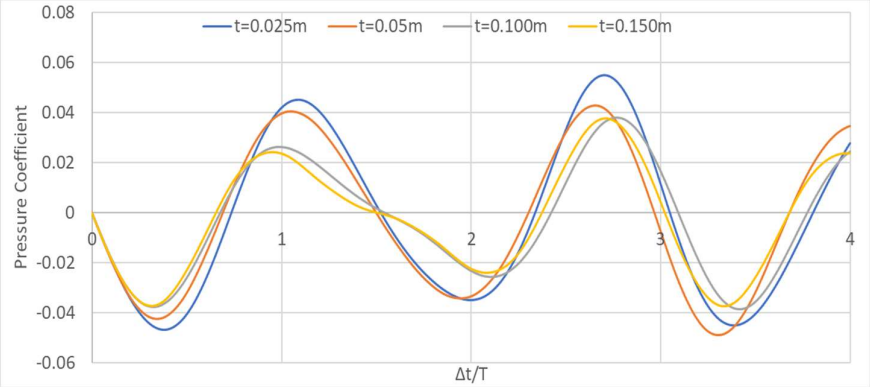

Fig 4.53 Variation of Pressure Co-efficient at 'D' for different baffle thickness

Variation in pressure coefficients is observed from the above graphs (fig 4.50 to 4.53) for different baffle thickness. At node B pressure coefficient is more compared to other three nodes.

d) Time history corresponding to exciting frequency '3ω'

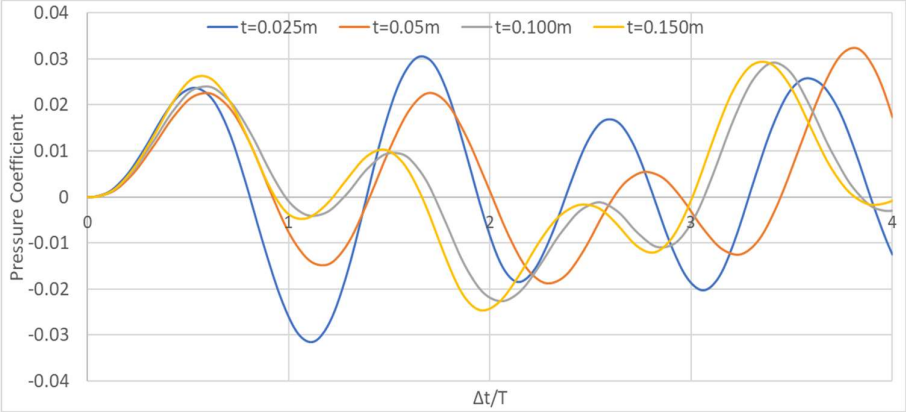

Fig 4.54 Variation of Pressure Co-efficient at 'A' for different baffle thickness

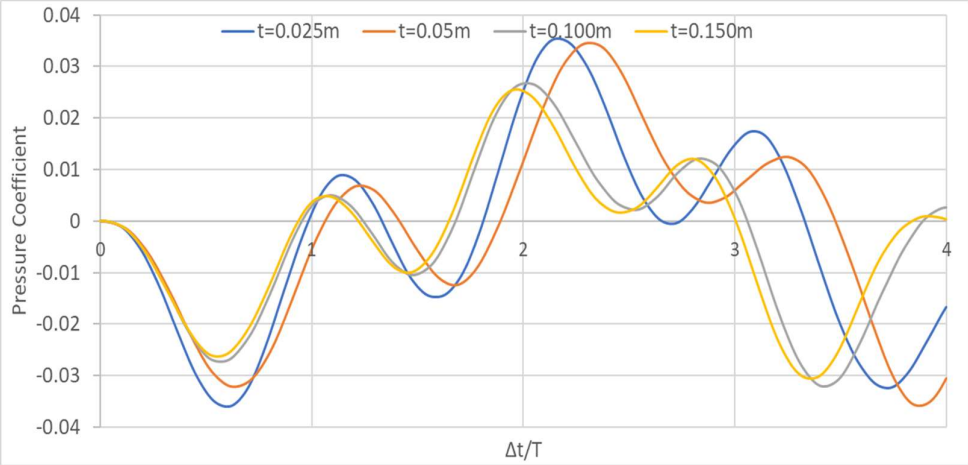

Fig 4.55 Variation of Pressure Co-efficient at 'B' for different baffle thickness

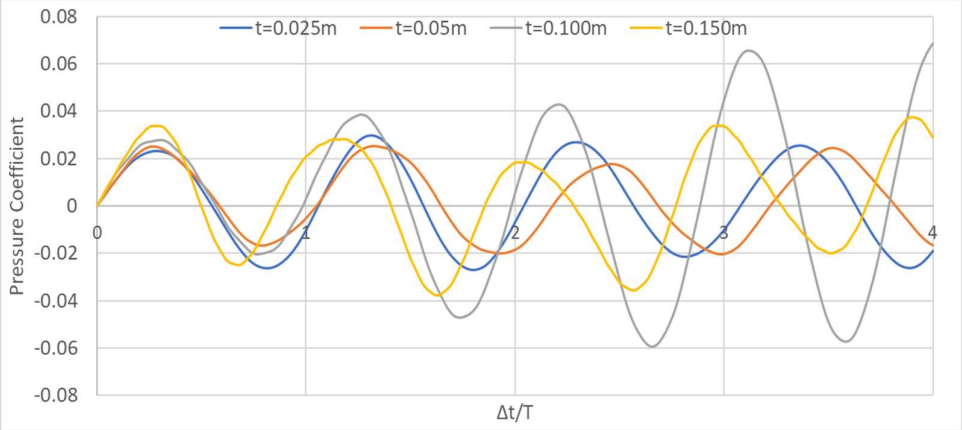

Fig 4.56 Variation of Pressure Co-efficient at 'C' for different baffle thickness

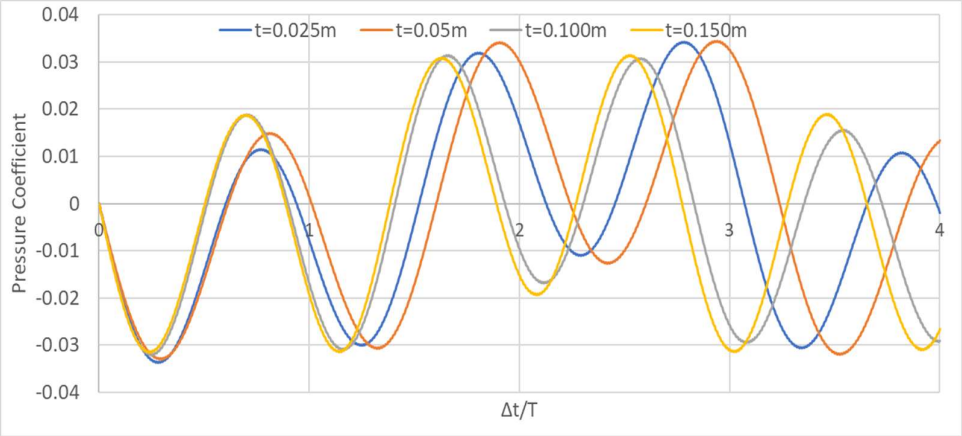

Fig 4.57 Variation of Pressure Co-efficient at 'D' for different baffle thickness

Variation of pressure coefficients at four corner nodes for forcing frequency equal to three times the natural frequency for different baffle wall thickness is plotted (fig 4.54-4.57). Variations are irregular in nature and it is difficult to draw any conclusions.

e) Time history corresponding to exciting frequency '3 rad/sec'

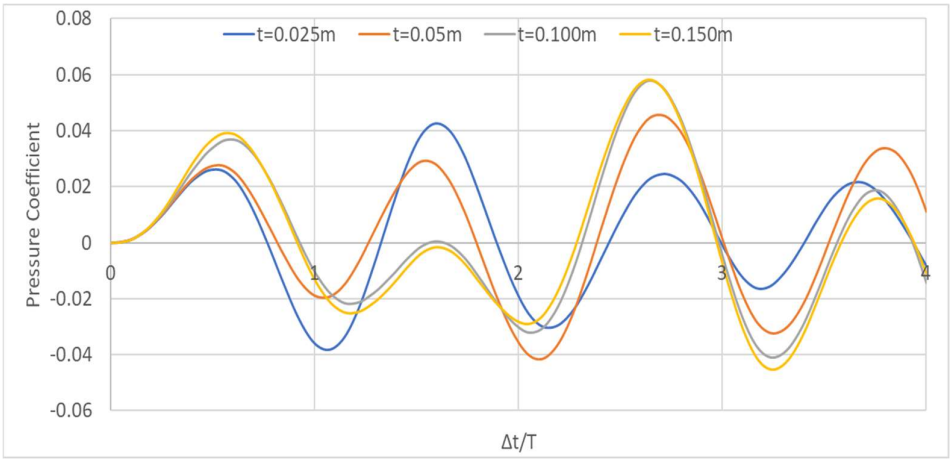

Fig 4.58 Variation of Pressure Co-efficient at 'A' for different baffle thickness

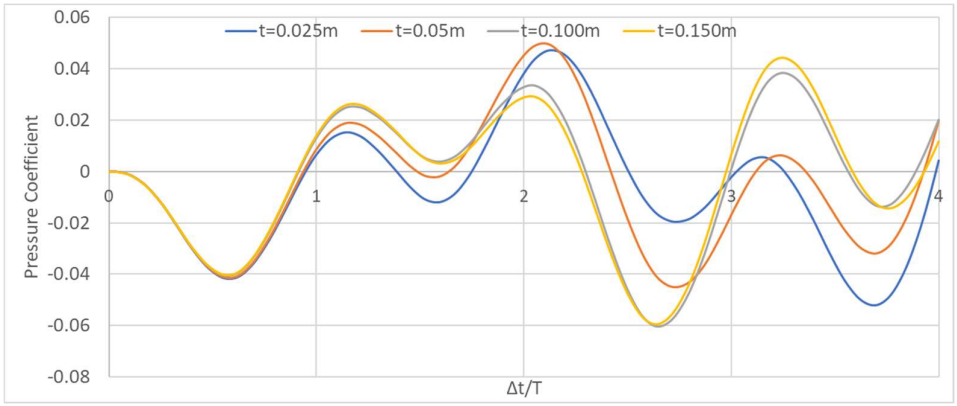

Fig 4.59 Variation of Pressure Co-efficient at 'B' for different baffle thickness

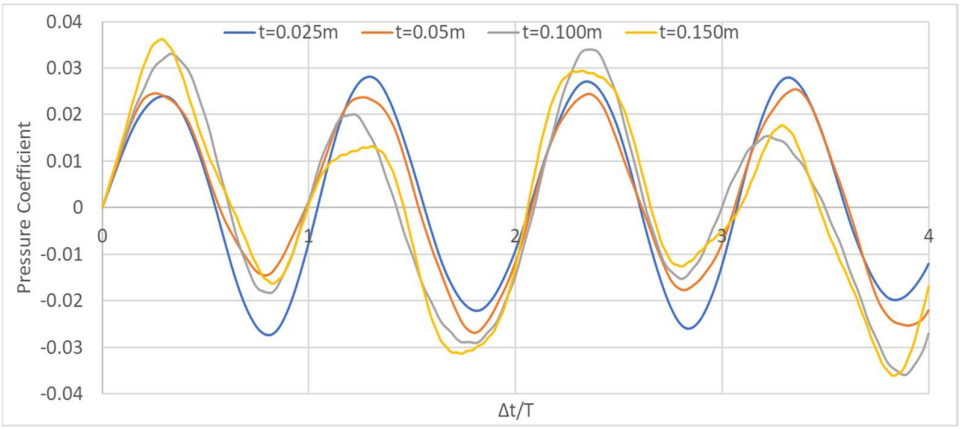

Fig 4.60 Variation of Pressure Co-efficient at 'C' for different baffle thickness

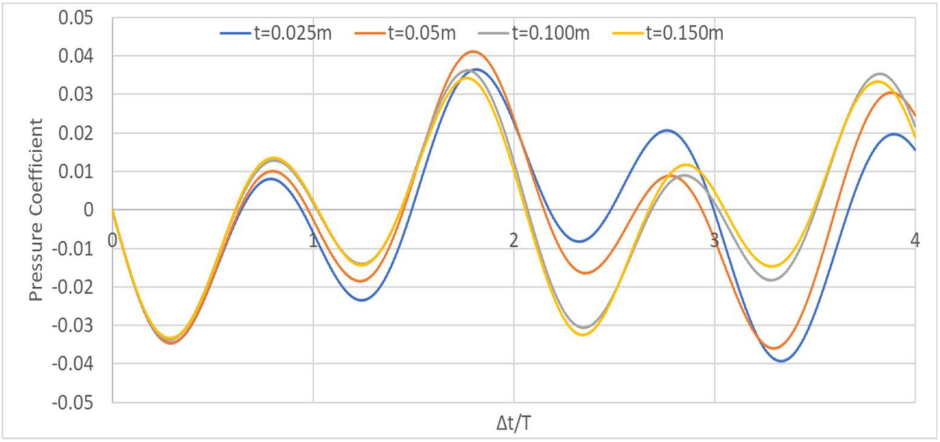

Fig 4.61 Variation of Pressure Co-efficient at 'D' for different baffle thickness

Pressure coefficients time histories are plotted at four corner nodes for forcing frequency equal to 3 rad/sec for different baffle wall thickness (fig 4.58-4.61). Variation in maximum pressure coefficients for different baffle thickness is less and may be ignored.

4.2.2.3 Change in Baffle position

Here the baffle has been positioned at different locations of a 12m tank which has 5m of fluid height, 4m of baffle height and 200mm of baffle thickness. Time histories are plotted for different baffle position.

a) Time history corresponding to exciting frequency 'ω'

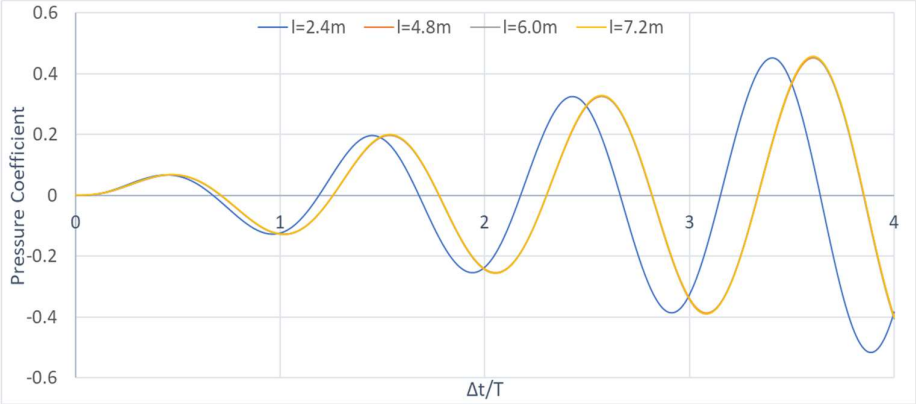

Fig 4.62 Variation of Pressure Co-efficient at 'A' for different baffle position

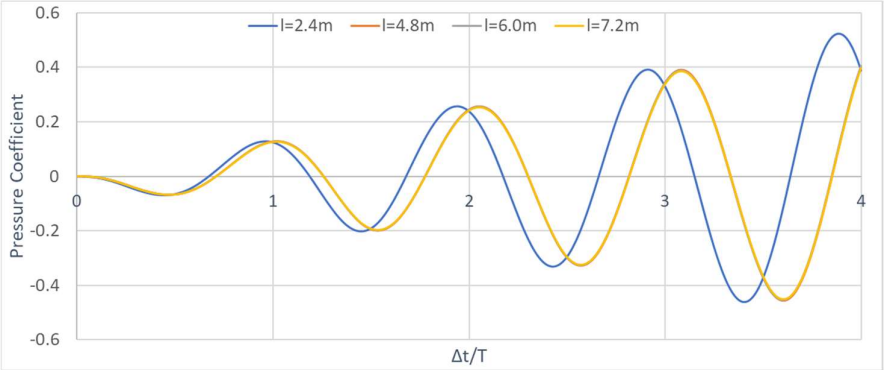

Fig 4.63 Variation of Pressure Co-efficient at 'B' for different baffle position

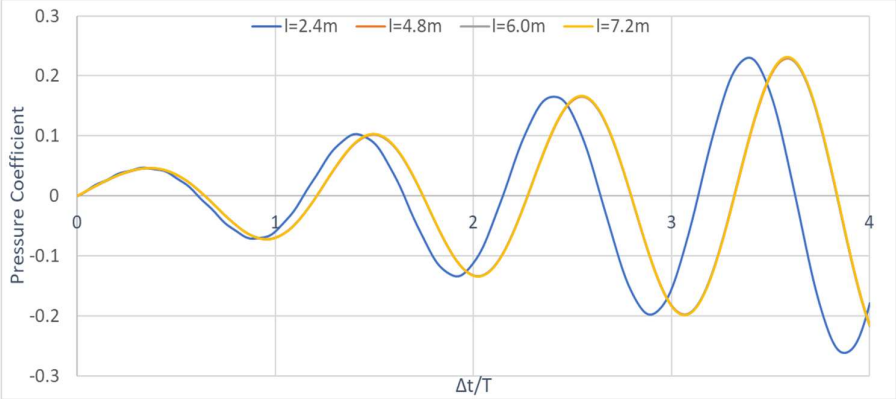

Fig 4.64 Variation of Pressure Co-efficient at 'C' for different baffle position

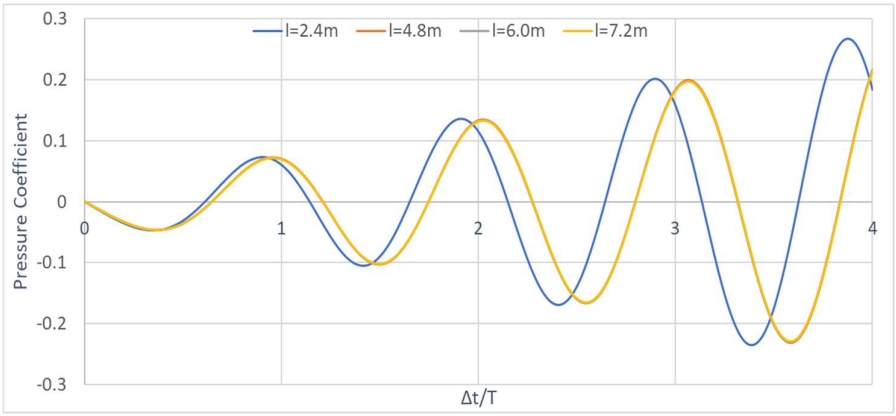

Fig 4.65 Variation of Pressure Co-efficient at 'D' for different baffle position

Pressure coefficients time histories are plotted at four corner nodes for forcing frequency equal to natural frequency (ω) for different baffle position (fig 4.62-4.65). Variation in pressure coefficients at all four nodes for baffle positioned at 2.4m is different from other three baffle locations.

b) Time history corresponding to exciting frequency '0.75ω'

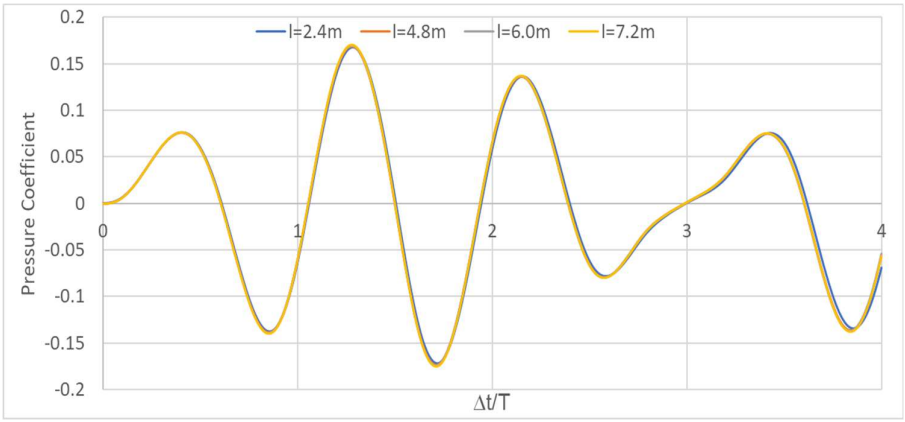

Fig 4.66 Variation of Pressure Co-efficient at 'A' for different baffle position

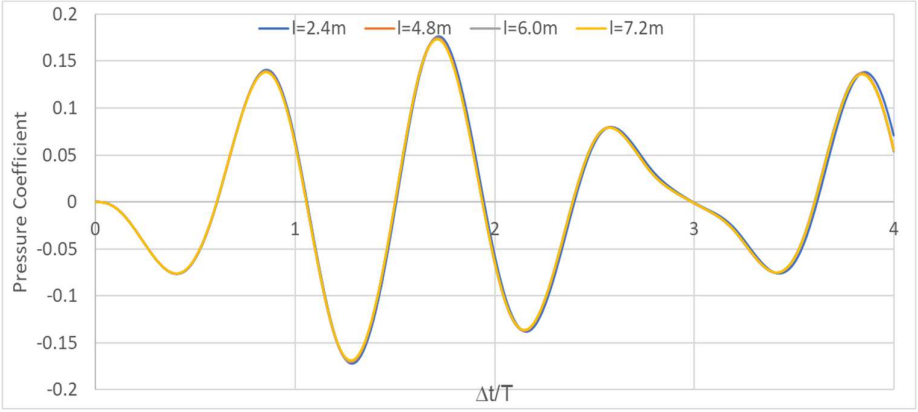

Fig 4.67 Variation of Pressure Co-efficient at 'B' for different baffle position

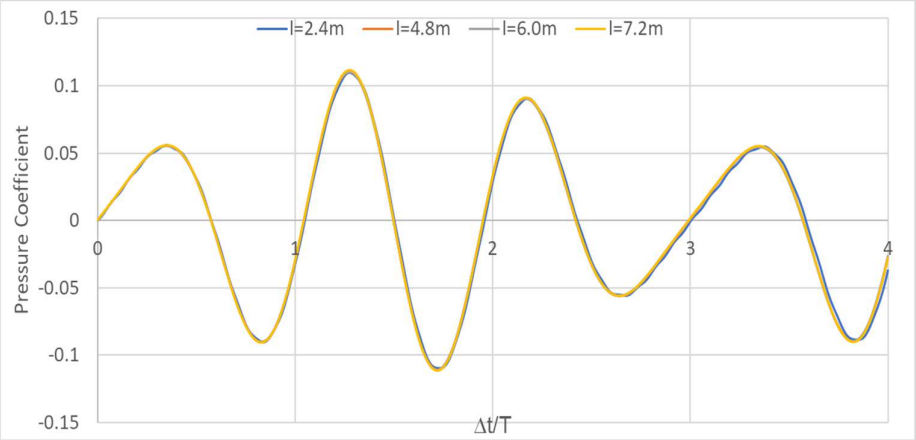

Fig 4.68 Variation of Pressure Co-efficient at 'C' for different baffle position

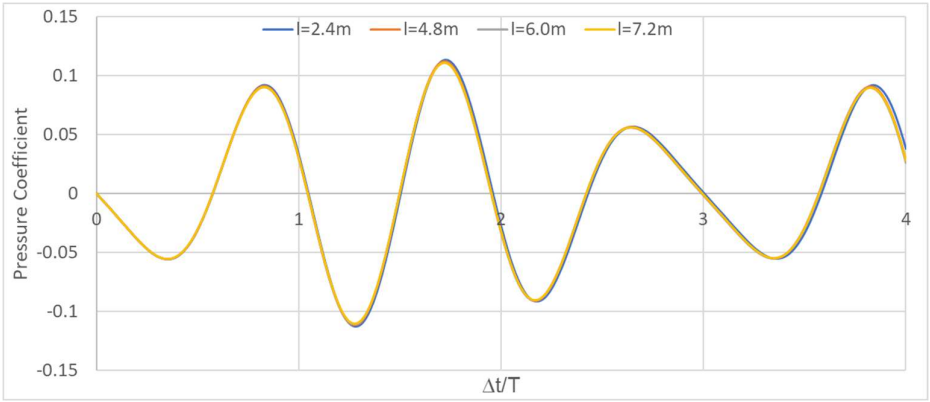

Fig 4.69 Variation of Pressure Co-efficient at 'D' for different baffle position

It is observed from the above figures that there is no change of pressure coefficients for different baffle position at all four nodes (fig 4.66-4.69). It reveals that for exciting frequency of 0.75ω dynamic response is not dependent on baffle positions.

c) Time history corresponding to exciting frequency '1.5ω'

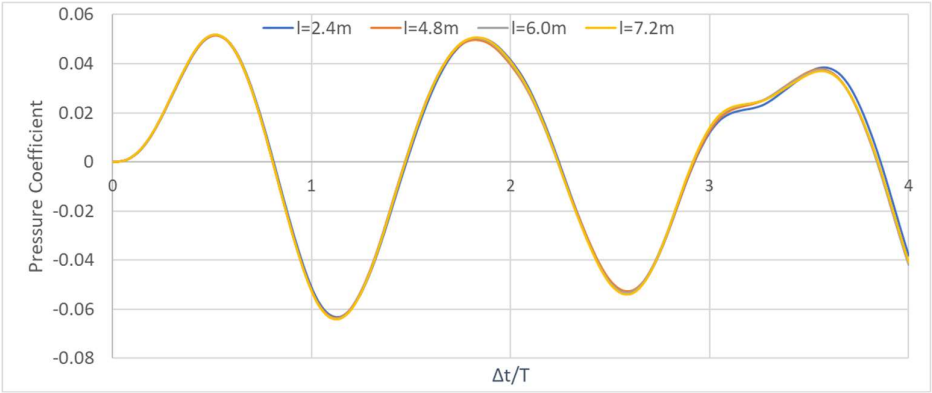

Fig 4.70 Variation of Pressure Co-efficient at 'A' for different baffle position

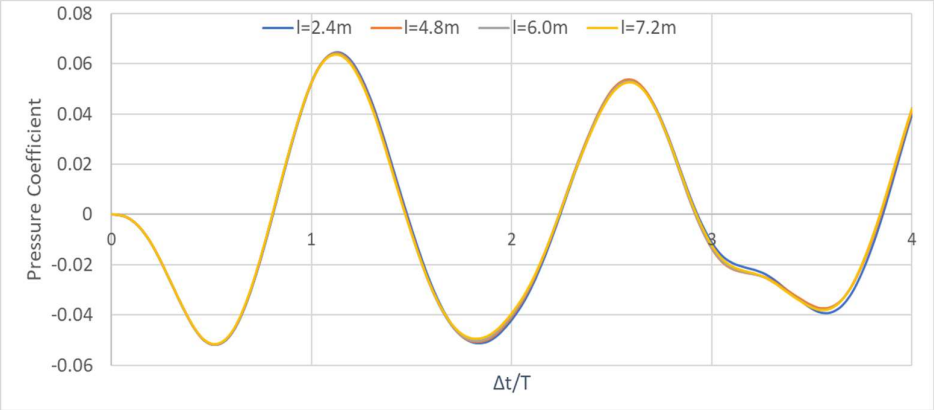

Fig 4.71 Variation of Pressure Co-efficient at 'B' for different baffle position

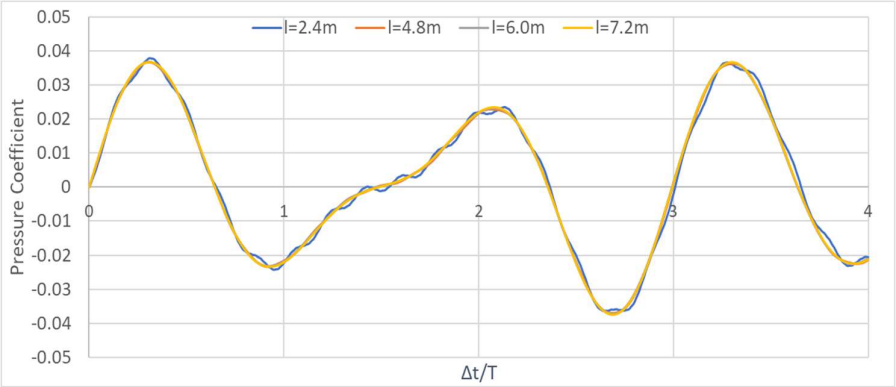

Fig 4.72 Variation of Pressure Co-efficient at 'C' for different baffle position

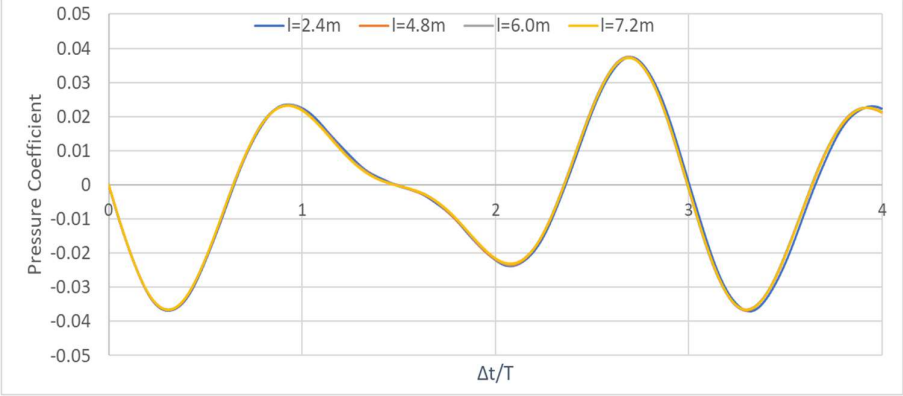

Fig 4.73 Variation of Pressure Co-efficient at 'D' for different baffle position

From the above graphs it can be concluded that baffle position is not important in dynamic response for forcing frequency of 1.5w.

d) Time history corresponding to exciting frequency '3ω'

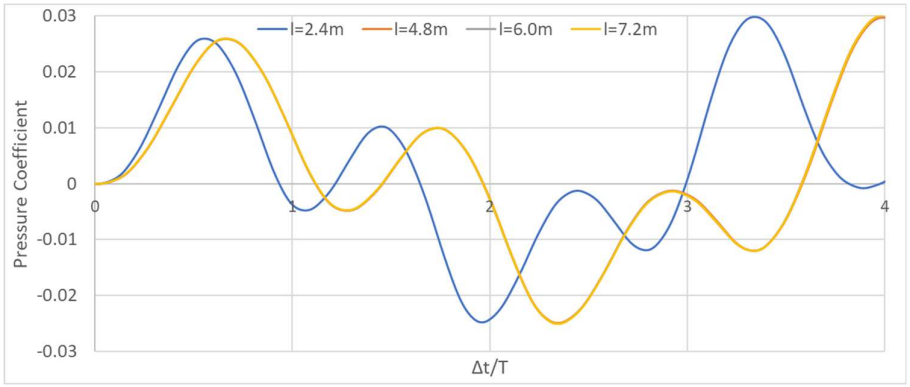

Fig 4.74 Variation of Pressure Co-efficient at 'A' for different baffle position

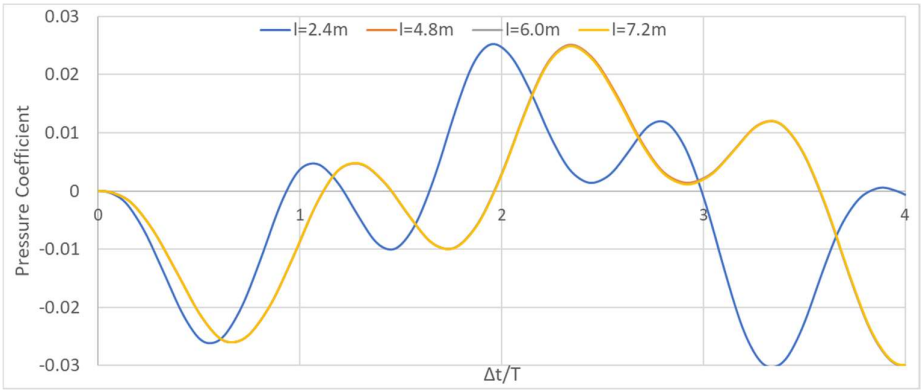

Fig 4.75 Variation of Pressure Co-efficient at 'B' for different baffle position

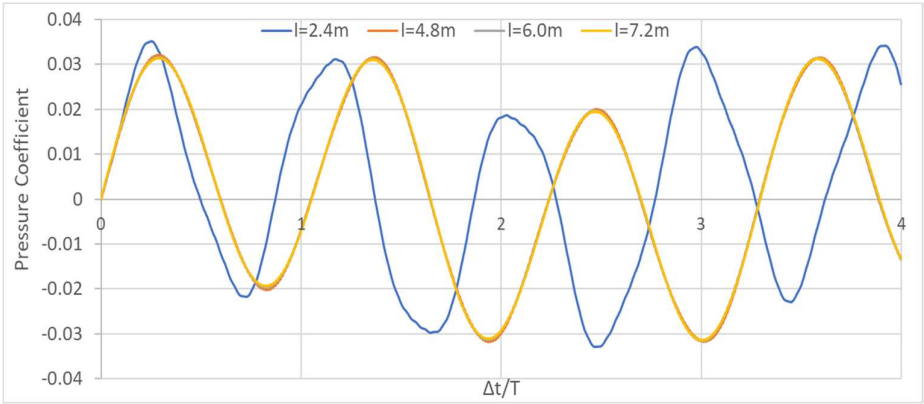

Fig 4.76 Variation of Pressure Co-efficient at 'C' for different baffle position

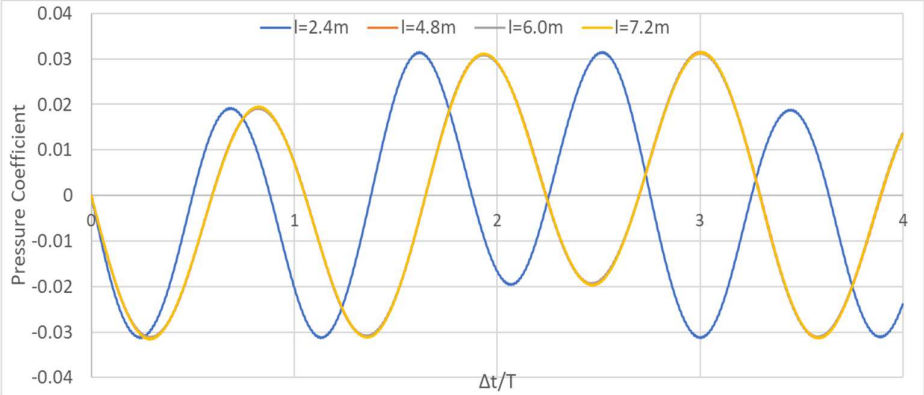

Fig 4.77 Variation of Pressure Co-efficient at 'D' for different baffle position

Pressure coefficients time histories are plotted for exciting frequency equal to three times the natural frequency for different baffle position (fig 4.74-4.77). Variation in pressure coefficients for baffle wall located at 2.4m is different from other three baffle locations 4.8m, 6m and 7.2m.

e) Time history corresponding to exciting frequency '3 rad/sec'

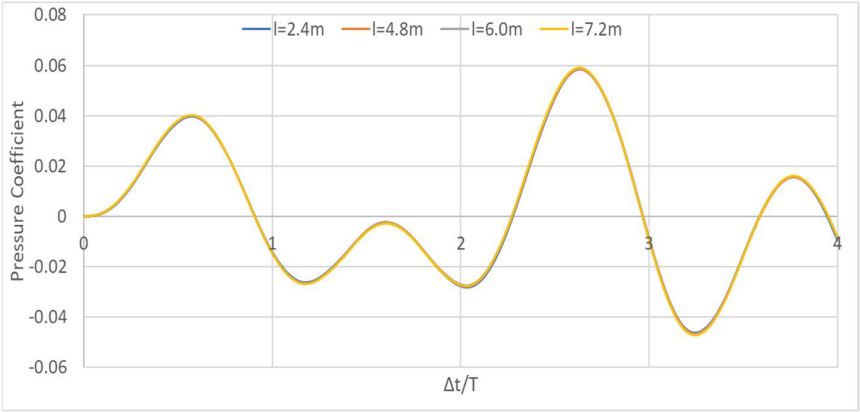

Fig 4.78 Variation of Pressure Co-efficient at 'A' for different baffle position

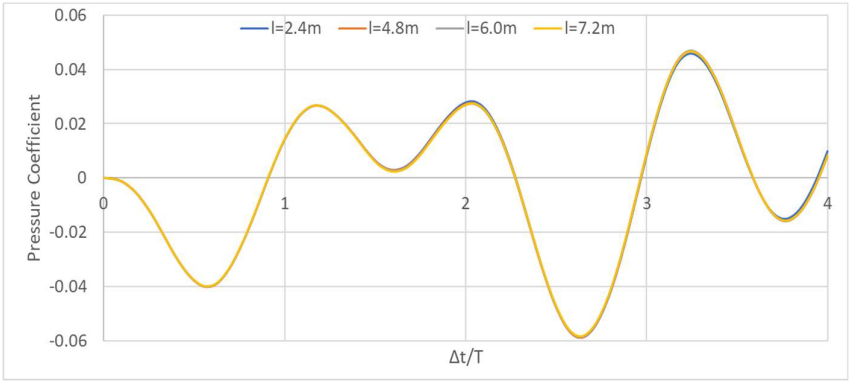

Fig 4.79 Variation of Pressure Co-efficient at 'B' for different baffle position

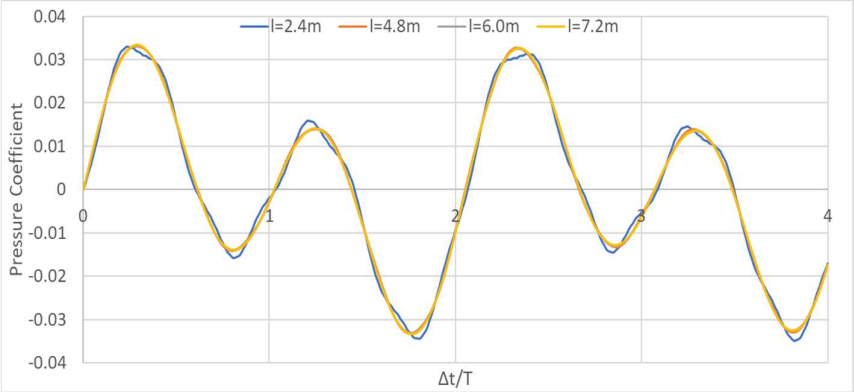

Fig 4.80 Variation of Pressure Co-efficient at 'C' for different baffle position

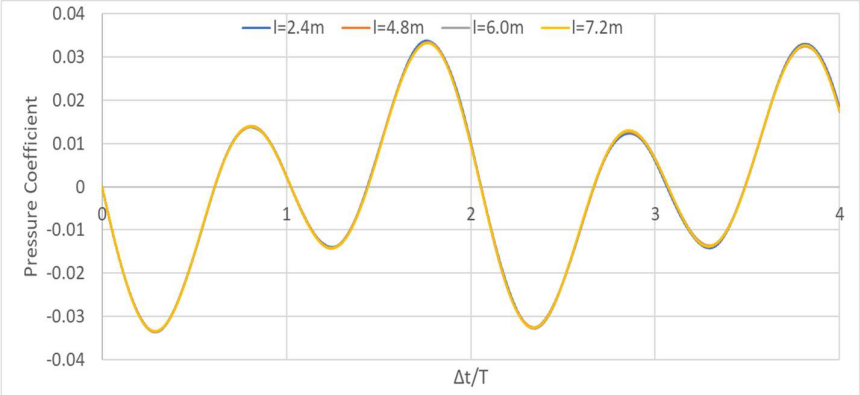

Fig 4.81 Variation of Pressure Co-efficient at 'D' for different baffle position

From the above graphs it is observed that there is no change in pressure coefficients for different baffle position if the coupled system is excited with an arbitrary frequency of 3 rad/sec.

4.2.2.4 Change in Baffle height

Here for a 12m tank with 5m fluid height, 100mm baffle thickness and baffle positioned at 2.4m from left, time histories are plotted for baffle height of 1m, 2m, 3m and 4m.

a) Time history corresponding to exciting frequency 'ω'

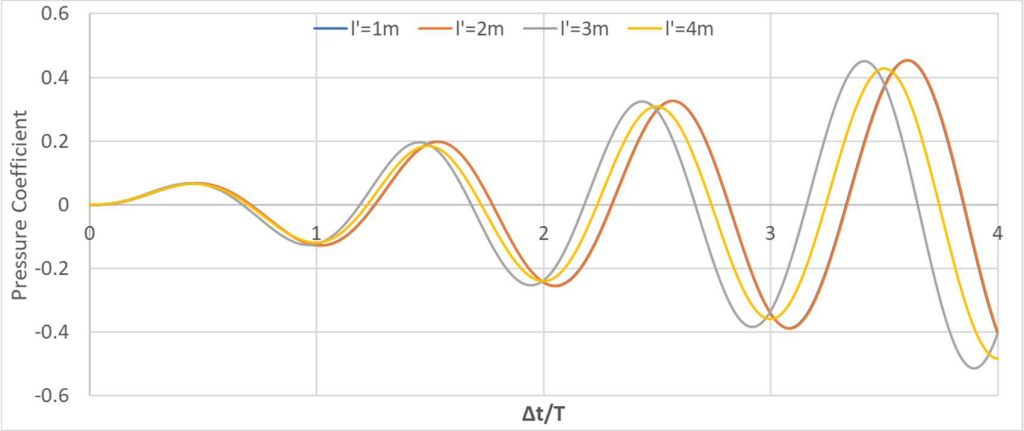

Fig 4.82 Variation of Pressure Co-efficient at 'A' for different baffle height

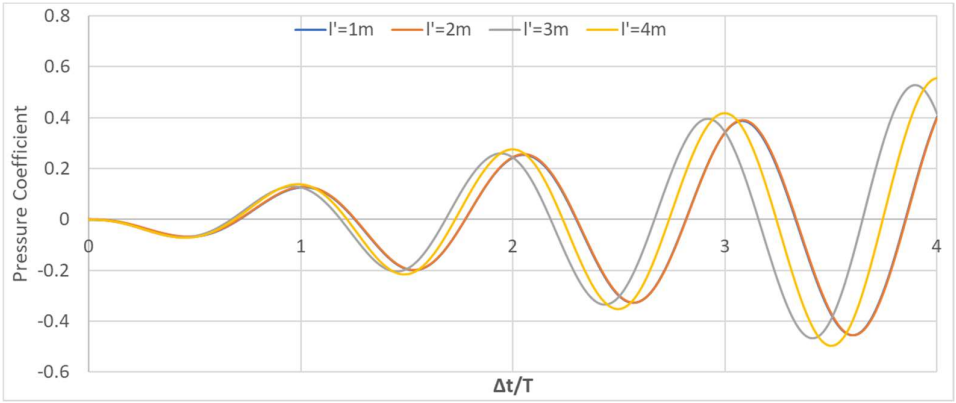

Fig 4.83 Variation of Pressure Co-efficient at 'B' for different baffle height

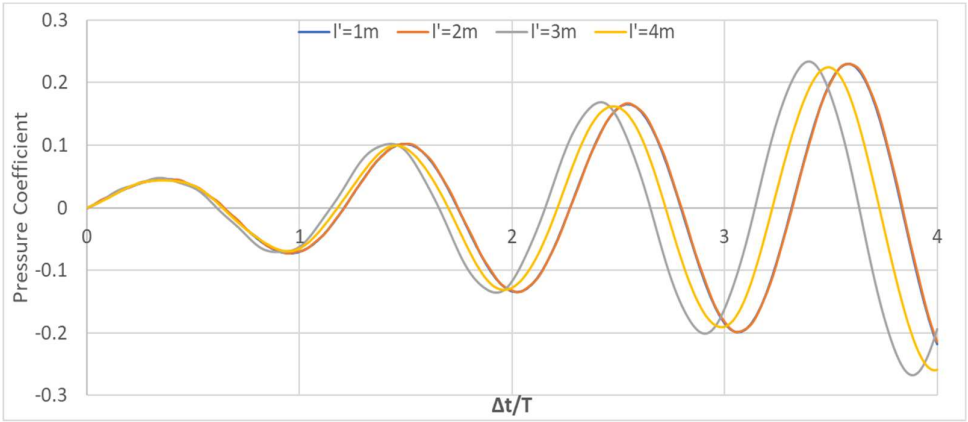

Fig 4.84 Variation of Pressure Co-efficient at 'C' for different baffle height

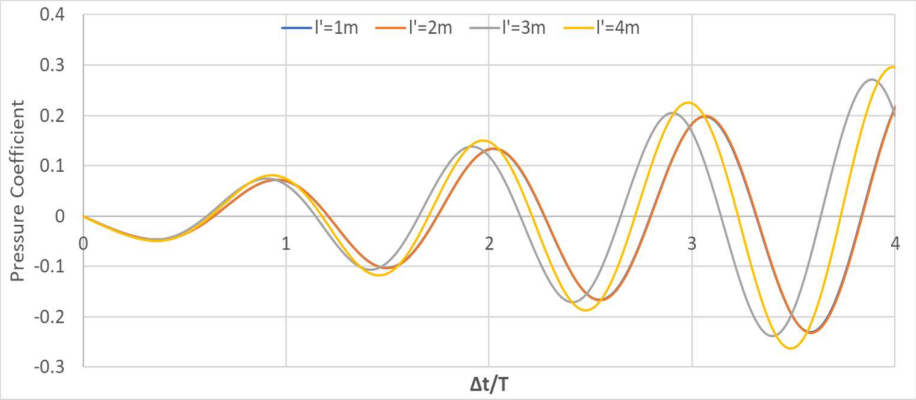

Fig 4.85 Variation of Pressure Co-efficient at 'D' for different baffle height

It has been observed that there is change in pressure coefficients for different baffle height when the coupled system is excited with a frequency equal to natural frequency. Almost similar variation pattern is observed at all four nodes A, B, C and D (fig 4.82-4.85).

b) Time history corresponding to exciting frequency '0.75ω'

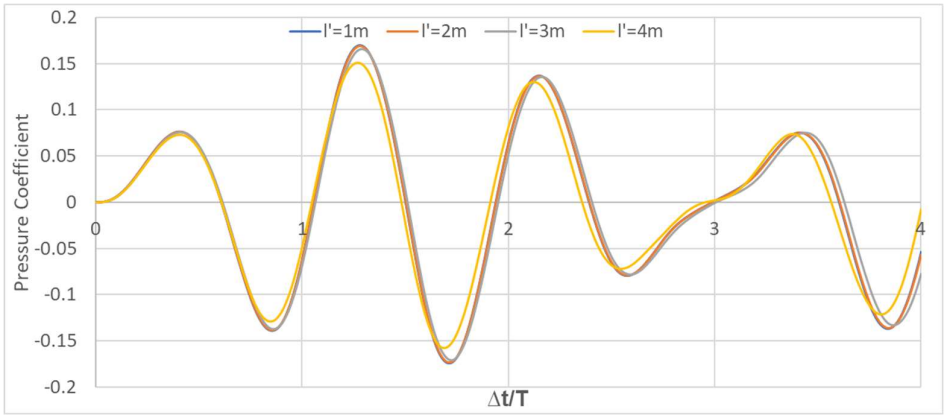

Fig 4.86 Variation of Pressure Co-efficient at 'A' for different baffle height

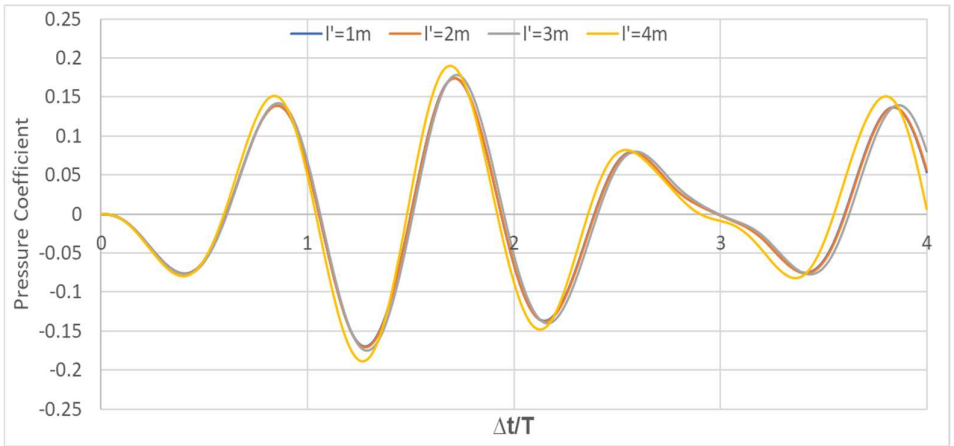

Fig 4.87 Variation of Pressure Co-efficient at 'B' for different baffle height

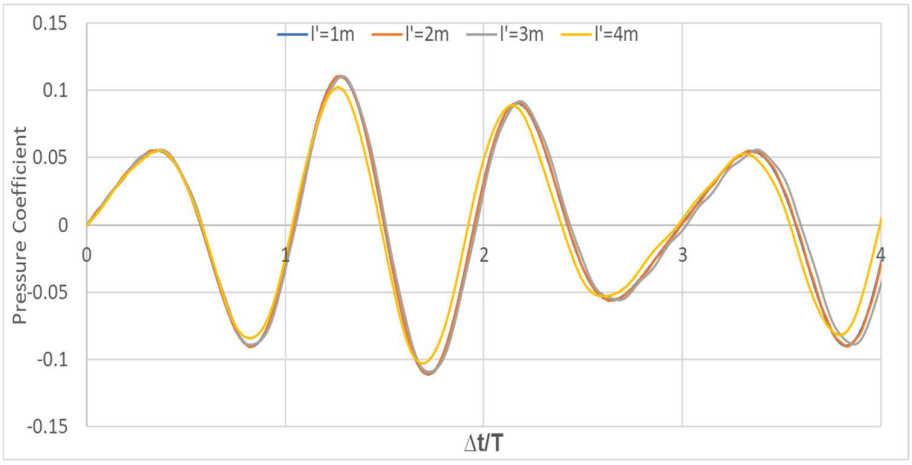

Fig 4.88 Variation of Pressure Co-efficient at 'C' for different baffle height

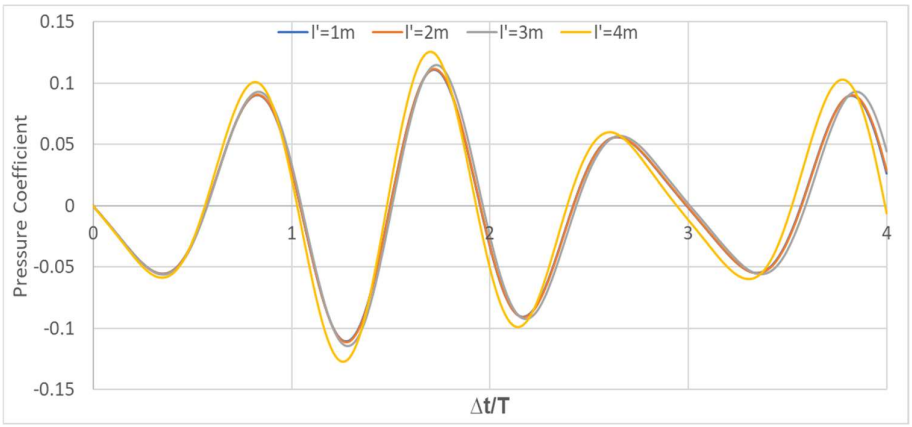

Fig 4.89 Variation of Pressure Co-efficient at 'D' for different baffle height

It has been observed from the above graphs that there is no notable change in pressure coefficients for different baffle height when the coupled system is subjected to an exciting frequency of 0.75ω.

c) Time history corresponding to exciting frequency '1.5ω'

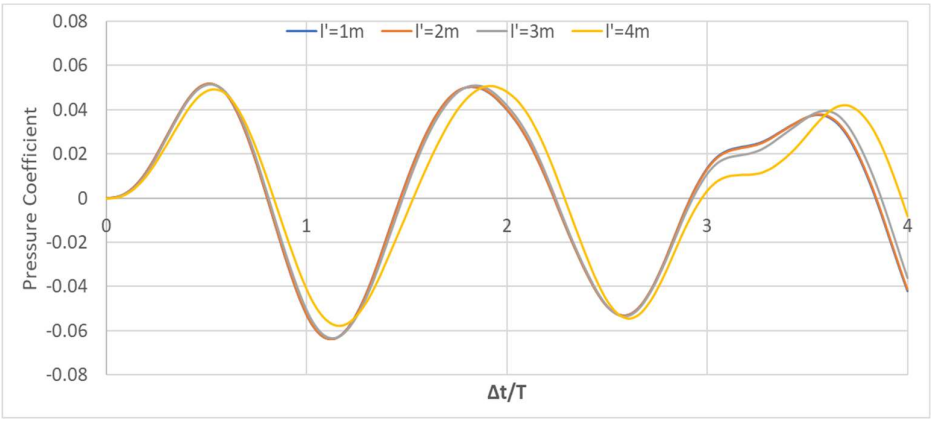

Fig 4.90 Variation of Pressure Co-efficient at 'A' for different baffle height

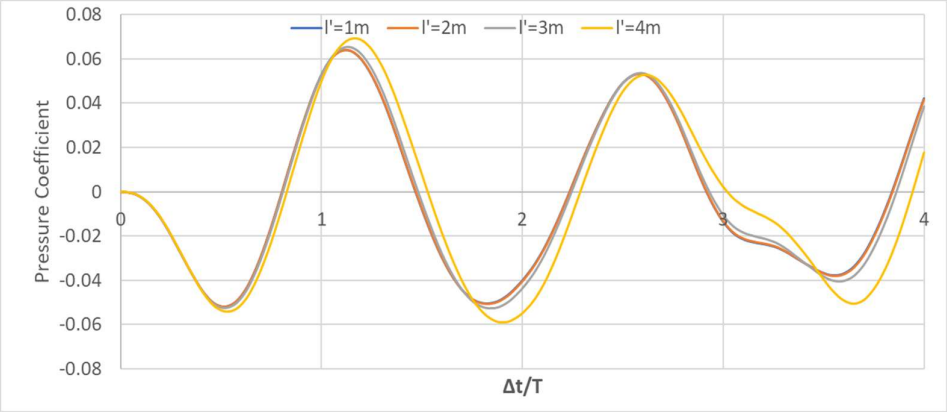

Fig 4.91 Variation of Pressure Co-efficient at 'B' for different baffle height

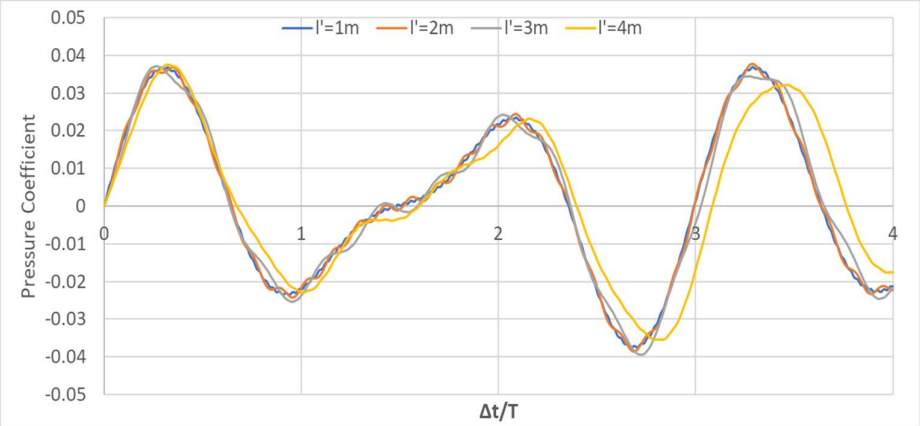

Fig 4.92 Variation of Pressure Co-efficient at 'C' for different baffle height

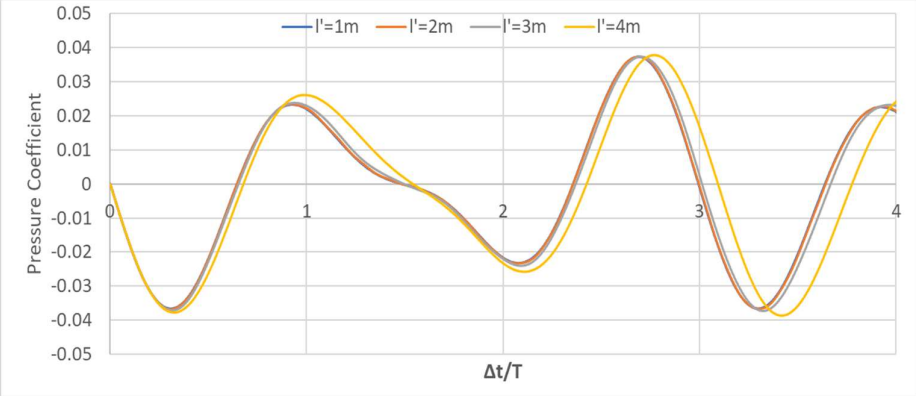

Fig 4.93 Variation of Pressure Co-efficient at 'D' for different baffle height

It has been observed from the figure 4.90-4.93 that there is no notable change in pressure coefficients for different baffle height for exciting frequency of 1.5ω. Response with respect to baffle height of 4m is slightly different from other baffle heights.

d) Time history corresponding to exciting frequency '3ω'

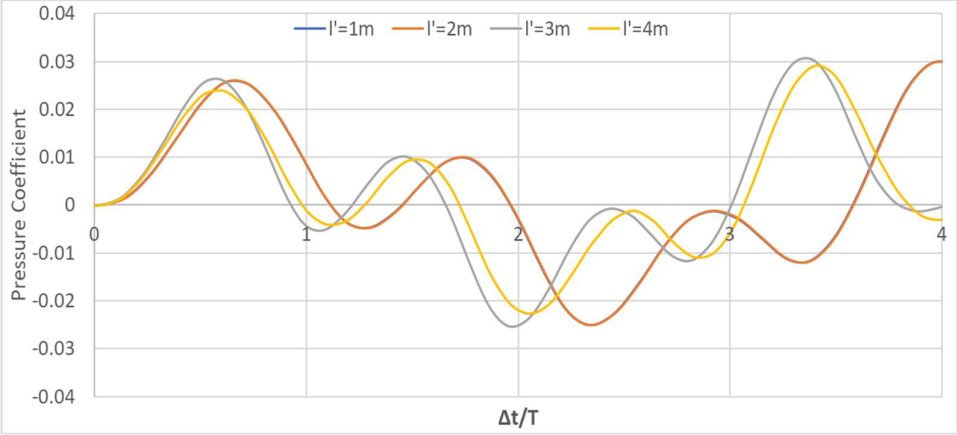

Fig 4.94 Variation of Pressure Co-efficient at 'A' for different baffle height

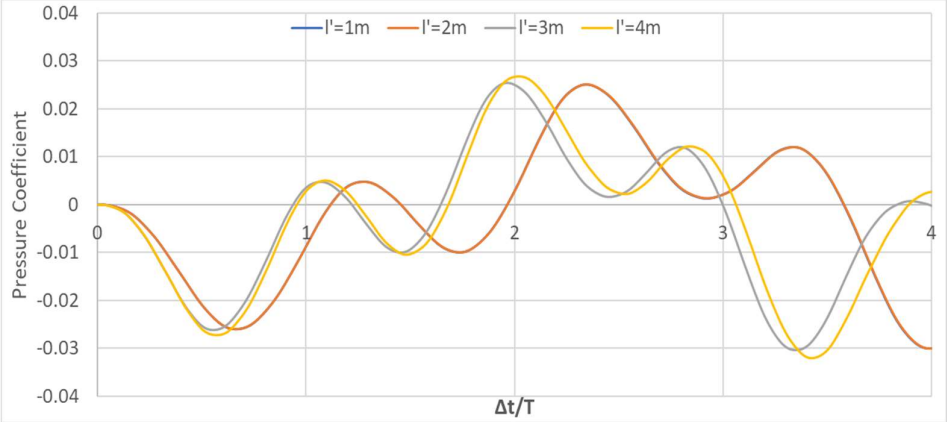

Fig 4.95 Variation of Pressure Co-efficient at 'B' for different baffle height

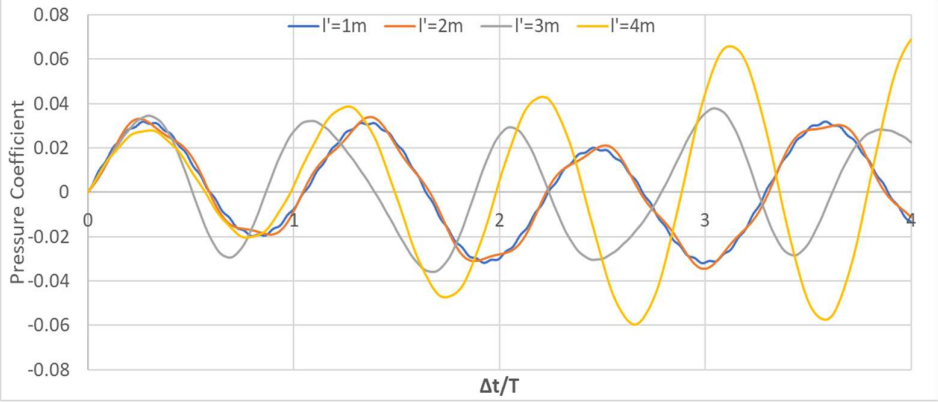

Fig 4.96 Variation of Pressure Co-efficient at 'C' for different baffle height

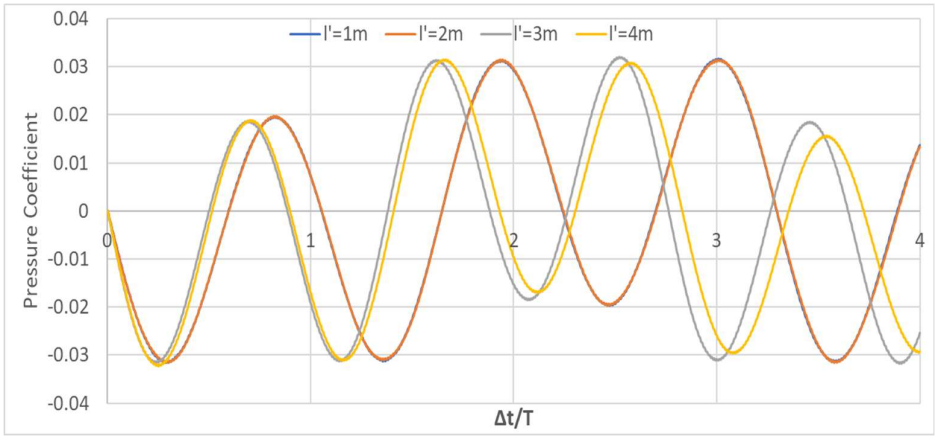

Fig 4.97 Variation of Pressure Co-efficient at 'D' for different baffle height

Variation in pressure coefficients is observed at all four nodes for different baffle height when the system is excited with forcing frequency of 3ω (fig 4.94 to 4.97).

e) Time history corresponding to exciting frequency '3 rad/sec'

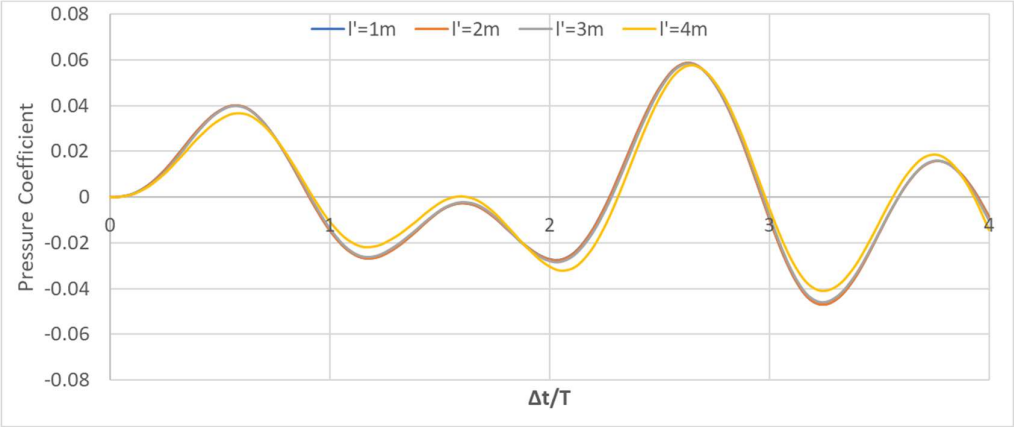

Fig 4.98 Variation of Pressure Co-efficient at 'A' for different baffle height

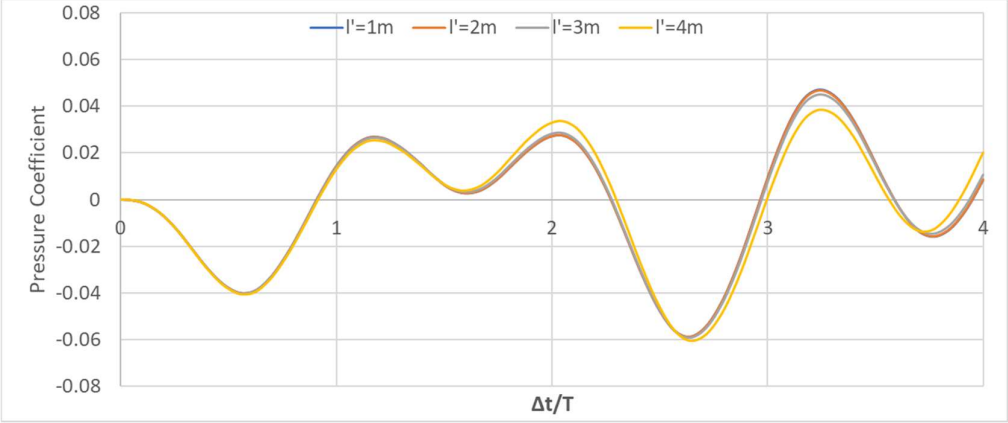

Fig 4.99 Variation of Pressure Co-efficient at 'B' for different baffle height

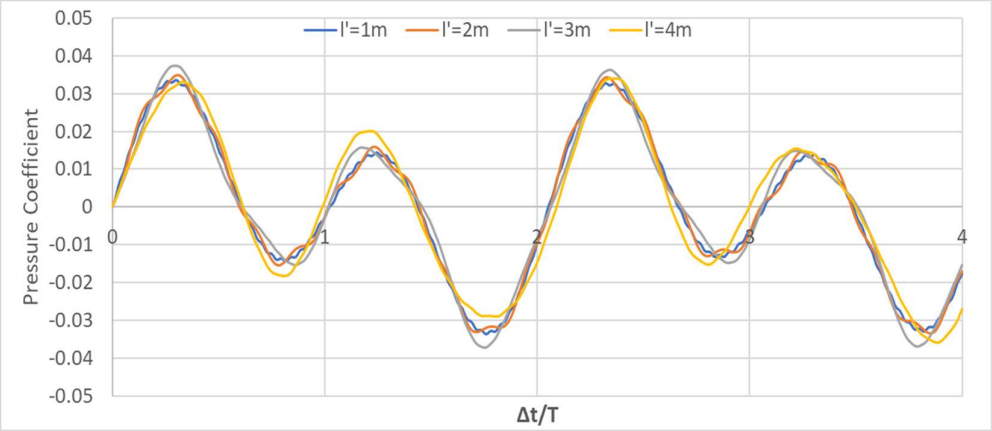

Fig 4.100 Variation of Pressure Co-efficient at 'C' for different baffle height

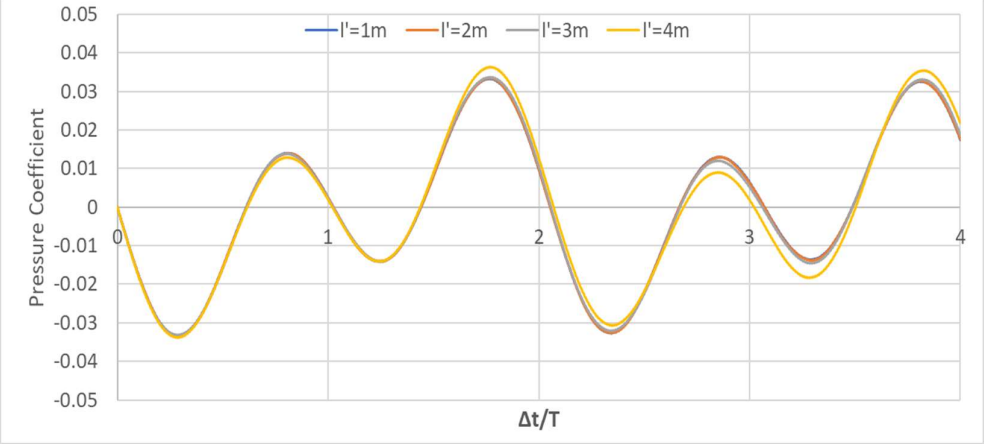

Fig 4.101 Variation of Pressure Co-efficient at 'D' for different baffle height

No notable variations in pressure coefficients have been observed for different baffle height when the system is excited with forcing frequency of 3 rad/sec (fig 4.98 to 4.101).

4.2.2.5 Variation of Maximum Pressure coefficient

A tank of 12m length and baffle wall of 200 mm thickness placed at middle of the tank are considered in the analysis. Fluid height has been changed to get different H/L ratio. Here variation of maximum pressure coefficients at node A, B, C and D for different exciting frequencies $0.2\omega_1$, $0.4\omega_1$, $0.6\omega_1$, $0.8\omega_1$, ω_1, $1.2\omega_1$, $1.4\omega_1$, $1.6\omega_1$, $1.8\omega_1$, ω_2 and ω_3 with different H/L ratios are plotted where ω_1, ω_2 and ω_3 are three fundamental frequencies of tank-baffle system for different tank and baffle wall dimensions.

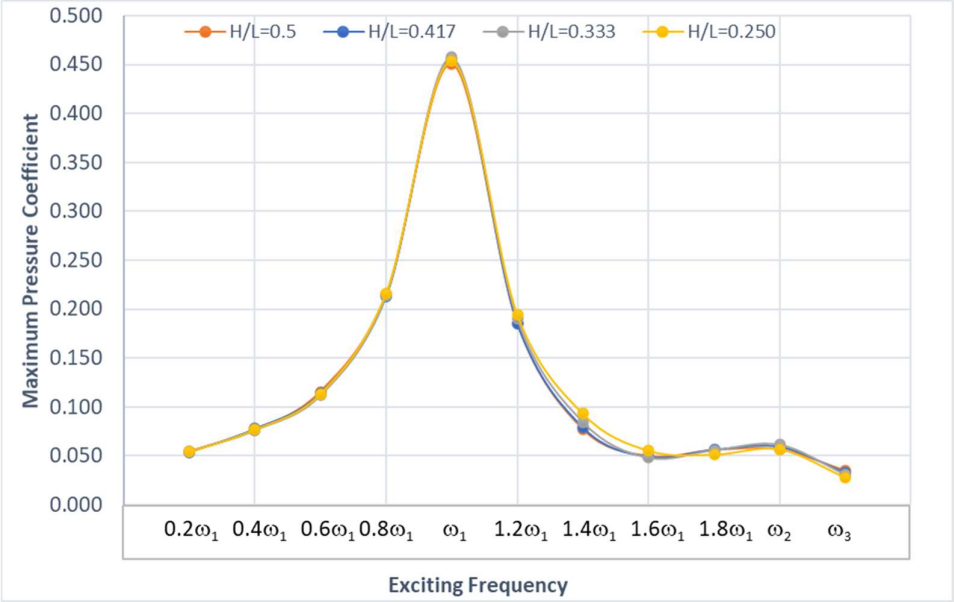

Fig 4.102 Variation of maximum Pressure Co-efficient at 'A' for different exciting frequencies and H/L ratios

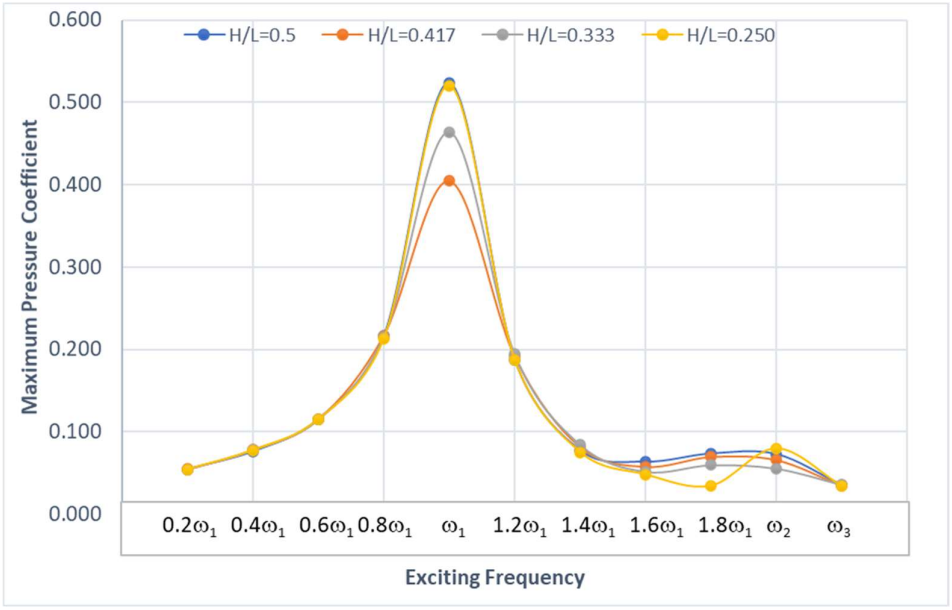

Fig 4.103 Variation of maximum Pressure Co-efficient at 'B' for different exciting frequencies and H/L ratios

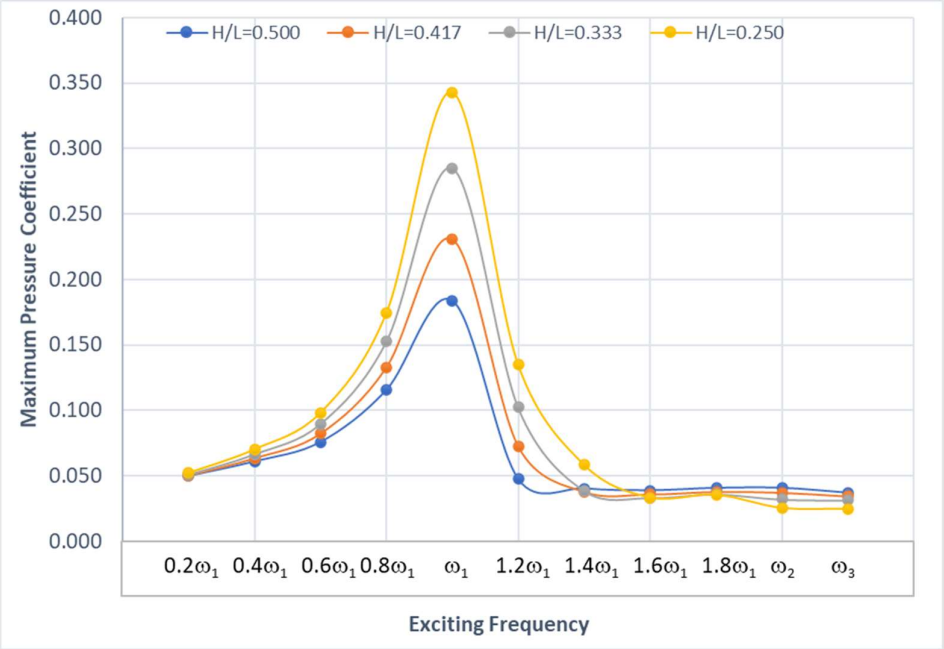

Fig 4.104 Variation of maximum Pressure Co-efficient at 'C' for different exciting frequencies and H/L ratios

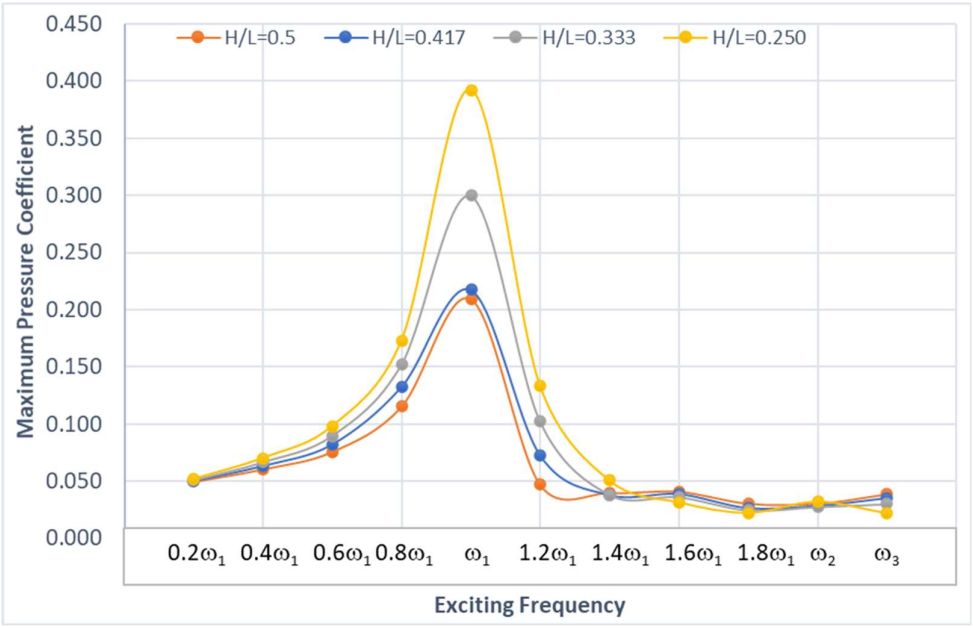

Fig 4.105 Variation of maximum Pressure Co-efficient at 'D' for different exciting frequencies and H/L ratios

Maximum pressure coefficients for different exciting frequencies have been plotted and it has been observed that pressure is maximum when the system is excited with frequency equal to natural frequency of the system. Resonant condition is clearly depicted from the above graphs (fig 4.102-4.105).

CHAPTER-5
CONCLUSION

The fundamental time period and the hydrodynamic pressure within rectangular tank with vertical elastic baffle with different excitations are determined considering baffle-fluid interaction. The fluid within the tank is considered to be linearly compressible. Pressure and displacement based finite element method are used to simulate the fluid within tank and baffle wall respectively. Based on the present study the following conclusions may be drawn.

a) The time period of tank increases with the increase of length of tank. This time period of tank with baffle is slightly greater than to those of tank without baffle. However, for comparatively smaller tank, the third time periods are almost same for tank with and without baffle and similar variation is observed in case of first time period of tank with and without baffle for comparatively large tank.
b) The height of the fluid within the tank is also an important parameter for free vibration analysis of rectangular tank with elastic baffle. In this case, the time period increases with the increase of fluid height.
c) The height of baffle also influences the time period of tank. The time periods for first and third mode increase with the increase of baffle height. It means the free vibration responses increase with the increase of flexibility of baffle wall. However, this effect is very little for second time period.
d) The time period decreases with increase in the distance between the tank wall and baffle for first two time periods. These time periods attain highest values when it is near to the tank wall and they have lowest value when it is placed near the midpoint of tank. But the third time period decreases up to one fourth distance from tank wall, after that the time period increases up to the midpoint of the tank and attains maximum value at the midpoint of tank.
e) The time period of tank decreases with the increase of baffle thickness for first and third time period because the higher thickness of baffle reduces the flexibility of baffle hence reduces time period of baffle-liquid coupled system. However, very little variation has been observed for second time period and can be neglected.

f) Pressure coefficients along walls are maximum when the frequency of externally applied force is close to the natural frequency of fluid-baffle system and resonant frequency results amplified response.

g) Baffle wall thickness influences the dynamic response and comparatively thin wall section results less pressure coefficients.

h) Hydrodynamic pressure at bottom surface of tank increases with decrease in fluid height.

i) Hydrodynamic pressure at bottom surface of tank increases with increase in tank length. However, there is no notable variation in pressure at free surface due to change in tank length.

5.1 Future Scope of works

The present work is an investigation of fundamental time periods of rectangular water tank with vertical elastic baffle and also to calculate the hydrodynamic pressure within the tank subjected to sinusoidal excitation with different frequencies. There are certain other aspects that may be considered for further research:

- The present study is limited to the forced vibration analysis of tank considering vertical baffle. The study may be extended for horizontal baffle.
- The responses of rectangular tank with elastic baffle may be determined against earthquake excitations.
- The present problem may be extended to three-dimensional form with or without baffle.
- The analysis may also be performed for cylindrical and other types of tanks.
- Non-linear wave theory may be used to simulate the water or other fluid motion within the tank

References:

i. Ranjan Adhikary and Kalyan Kumar Mandal (2017) "Dynamic analysis of water storage tank with rigid block at bottom", Ocean Systems Engineering, Vol. 8, No. 1 (2018) 57-77; DOI: https:// doi.org/10.12989/ose.2018.8.1.057

ii. Waghmare, M.V., Madhekar, S.N. and Matsagar, Vasant(2015) "Behavior of elevated water storage tanks under seismic events", V. Matsagar (ed.), Advances in Structural Engineering, Springer India 2015

iii. Hadj-Djelloul, Nasser Dine, Djermane, Mohammed, Sharari, Noor and Merabti, Soufiane(2020) "Dynamic behavior of elevated water tanks under seismic excitation", International Journal of Innovative Technology and Exploring Engineering (IJITEE),ISSN: 2278-3075, Volume-9 Issue-9, July 2020

iv. Kalyan Kumar Mandal and Munna Aziz "An Eulerian approach for dynamic analysis of reservoir adjacent to concrete gravity dam", SN Applied Sciences (2019) 1:709/ https://doi.org/10.1007/s42452-019-0693-z

v. Kalyan Kumar Mandal (2023) "Finite element based total response analysis of rectangular liquid containers against different excitations", Ocean Systems Engineering, Vol. 13, No. 1 (2023) 57-77; DOI: https:// doi.org/10.12989/ose.2023.13.1.057

vi. Santosh Kumar Das, Kalyan Kumar Mandal and Arup Guha Niyogi, "Finite element-based direct coupling approach for dynamic analysis of dam–reservoir system", Innovative Infrastructure Solutions (2023) 8:44 https://doi.org/10.1007/s41062-022-01013-5, Springer Nature Switzerland AG 2022

vii. Nayana R, Neenu K Mathew and Asha Joseph (2015) " Dynamic Response of Ground Supported Rectangular Water Tank", Special Issue – 2015, International Journal of Engineering Research & Technology (IJERT), ISSN: 2278-0181, NCRACE-2015 Conference Proceedings

viii. Jung, J.H., Yoon, H.S., Lee, C.Y. and Shin, S.C.(2012) "Effect of the vertical baffle height on the liquid sloshing in a three-dimensional rectangular tank", J.H. Jung et al. / Ocean Engineering 44 (2012) 79–89

ix. Vahid Lotfi and Ali Samii, "Dynamic analysis of concrete gravity dam-reservoir systems by Wavenumber approach in the frequency domain"

x. Drosos, G.C., Dimas, A.A. and Karabalis, D.L.(2008) "Discrete models for seismic analysis of liquid storage tanks of arbitrary shape and fill height", Journal of Pressure Vessel Technology, Transactions of the ASME · November 2008, Vol. 130 / 041801-1

xi. Majid Pasbani Khiavi, Adel Ferdousi and Abdolrahman Moallemi Khiavi "A Probabilistic Model for Evaluation of the Dynamic Behavior of a Concrete Gravity Dam considering

the Fluid Structure Interaction", Hindawi, Advances in Civil Engineering, Volume 2023, Article ID 9927608, 12 pages https://doi.org/10.1155/2023/9927608

xii. Prashant A Bansode and V. P. Datye, "Seismic Analysis of Elevated Water Tank with Different Staging Configuration", MAT Journals, Journal of Geotechnical Studies, Volume 3 Issue 1

xiii. Malhotra, Praveen K., Wenk, Thomas and Wieland, Martin(2000) "Simple procedure for seismic analysis of liquid-storage tanks", Structural Engineering International 3/2000

xiv. Aregawi, Birhane and Kassahun, Abdulaziz(2017) "Dynamic response of ground supported rectangular water tanks to earthquake excitation", Momona Ethiopian Journal of Science (MEJS), V9(1):66-75, 2017, CNCS, Mekelle University, ISSN:2220-184X

xv. Santosh Kumar Das, Kalyan Kumar Mandal and Arup Guha Niyogi, "A finite element based approach to observe hydrodynamic pressure in reservoir adjacent to concrete gravity dam", Ocean Systems Engineering, Vol.12, No.4(2022) 385-402, https://doi.org/10.12989/ose.2022.12.4.385

xvi. Ikeda, T. and Nakagawa, N.(1996) "Non-Linear vibrations of a structure caused by water sloshing in a rectangular tank", Journal of Sound and Vibration (1997) 201(1), 23-41

xvii. Jiaqi Ren, Wenwei Yang and Yin Wang "Study on the Response Characteristics of Elevated Cylindrical Liquid Storage Tanks under Seismic Excitation", DOI: https://doi.org/10.21203/rs.3.rs-2810378/v1, April 20th, 2023

xviii. Omidinasab, F. and Shakib, H.(2011) "Seismic response evaluation of the RC elevated water tank with fluid-structure interaction and earthquake ensemble", KSCE Journal of Civil Engineering (2012) 16(3):366-376, Vol. 16, No. 3 / March 2012

xix. Nandagopan M. and Shinu Shajee "Dynamic Analysis of RCC Water Tanks with Varying Height of Water Level", International Journal of Innovative Research in Science, Engineering and Technology, Vol. 6, Issue 4, April 2017

xx. Kotrasová, Kamila and Kormaníková(2017) "Liquid storage cylindrical tank - earthquake analysis", MATEC Web of Conferences 125, 04009 (2017)

xxi. Aliakbar Qutubuddin Ali and Deepa P. Telang, "A Survey on Dynamic Analysis of Elevated Water Tank for Different Staging Configuration, International Journal of Computer Science and Mobile Computing, IJCSMC, Vol. 6, Issue. 5, May 2017, pg.194 – 201

xxii. Mustafa Arafa, "Finite element analysis of sloshing in liquid-filled containers", Production Engineering & Design For Development, PEDD7, Cairo, February 7 – 9, 2006

xxiii. M. Yazdanian, S.V. Razavi and M. Mashal, " Seismic Analysis of Rectangular Concrete Tanks by Considering Fluid and Tank Interaction", Journal of Solid Mechanics Vol. 8, No. 2 (2016) pp. 435-445

xxiv. Visuvasam, J., Simon, J., Packiaraj, J. S., Agarwal, R., Goyal, L. and Dhingra. V.(2017) "Seismic response of elevated rectangular water tanks considering soil structure interaction", IOP Conf. Series: Materials Science and Engineering 263 (2017) 032036

xxv. Dongya Zhao, Zhiqiang Hu, Gang Chen, Serena Lim, Shuqi Wang, "Nonlinear sloshing in rectangular tanks under forced excitation", International Journal of Naval Architecture and Ocean Engineering xxx (2017) 1-21

xxvi. Wakchaure M. R and Besekar Sonal S. "Behaviour of Elevated Water Tank under Sloshing Effect", International Journal of Engineering Research & Technology (IJERT), ISSN: 2278-0181, Vol. 3 Issue 2, February – 2014

xxvii. Patel, Chirag N., Vaghela, Shashi N. and Patel, H.S.(2012) "Sloshing response of elevated water tank over alternate column proportionality", IJAET/Vol.III/ Issue IV/Oct.-Dec., 2012/60-63

xxviii. M.S. Bhandiwad and B. M. Dodamani "Porous Baffle Performance in a Sloshing Tank", SSRG International Journal of Civil Engineering, Volume 9 Issue 12, 1-6, December, 2022

xxix. Zhao, Chunfeng, Chen, Jianyun, Xu, Qiang, Wang, Jingfeng and Wang, Bo(2015) "Investigation on sloshing and vibration mitigation of water storage tank of AP1000", C. Zhao et al. / Annals of Nuclear Energy 90 (2016) 331–342

xxx. Dona Rose K J, M Sreekumar and A S Anumod "A Study of Overhead Water Tanks Subjected to Dynamic Loads", International Journal of Engineering Trends and Technology (IJETT) – Volume 28 Number 7 - October 2015

xxxi. Helou, Sameer H.(2014) "Seismic induced forces on rigid water storage tanks", Asian Journal of Engineering and Technology (ISSN: 2321 – 2462) Volume 02 – Issue 04, August 2014

xxxii. Bang-Fuh Chen, Bing-Han Lin and Po-Chih Chen "Investigation of Sloshing Response in Rectangular Container with Flexible Baffle" Proceedings of the 9th International Symposium on Fluid-Structure Interactions, Flow-Sound Interactions, Flow-Induced Vibration & Noise July 8-11, 2018, Toronto, Ontario, Canada

xxxiii. Suyash Nerkar and Chittaranjan Nayak "Seismic Behaviour of Elevated Storage Reservoir by Finite Element Method", International Journal of Advanced Technology in Engineering and Science, Vol No-4, Special Issue No.01, March 2016

xxxiv. Chaithra M, Krishnamoorthy A and Naurin Nafisa P M "Analysis of Soil - Structure Interaction on Response of Tanks Filled with Fluid" International Journal of Civil

Engineering and Technology (IJCIET) Volume 8, Issue 7, July 2017, pp. 813–819, Article ID: IJCIET_08_07_088, ISSN Print: 0976-6308 and ISSN Online: 0976-6316

xxxv. Bachir, Meziani and Ouerdia, Ourrad (2014) "Capillary effect on the sloshing of a fluid in a rectangular tank submitted to sinusoidal vertical dynamical excitation", www.sciencedirect.com/science/journal/10016058, 2014,26(2):326-338 Journal of Hydrodynamics

xxxvi. Hadj-Djelloul, N. and Djermane, M.(2019) "Effect of geometric imperfection on the dynamic of elevated water tanks", Civil Engineering Journal, Vol. 6, No. 1, January, 2020

xxxvii. Juan C. Virella, Carlos A. Prato and Luis A. Godoy "Linear and nonlinear 2D finite element analysis of sloshing modes and pressures in rectangular tanks subject to horizontal harmonic motions", Journal of Sound and Vibration 312 (2008) 442–46

xxxviii. Rubesh Raja V. and Ponnusamy Palanisamy " Numerical modelling of nonlinear baffles on sloshing suppression of rectangular tanks under horizontal excitation", Ocean Engineering, Volume 267, 1 January 2023, 113277

xxxix. V.S. Sanapala, Rajkumar M, K. Velusamy and B.S.V. Patnaik "Numerical simulation of parametric liquid sloshing in a horizontally baffled rectangular container", Journal of Fluid and Structures 76(2018) 229-250

xl. Fabbrocino, Giovanni, Iervolino, Iunio, Orlando, Francesca and Salzano, Ernesto(2005) "Quantitative risk analysis of oil storage facilities in seismic areas", G. Fabbrocino et al. / Journal of Hazardous Materials A123 (2005) 61–69

xli. Yanmin Guan, Caihong Yang and Ping Chen and Li Zhou "Numerical investigation on the effect of baffles on liquid sloshing in 3D rectangular tanks based on nonlinear boundary element method", International Journal of Naval Architecture and Ocean Engineering 12(2020) 399-413